UNIVERSITA' DEGLI STUDI DI MILANO

SCUOLA DI DOTTORATO IN SCIENZE FARMACOLOGICHE

Corso di Dottorato in Farmacologia, Chemioterapia e Tossicologia Medica

Settore Scientifico Disciplinare BIO/14

Ciclo XXIV

ADIPOSE-DERIVED STEM CELLS (ASCs) FOR FUTURE CELLULAR THERAPIES IN MUSCLE-SKELETAL TISSUES REGENERATION

Tutor: Prof. Anna T. BRINI

Coordinatore: Prof. Alberto E. PANERAI

Dottorando

ARRIGONI ELENA

Anno Accademico 2010/2011

INDEX

__ABSTRACT__

Every year several patients have to deal with bone tissue loss due to trauma or diseases. Bone tissue engineering aims to restore or repair musculoskeletal disorders through the development of bio-substitutes that require the use of cells and scaffolds which should possess both adequate mechanical properties and interconnecting pores to allow cellular infiltration, graft integration and vascularization. The ideal cell for tissue engineering should possess a potential plasticity with the ability to functionally repair the damaged tissue, and it should be available in large amount. Mesenchymal stem cells (MSCs) are present in many adult tissues, and adipose tissue represents an attractive source of MSCs for researchers and clinicians of nearly all medical specialties. Adipose-derived stem cells (ASCs) are similar to MSCs isolated from bone marrow, placenta, and umbilical cord blood in morphology, immunophenotype, and differentiation ability, and they represent a promising approach of bone regeneration. Additional features of ASCs are their immunoregolatory and anti-inflammatory properties both *in vivo* and *in vitro* and their low immunogenicity.

Since several years our laboratory is studying mesenchymal stem cells isolated from human and animal adipose tissues. Human ASCs (hASCs) have been characterized by their immunophenotype, their self-renewal potential, and they have been induced to differentiate towards adipogenic, osteogenic and chondrogenic lineages. The ability of hASCs to grow in the presence of several scaffolds has also been tested. hASCs adhered to the surface of tested biomaterials, filling the pores and forming a 3D web-like structure, allowing these progenitor cells to osteo-differentiate more efficiently respect to cells maintained on polystyrene. Since our interest was to regenerate muscle-skeletal defects by ASCs in pre-clinical models, we first studied ASCs isolated from adipose tissue of rat (rASCs), rabbit (rbASCs) and pig (pASCs), considered good models in the orthopaedic field. We have shown that animal ASCs behaved similarly to the human ones, and, in collaboration with the Faculty of Veterinary Medicine of University of Milan and the IRCCS Galeazzi

Orthopaedic Institute of Milan, we have tested the ability of autologous ASCs to regenerate a full-thickness critical-size bone defect in rabbits. The experimental study was conducted on the tibiae of 12 New Zealand rabbits, and from 6 rabbits out of 12 we have collected adipose tissue from the interscapular region. We have isolated $2.8 \times 10^5 \pm 1.9 \times 10^5$ rbASCs per ml of raw tissue, and after 3-4 days in culture the cells showed the typical fibroblast-like morphology. One week later, all the 6 cellular populations started to steadily proliferate, and they generated fibroblast (CFU-F) and osteoblast (CFU-O) colonies, highlighting the presence of osteogenic progenitors. Indeed, when rbASCs were induced to osteo-differentiate, either after 7 and 14 days, we have observed an up-regulation of specific osteogenic markers, such as alkaline phosphatase (ALP, +28.9%), collagen (+105.9%) and extracellular calcified matrix (+168.1%), compared to undifferentiated cells. In parallel, testing HA, the scaffold selected for the *in vivo* experiment, we found that rbASCs were osteoinduced; indeed the presence of HA granules increased per se the amount of collagen production (+48.2%).

1.5×10^6 undifferentiated rbASCs were seeded on custom-made HA disks (8 mm Ø x 4 mm ↕), and the day after, each bioconstruct was implanted into the lesion created in the tibia of each rabbit. We had an additional experimental group of defects where the same number of rbASCs were inserted in the lesion as a semi-liquid suspension; moreover, as controls, we treated 6 lesioned tibia with just the scaffolds, and we left 6 untreated lesioned bone.

8 weeks after surgery animals were sacrificed and the tibia explanted. A macroscopic analysis showed no bone resorption, no abnormal bone callous formation, no fractures, infection or inflammatory reactions, and all the bone defects were completely filled without any significant differences among the four groups.

Interestingly, in the presence of scaffold seeded with rbASCs, histology and immunohistochemistry showed a new bone tissue more mature and similar to the native bone. These data have also been confirmed by biomechanical tests: indeed, the mechanical properties of the bone defect treated by rbASCs-HA were improved, suggesting that these constructs bore mechanical loading with an increase in stiffness of 19.8% and in hardness of 31.6% respect to just HA treated group, indicating that the bioconstructs made out of autologous rbASCs and hydroxyapatite might ameliorate the treatment for large bone defects. We would suggest the use of ASCs as a safe cellular therapy in future clinical

applications where a large bone defect needs to be treated. These promising results on small size animals allow us to plan a new study on large size animals such as minipigs.

However, before moving to the clinic, we know that there are several important aspects that need to be faced regarding safeness and the features of the candidate patients:

1. may the "quality" of hASCs be affected by the donor's physiological or pathological conditions?
2. may the use of pharmacological treatment enhance cellular plasticity of multipotent cells?
3. may the use of immunoselected hASCs ameliorate tissue regeneration in the field of muscle-skeletal?

We have addressed some of these aspects, comparing different populations of hASCs from subcutaneous adipose tissue of healthy-young-female donors (hASCs<35 y/o, n=12, mean age 31±4 years, BMI=23.5±1.6), and from middle-age ones (hASCs>45 y/o n=14, mean age 56±7 years, mean BMI=28.4±1.8). The cellular yield of hASCs derived from older donors was 2.5 fold greater than the one of hASCs<35 y/o, whereas hASCs from younger donors were more clonogenic than hASCs isolated from older ones, with an increase of 129%. No significant differences were observed looking at their immunophenotype.

When hASCs were induced to differentiate into cells of the adipogenic and osteogenic lineages, the donor's age did not affect their adipogenic differentiation, whereas the osteogenic one was significantly affected by age both in the absence and in the presence of three-dimensional scaffolds, showing a decreased ALP basal levels of about 10-fold in hASCs>45 y/o respect to hASCs<35 y/o.

These results seems to indicate that ASCs from different donors could behave differently.

Trying to overcome this aspect we have used different approaches, and we have studied if Reversine, a synthetic purine already known to increase plasticity of terminally differentiated cells, might improve the differentiation ability of hASCs. 72 hours treatment with 50 nM Reversine induced hASCs to differentiate into osteoblast like-cells (+45% of alkaline phosphatase activity), smooth muscle cells (+89% of α-actin expression) and skeletal muscle cells (myotubes formation) compared to control hASCs.

Moreover, since it is known that CD34 and L-NGFR positive cells define a subset of high proliferative and multipotent MSCs, we have immunoselected, these progenitor cells from hASC populations. In contrast to the whole population, the immunoseparated fractions

maintained their undifferentiate state and their ability to differentiate much longer during culture. We have shown that both CD34+ and L-NGFR+ hASCs can be used as alternative candidates for tissue engineering and regenerative medicine applications. In particular, due to the improved ability of L-NGFR positive cells to adipo- and chondro-differentiate, they appear an ideal tool in reconstructive plastic surgery and cartilage regeneration.

From our data, and the ones from researchers in other fields, we believe that in the near future adipose-derived stem cells might be considered a safe tool in regenerative medicine. Furthermore, to improve this "cellular therapy", we could either pre-treat ASCs with molecules, such as drugs and/or siRNAs known to affect specific differentiation pathways, or by selecting subpopulations of progenitor cells which may be used as allogenic implants. Next step will be to confirm our *in vivo* data in a large size animal model such as minipig, and then to test if pre-treated cells or selected population might be used in an autologous and allogenic small size animal model.

INTRODUCTION

CHAPTER 1

1. STEM CELLS

Stem cells are biological cells characterized by two properties: the ability to self-renewal maintaining their undifferentiated state (symmetric division), and the ability to give rise to cells identical to the mother cells and to differentiated daughter cells with different characteristics (asymmetric division) [Weiss and Troyer, 2006] (Figure 1).
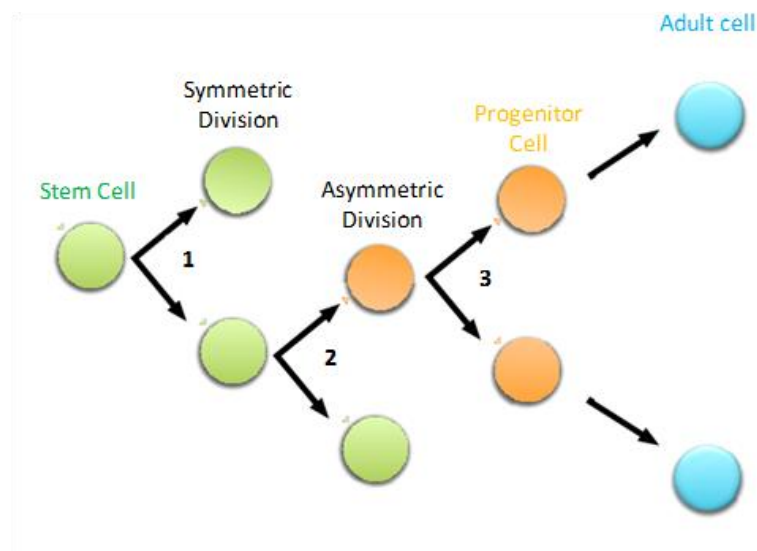
Figure 1. Stem cells division. Green dots: stem cells; orange dots: progenitor cells; light blue dots: differentiated cells. 1. symmetric stem cells division; 2. asymmetric stem cells division; 3. progenitor division and terminal differentiation (modified by [Weiss and Troyer, 2006]).

Stem cells are distinguished by their ability to produce mature cells belonging to different genealogies (Figure 2):

Totipotent Stem Cells able to differentiate into embryonic and extra-embryonic cell types. These cells are produced from the fusion of an egg and sperm cell.

Pluripotent Stem Cells, cells that originate from the inner cell mass of the blastocyst and that can give rise to any fetal or adult cell type of the three germ layers (mesoderm, endoderm and ectoderm), but they are not able to generate an adult organism.

Multipotent Stem Cells able to differentiate into a number of cells, but only those of a closely related family of cells; however, has been demonstrated the ability of these cells to trasndifferentiate into cell lineages of different embryonic origin.

Unipotent Stem Cells able to differentiate into only one type of tissue/cell type.
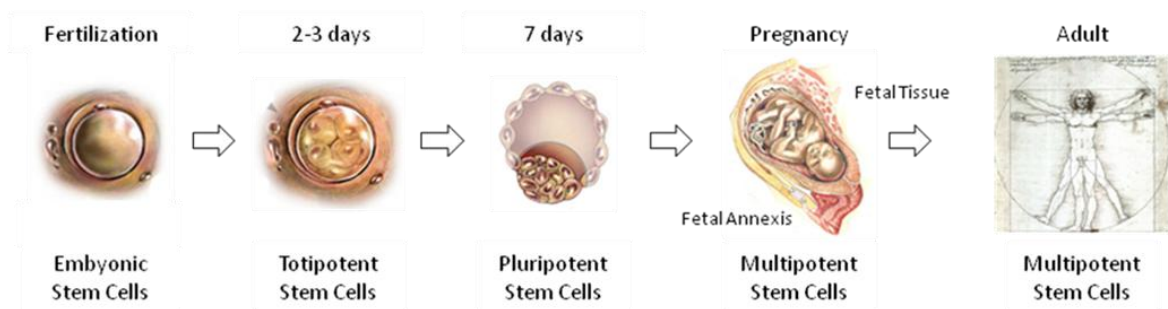
Figure 2. Source of stem cells (modified by http://www.sciencecases.org/superman_ethics/primer.asp).

1.1. STEM CELLS FROM ADULT TISSUES

At the end of embryogenesis each tissue is characterized by heterogeneous populations of cells at different stages of maturation, including a population of undifferentiated cells called adult stem cells [Atala, 2007]. Adult stem cells are responsible of the maintaining of tissue homeostasis [Tarnowski and Sieron, 2006], and of the replacing of terminally differentiated cells lost during senescence or due to trauma and injury [Barry and Murphy, 2004]. These cells are located in a specialized compartment defined "stem cell niche": it is an anti-proliferative and anti-differentiative environment, with the ability to recall and reprogram themselves [Xie and Spradling, 2000; Shinohara et al., 2001, 2002]. In the tissues it is possible to find a tissue's hierarchy, important to minimizing the occurrence of pathological states. Stem cells are characterized by a high proliferation rate that permit to protect the integrity of the stem cell compartment, and are also able to produce committed progenitor stem cells which can give rise to mature and functionally differentiated cells [Piscaglia, 2008].

Adult stem cells, in the presence of specific chemical and physical stimuli, can give rise to cells derives of the three primary germ layers: mesoderm, ectoderm and endoderm [Caplan, 2007].

It has been observed that neural stem cells can give rise to blood and skeletal muscle cells when transplanted into an ectopic site [Panchision et al., 1998]. Another study has shown that mesenchymal stem cells isolated from adipose tissue can differentiate into pancreatic-β cells [Timper et al., 2006]. For these reason, adult mesenchymal stem cells could be considered suitable candidates for applications in tissue engineering and regenerative medicine.

1.1.1. MESENCHYMAL STEM CELLS (MSCs)

The presence in the bone marrow of non-hematopoietic stem cells, was suggested by Friedenstein in 1968. These cells, after several passages in culture, showed a typical fibroblast-like morphology able to give rise to different cell lineages such as osteoblasts, chondrocytes and adipocytes [Friedenstein et al., 1968]. The bone marrow is still the main source of Mesenchymal Stem Cells (MSCs), but several studies have identified these cells in other tissues such as periosteum, dental pulp, skeletal muscle, synovial membrane, trabecular bone tissue, and adipose tissue [Arai et al., 2002; Noth et al., 2002; Zuk et al., 2002; De Ugarte et al., 2003; Sakaguchi et al., 2004]. Adipose tissue is also an abundant source of stem cells (Adipose-derived Stem Cells, ASCs) and it is a tissue easily accessible by a minimally invasive liposuction procedure; in addition, a significant number of ASCs can be isolated from a small volume of subcutaneous fat, expanded and subsequently differentiated or cryopreserved. ASCs show high plasticity and are able to differentiate in mesenchymal-derived tissues, such as:

Adipocytes: specific medium, characterized by dexamethasone, indomethacin, insulin, and isobutyl-methylxanthine, induce ASCs differentiation towards the adipogenic lineage with lipid vacuoles accumulation [Yu et al., 2011].

Chondrocytes: pellet culture maintained in specific inductive medium characterized by transforming growth factor β (TGF-β), ascorbic acid, and dexamethasone, induce ASCs chondrogenic differentiation able to secrete extracellular matrix proteins, such as collagen

type II, VI and proteoglycans and expressing biochemical markers of mature chondrocytes [Erickson et al., 2002; Wickham et al., 2003].

Osteoblasts: in the presence of ascorbic acid, β-glycerolphosphate, dexamethasone and vitamin D3, ASCs express osteogenic markers [Halvorsen et al., 2001; Zuk et al., 2001; Zuk et al., 2002; de Girolamo et al., 2007].

Cardiomyocytes: when exposed in culture with 5'-azacytidine, ASCs express specific proteins of cardiac myocytes, such as troponin I [Fraser et al., 2006a]. This suggests that ASCs can be used in the treatment of ischemic damage.

Smooth Muscle Fibrocells: specific inductive media, characterized by 1% FBS and heparin, induce ASCs differentiation with an up-regulation of smooth muscle α-actin and caldesmin [Rodriguez et al., 2006].

Myocytes: in the presence of horse serum (HS), ASCs express early markers of myogenic differentiation such as myoD and myogenin [Mizuno et al., 2002; Lee and Kemp, 2006].

ASCs are also able to trans-differentiate in cell types of the non-mesodermal origin, such as neurons: human and murine ASCs cultured in the presence of antioxidants and in the absence of serum, acquire a bipolar morphology expressing nestin, intermediate filament, and fibrillary glial protein M [Safford et al., 2004; Fujimura et al., 2005]. Moreover, ASCs are also able to differentiate into endothelial and epithelial cells, hepatocytes and pancreatic-β cells [Seo et al., 2005; Timper et al., 2006; Banas et al., 2007] (Figure 3).
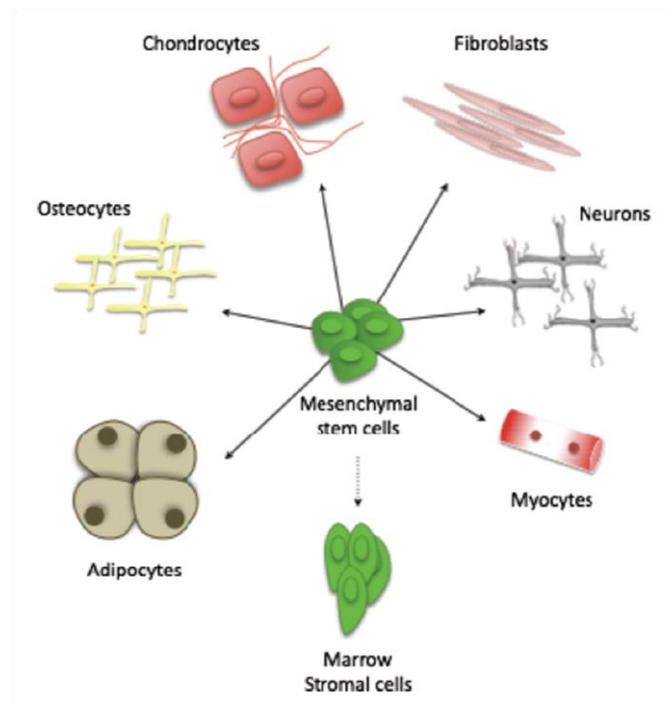
Figure 3. Mesenchymal stem cells can differentiate into several mesenchymal tissues such as bone, cartilage, muscle, bone marrow, adipose tissue and tendon.

An overview of MSCs characteristics is summarized in Table 1.

SOUCE		DIFFERENTIATION
Bone Marrow		Osteoblasts
Trabecular Bone		Chondrocytes
Periosteum		Adipocytes
Articular Cartilage		Cardiac Muscle
Synovial Membrane		Fibroblasts
Synovial Fluid		Myofibroblasts
Muscle		Skeletal Muscle
Adipose Tissue	**Mesenchymal Stem Cells (MSCs)**	Pericytes
Tendon		Tenocytes
Blood		Retina Cells
Blood Vessels		Neuronal Cells
Umbilical Cord Vessels		Astrocytes
Fetal Tissue		Hepatocytes
Spleen and Thymus		Pancreatic Cells
Skin		Hematopoietic Supporting Stroma

Table 1. Sources and cell types derived from mesenchymal stem cells (MSCs) [Pountos and Giannoudis, 2005].

In addition, ASCs and, more generally MSCs, present important properties such as the ability to maintain their undifferentiated state and to proliferate during *in vitro* expansion [Bruder et al., 1997]. The doubling time of ASCs is directly related to several factors, such as

donor age [de Girolamo/ Arrigoni et al., 2009], donor site (subcutaneous or visceral, unpublished data), surgery, and also culture conditions [Gimble, 2003; Izadpanah et al., 2006].

Great effort has been applied to identify specific surface markers on mesenchymal stem cells for their identification *in vivo* and *in vitro*: ASCs express CD9, CD10 (membrane metalloendopeptidase), CD13 (aminopeptidase), CD29 (β1 integrin), CD44 (receptor that binds hyaluronic acid), CD49d (α4 integrin), CD54 (intracellular adhesion molecule 1 or ICAM-1), CD55, CD59, CD71 (transferrin receptor), CD73 (lymphocyte-vascular adhesion protein-2), CD90 (thymocyte differentiation antigen 1), CD105 (endoglin), CD106 and CD166 (Activated leukocyte cell adhesion molecule). ASCs express class I histocompatibility antigen HLA-ABC and do not express class II molecules HLA-DR. These cells do not express hematopoietic markers CD14, CD31 and CD45 [Pittenger et al., 1999; Noort et al., 2002; Zuk et al., 2002; de Girolamo/ Arrigoni et al., 2008].

One of the features that makes the use of MSCs interesting in a clinical setting, is their ability to migrate to the damaged tissue or toward inflammatory sites after intravenously administration [Devine et al., 2001]. This ability has been demonstrated in bone fractures [Devine et al., 2002], myocardial infarction and cerebral ischemia [Saito et al., 2002; Jiang et al., 2005; Erbs et al., 2007]. The mechanism by which MSCs migrate across the endothelium to the injury site has not yet been understood, but it is reasonable to assume that the damaged tissue expresses receptors or ligands that facilitate the transport, adhesion and transmigration of MSCs, like the recruitment of lymphocytes to the inflammation site. Essential molecules for the transmigration of leukocytes from the blood to the tissue, such as integrins, selectins and chemokine receptors are also expressed by MSCs [Krampera et al., 2006; Chamberlain et al., 2007].

Several studies have shown that MSCs have immunomodulatory properties: MSCs are able to inhibit the function of most cells involved in immune response, such as B and T lymphocytes, dendritic cells and natural killer cells [Sotiropoulou et al., 2006]. MSCs inhibited *in vitro* proliferation, differentiation and chemotaxis of human B cells; moreover, these cells inhibit the proliferation of T cells, and activated T cells can increase the immunosuppressive properties of MSCs [Corcione et al., 2006]. Up to now, the mechanisms underlying the immunosuppressive activity of MSCs, have not be elucidated, but both the direct contact between MSCs and cells of the immune system, and also the release by MSCs

of soluble factors such as TGF-β, HGF, and prostaglandin E2 (PGE-2) seem to be important for this function [Zappia et al., 2005].

One of the important properties of MSCs is also the tropism for cancer cells, which makes them as cellular vehicles for the release of anticancer agents. The MSCs can be engineered to release IFN-β, cytosine deaminase, or oncolytic viruses. These approaches have been evaluated in preclinical models and have demonstrated significant antitumoral efficacy [Josiah et al., 2010; Pessina et al., 2011]. Some studies have reported that MSCs can promote tumor growth: subcutaneous co-injection of ASCs with lung carcinoma cells (H460) or glioma cells (U87MG) in nude mice, leads to an increase in tumor size [Yu et al., 2008]. In conflict with the studies reporting a role of MSCs in promoting tumor growth, other studies show that MSCs are able to inhibit tumor expansion: MSCs inhibited the proliferation of human liver cancer cells and the expression of oncogenes *in vivo* and *in vitro* [Qiao et al., 2008]. The effect of MSCs on tumor progression can be explained considering the heterogeneity of MSCs, the injected dose, the patient variability and the time of cells administration: in early tumor development studies, the ability of MSCs to support tumor growth may depend on both their immunosuppressive effect and on their ability to promote angiogenesis, a key event in cancer development and in the process of metastatization.

1.2. CANCER STEM CELLS (CSCs)

Tumorigenicity is a multistep process and requires the accumulation of genetic mutations that lead to the transformation from normal to tumor cells. In a tissue, all proliferating cells may undergo to malignant transformation, including stem cells and committed progenitor cells. Several studies have shown that in most tumors, it is possible to find a hierarchical organization of functionally distinct subpopulations: the majority of tumor cells are not able to support the growth of the tumor or to give rise to metastases. At the top of the hierarchical organization there is a small subpopulation of tumor cells responsible of tumor progression: these cells are known as Cancer Stem Cells (CSCs) which possess some characteristics of stemness. CSCs may generate tumors through the stem cells processes of self-renewal and differentiation into multiple cell types (Figure 4). Such cells are proposed

to persist in tumors as a distinct population and cause relapse and metastasis by giving rise to new tumors.
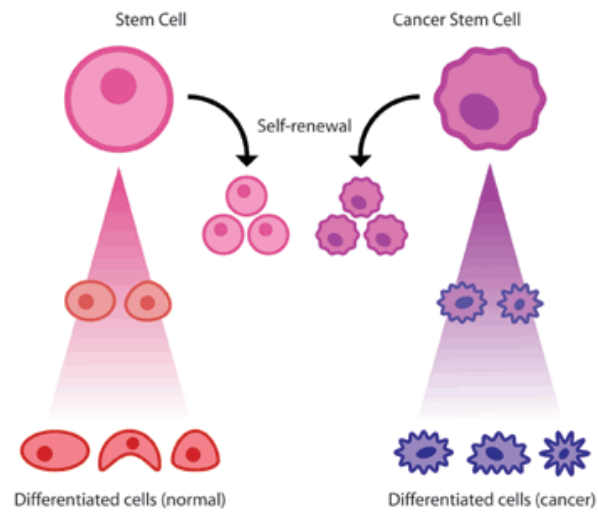
Figure 4. Normal and cancer stem cells show similar properties, included their ability to self-renewal and to differentiate (http://www.childrenshospital.org/gallery/index.cfm?G=67).

The existence of CSCs is a subject of debate within medical research, because many studies have not been successful in discovering the similarities and differences between normal tissue stem cells and cancer stem cells [Gupta et al., 2009]. CSCs must be capable of continuous proliferation and self-renewal in order to retain the many mutations required for carcinogenesis, and to sustain the growth of a tumor since differentiated cells cannot divide indefinitely. There is also debate on the cell of origin of CSCs - whether they originate from stem cells that have lost the ability to regulate proliferation, or from more differentiated population of progenitor cells that have acquired abilities to self-renew (Figure 5).

CSCs have recently been identified in several solid tumors, including brain cancer [Singh et al., 2003], breast cancer [Al-Hajj et al., 2003], prostate cancer [O'Brien et al., 2007] and melanoma [Schmidt et al., 2011]. The existence of CSCs has several implications in terms of future cancer treatment and therapies. These include disease identification, selective drug targets, prevention of metastasis, and development of new intervention strategies. Normal somatic stem cells are naturally resistant to chemotherapeutic agents: they have various pumps (such as Multiple Drug Resistance, MDR) that pump out drugs, DNA repair proteins

and they also have a slow rate of cell turnover [Lu and Shervington, 2008]. CSCs may also express proteins that would increase their resistance towards chemotherapeutic agents.
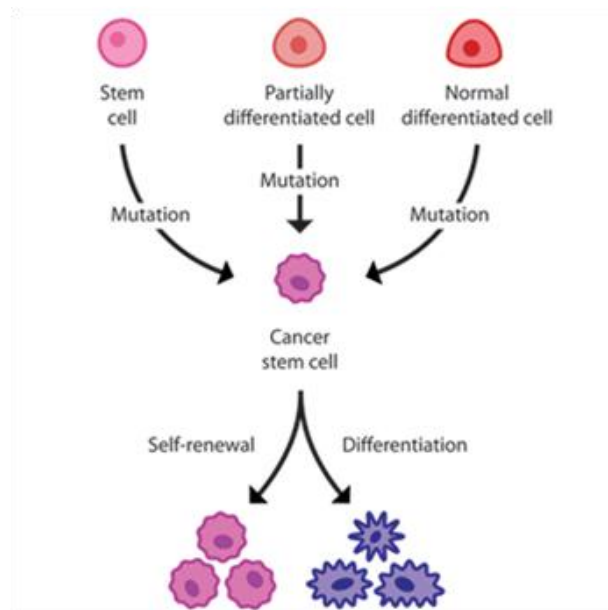
Figure 5. Origins of cancer stem cells. One theory is that a mutation occurs in a normal tissue stem cell, endowing it with cancerous properties and causing it to become a cancer stem cell. Another theory is that the mutation occurs in a normal differentiated cell. There also appear to be cases in which a partially differentiated cell, known as a progenitor cell, can become a cancer stem cell. In any of these scenarios, the cancer stem cell is able to self-renew, creating more cancer stem cells, and to differentiate, creating the various types of cancer cells that make up a tumor (http://www.childrenshospital.org/gallery/index.cfm?G=67).

These surviving CSCs then repopulate the tumor, causing relapse. By selectively targeting CSCs, it would be possible to treat patients with aggressive, non-resectable tumors, as well as preventing the tumor from metastasizing. The hypothesis suggests that upon CSCs elimination, cancer would regress due to differentiation and/or cell death. A number of studies have investigated the possibility of identifying specific markers that may distinguish CSCs.

Several studies have suggested that the fraction of CSCs of the various tumor types could be identified by the expression of the transmembrane glycoprotein CD133. Glioblastoma CD133 positive cells are able to induce tumor formation when injected into the skull of NOD/SCID mice [Singh et al., 2004]. However, it is shown that in 40% of glioblastoma, cells do not express CD133 [Beier et al., 2007] and this suggests the limits of selection of CD133 positive CSCs [Son et al., 2009]. Furthermore, CD133 is also expressed in normal stem cells

and in neuronal, hematopoietic, epithelial and endothelial progenitor cells. This glycoprotein may be useful to enrich the fraction of CSCs, but is requires the identification of other specific markers [Idikio, 2011].

1.3.   INDUCED PLURIPOTENT STEM CELLS (iPSCs)

Induced pluripotent stem cells (iPSCs) are differentiated non-pluripotent stem cell returned to a state of pluripotency through the introduction, in an adult somatic cells, of reprogramming factors, generally transcription factors which regulate gene activity. These cells are similar to natural pluripotent stem cells, in many aspects, such as the expression of stem cell genes and proteins, chromatin methylation patterns, and differentiative ability, but the full extent of their relation to natural pluripotent stem cells is still being assessed (Figure 6).
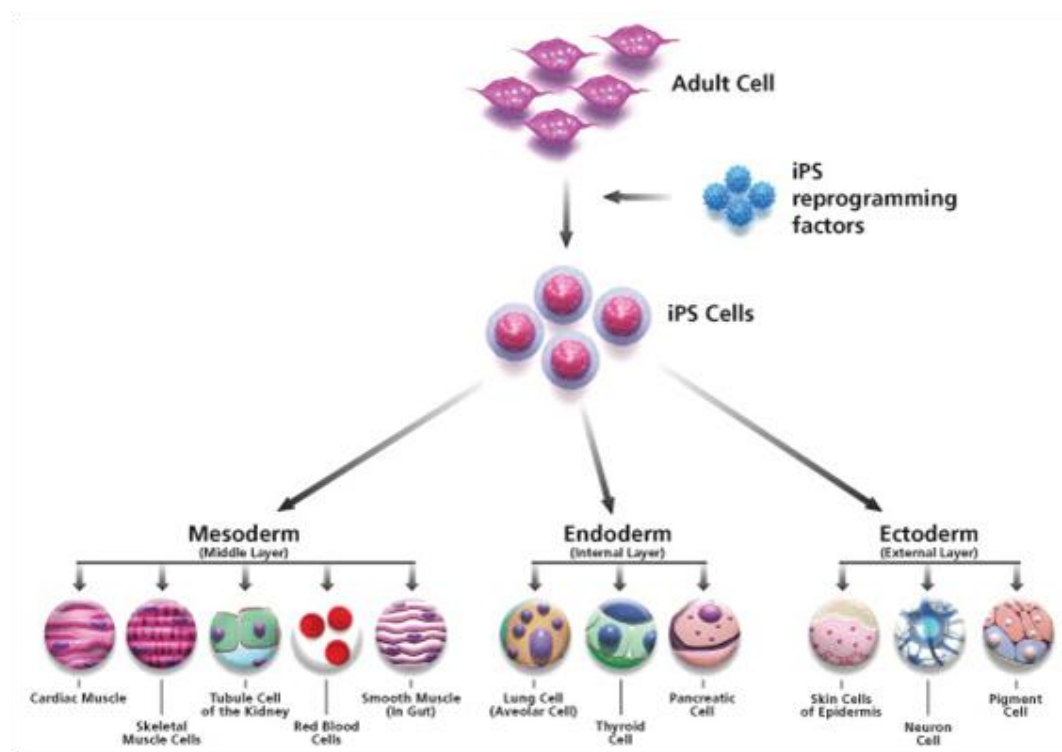
Figure 6. Adult cells are used for the derivation of induced pluripotent stem cells (iPSCs), followed by directed differentiation of these cells into cells that have a crucial role in the disease (http://www.sigmaaldrich.com/life-science/stem-cell-biology/ipsc.html).

The first successful iPSCs, which showed many similarities to embryonic stem cells, were created in 2006 by transducing the factors Oct-4, Sox-2, Klf.4, and c-Myc into mouse

fibroblasts via retroviruses; the same results were achieved a year later using adult human fibroblasts [Takahashi and Yamanaka, 2006] (Figure 7). This has been cited as an important advance in stem cell research and potentially have therapeutic uses, without the controversial use of embryos. Because iPSCs are developed from a patient's own somatic cells, it was believed that treatment of iPSCs would avoid any immunogenic responses.
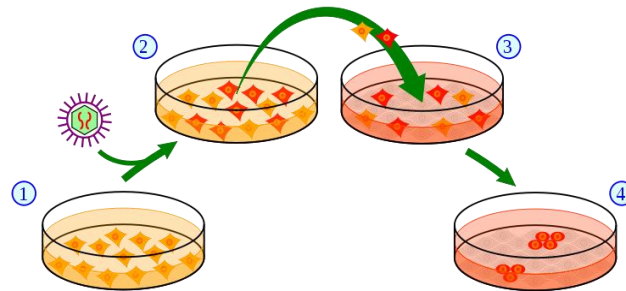
Figure 7. Generation of induced pluripotent stem cells. (1) Isolate and culture donor cells. (2) Transfect stem cell-associated genes into the cells by viral vectors. Red cells indicate the cells expressing the exogenous genes. (3) Harvest and culture the cells according to ES cell culture, using mitotically inactivated feeder cells (lightgray). (4) A small subset of the transfected cells become iPS cells and generate ES-like colonies.

Although the traditional method using transcription factors such as Oct4, Sox2, c-Myc, and Klf4, was good proof of concept that somatic cells can be reprogrammed to iPS cells, there are still many key challenges for this method to overcome: 1. The throughput of successfully reprogrammed cells has been incredibly low (0.01-0.1%) [Takahashi and Yamanaka, 2006]. The low efficiency rate may reflect the need for precise timing, balance, and absolute levels of expression of the reprogramming genes. 2. Genomic integration of the transcription factors limits the utility of the transcription factor approach because of the risk of mutations being inserted into the target cell's genome [Selvaraj et al., 2010]. 3. Some of the reprogramming factors are oncogenes that bring on a potential tumor risk. Inactivation or deletion of the tumor suppressor p53, which is the master regulator of cancer, significantly increases reprogramming efficiency [Marion et al., 2009]. One of the main strategies for avoiding problems (1) and (2) has been to use small compounds that can mimic the effects of transcription factors. These molecule compounds can compensate for a reprogramming factor that does not effectively target the genome or fails at reprogramming for another reason; thus they raise reprogramming efficiency. They also

avoid the problem of genomic integration, which in some cases contributes to tumor genesis. Melton et al. studied the effects of histone deacetylase (HDAC) inhibitor valproic acid. They found that it increased reprogramming efficiency 100-fold (compared to Yamanaka's traditional transcription factor method) [Huangfu et al., 2008]. In 2008, Ding et al. used the inhibition of histone methyl transferase (HMT) with BIX-01294 in combination with the activation of calcium channels in the plasma membrane in order to increase reprogramming efficiency [Shi et al., 2008] (Table 2).

YEAR	GROUP	STRATEGY	CONTRIBUTION
2006	Yamanaka et al.	First to demonstrate	iPS cells were first generated using retroviruses and the four key pluripotency genes; failed to produce viable chimera
2007	Yamanaka et al.	Different Selection method	iPS cells were generated again using retroviruses, but this time produced viable chimera (they used different selection method)
2007	Thomson et al	Vector	iPS cells were generated again using lentiviruses, and again produced viable chimera
2008	Melton et al.	Small Compound Mimicking	Using HDAC inhibitor valproic acid compensates for c-Myc
2008	Ding et al.	Small Compound Mimicking	Inhibit HMT with BIX-01294 mimics the effects of Sox-2, significantly increases reprogramming efficiency
2008	Hochedlinger et al.	Vector	The group used an adenovirus to avoid the danger of creating tumors; however, this led to lower efficiency
2008	Yamanaka et al.	Vector	The group demonstrated reprogramming with no virus (they used a plasmid)
2009	Ding et al.	Proteins	Used recombinant proteins; proteins added to cells via arginine anchors was sufficient to induce pluripotency
2009	Freed et al.	Vector	Adenoviral gene delivery reprogrammed human fibroblast to iPS cells
2009	Bielloch et al.	RNA	Embryonic stem-cell specific microRNA promoted iPS reprogramming
2011	Morrisey et al.	RNA	Demonstrated another method using micro RNA that improved the efficiency of reprogramming to a rate similar to that demonstrated by Ding

Table 2. This timeline summarizes the key strategies and techniques used to develop iPS cells over the past half-decade. Rows of similar colours represents studies that used similar strategies for reprogramming.

Reversine, a synthetic purine originally synthesized by Schultz and Ding [Chen et al., 2004], is also able to increase the plasticity of several terminally differentiated cell lines, such as

fibroblasts and murine C2C12, by inducing their de-differentiation to stem cells and their differentiation into osteoblasts and adipocytes in the presence of suitable stimulations [Anastasia et al., 2006; Chen et al., 2007; Anastasia et al., 2010] (Figure 8).

Another key strategy for avoiding problems such as tumor genesis and low throughput has been to use alternate forms of vectors: adenovirus, plasmids, and protein compounds [Okita et al., 2008; Shi et al., 2008]. Studies by Blelloch et al. in 2009 demonstrated that expression of ES cell-specific microRNA molecules (miR-291, miR-294 and miR-295) enhances the efficiency of induced pluripotency by acting downstream of c-Myc. More recently, Morrisey et al. demonstrated another method using microRNA that improved the efficiency of reprogramming to a rate similar to that demonstrated by Ding [Anokye-Danso et al., 2011].
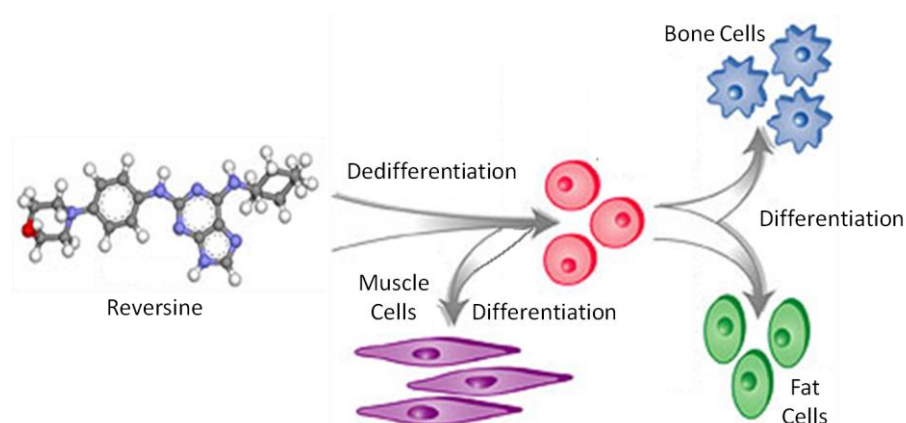
Figure 8. The synthetic chemical Reversine induces dedifferentiation of adult and differentiated cells. In the presence of specific stimuli, iPSCs are able to differentiate into several cell types (http://www.scripps.edu/news/press/122203.html).

It is foreseeable that such experiments will continue to find small compounds that improve efficiency rates. Ultimately, the goal is to discover a cocktail of reprogramming factors and compounds that efficiently and reliably reprogram somatic cells to iPS cells.

CHAPTER 2

2. MSCs AND OSTEOGENIC DIFFERENTIATION

Bone tissue is a specialized form of connective tissue and is the main element of the skeleton with the function of protection and support. It originates from the mesenchyme, it is composed by cells and intercellular substance and fibrillar or amorphous matrix. However, it differs markedly from all the other connective tissues due to the fact that its matrix is highly mineralized. Bone is a hallmark of all vertebrates and absolutely essential in terms of organ protection and support, brain and lung function, locomotion, support of haematopoiesis in the bone marrow, storage of minerals and providing attachment to muscles [Proff and Romer, 2009]. For this reason, it is able to modulate its structure and architecture as a result of mechanical stimuli, highlighting the dynamic properties and plasticity of this tissue (Table 3).

The cells that are found in bone tissue are osteoblasts, osteocytes, lining cells and osteoclasts, all derived from mesenchymal cells. The organic component of the extracellular matrix (ECM) consists of collagen type I fibres (97%), non-collagenous proteins, glycoproteins, proteoglycans, and lipids, important for the elasticity and resistance to fracture. The inorganic phase of ECM is mainly composed of mineral hydroxyapatite [$Ca_{10}(PO_4)_2 \bullet Ca(OH)_2$] (approximately 85%), calcium carbonate (about 10%) and other salts (magnesium phosphate, calcium fluoride), as well as traces of sodium, potassium, manganese and zinc, that are involved in the mechanical properties in term of hardness and resistance to the load.

FUNCTION OF BONE TISSUE	
MECHANICAL	**Protection**: bones can protect internal organs
	Structure: bones provide a frame to keep the body supported
	Movement: bones, skeletal muscles, tendons, ligaments and joints function together to generate movement
SYNTHETIC	**Blood production**: the marrow, located within the medullary cavity of long bones and interstices of cancellous bone, produces blood cells in a process called haematopoiesis
METABOLIC	**Mineral storage**: bones act as reserves of minerals important for the body (calcium and phosphorus)
	Growth factor storage: mineralized bone matrix stores important growth factors such as insulin-like growth factors, transforming growth factor, bone morphogenetic proteins and others
	Fat storage: yellow bone marrow acts as a storage reserve of fatty acids
	Acid-base balance: bone buffers the blood against excessive pH changes by absorbing or releasing alkaline salts
	Detoxification: bone tissues can store heavy metals and other elements, removing them from the blood and reducing their effects on other tissues
	Endocrine organ: bone controls phosphate metabolism by releasing fibroblast growth factor 23 (FGF-23), which acts on kidneys to reduce phosphate resorption. Bone cells also release a hormone called osteocalcin, which contributes to the regulation of blood sugar (glucose) and fat deposition. Osteocalcin increases both the insulin secretion and sensitivity, in addition to boosting the number of insulin-producing cells and reducing stores of fat

Table 3. Main function of bone tissue.

Bone tissue is externally covered by a connective tissue called periosteum, which is absent in the articular cartilage and in proximity of insertion of tendons and ligaments. There are two types of bone tissue: compact or cortical and spongy or trabecular bone (Figure 9). The compact bone tissue presents a complex structure responsible for the stability of the skeleton. Its main unit, the osteon consists of concentric deposition of collagen fibres, which are composed of a central canal (Haversian canal), containing blood vessels and unmyelinated nerve fibres, through which the bone communicates with the surrounding environment. In longitudinal sections are also present other canals (Volkmann canals), that contain connective tissue and vessels.

The spongy bone tissue, is designed to resist to compressive stress, to ensure elasticity and stability of the skeleton and to account for the main part of bone metabolism (about 70%). The compact and spongy bone tissues are made of the same elements, cells and matrix proteins, although they play different structural and metabolic functions [Neumann and Schett, 2007].
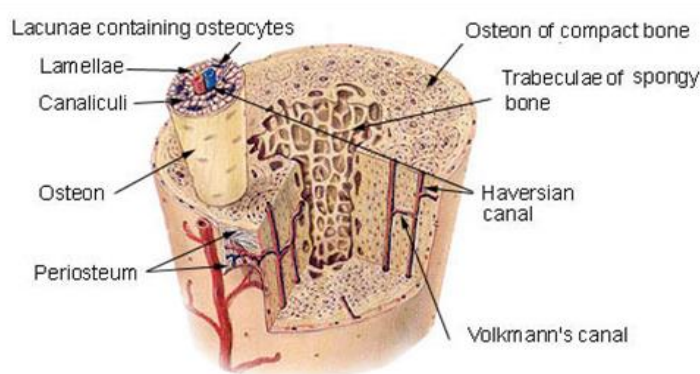
Figure 9. Bone schematic representation
(http://training.seer.cancer.gov/module_anatomy/unit3_2_bone_tissue.html).

The differentiation process of the various cell types of bone tissue represents an important field of research, because the knowledge about the genesis of osteoblasts, osteocytes and osteoclasts is relevant for understanding complex phenomena from a biological, pathological and clinical point of view, such as skeletal and mineral homeostasis and diseases. Under the control of specific growth and transcriptional factors, mesenchymal stem cells differentiate toward osteogenic lineage during a number of developmental stages, starting from commitment to osteo-progenitors, pre-osteoblasts and osteoblasts and finally osteocytes or lining cells. In contrast, osteoclasts derive from the fusion of differentiated mononuclear macrophages (pre-osteoclast). They reach the bone through the blood and in this environment they should establish a population of monocytes [Katagiri and Takahashi, 2002].

2.1. BONE REMODELING

In order to maintain stability and integrity, bone is constantly undergoing remodeling [Lerner, 2006]: during its lifespan, bone tissue is constantly subject to cycles of resorption

and deposition, with the purpose to fill the metabolic and functional requirements of the bone tissues and to adapt the structure of the skeleton to mechanical stress which it is subjected.

Bone remodeling is a complex process that involves bone resorption performed by osteoclasts, followed by bone formation carried out by osteoblasts. In this process, these cells closely collaborate in basic multicellular units (BMU) [Hadjidakis and Androulakis, 2006]. Different cells populations are involved (Figure 10):

Pre-osteoblasts, osteoprogenitor cells derived from mesenchymal cells. These cells can divided during the lifespan of an individual and they can differentiate, in the presence of specific stimuli (parathyroid hormone PTH, growth hormone GH and TGF-β) into mature osteoblast.

Osteoblasts, cells with an intense osteogenic activity involved in the bone formation by synthesizing and secreting all the components of the bone matrix. Osteoblasts are rich of the enzyme alkaline phosphatase, which plays a central role either in the formation of bone mineral matrix, and in the synthesis and secretion of collagen fibres. Generally, osteoblasts are walled in the extracellular matrix deposited by themselves and they become osteocytes or lining cells [Rosen and Spiegelman, 2000; Karsenty and Wagner, 2002].

Osteocytes, cells of mature bone tissue implicated in its preservation and able to induce bone remodeling. They are terminally differentiated cells that develop from osteoblasts and are located in lacunae within the bony matrix [Ehrlich and Lanyon, 2002]. Osteocytes have cytoplasmic processes located in canaliculi important to make contact with the processes from neighbouring osteocytes. Their functions include bone formation, matrix maintenance, and calcium homeostasis. They have also been shown to act as mechano-sensory receptors regulating the bone's response to stress and mechanical load.

Lining cells, temporarily inactive flat cells localized on the surfaces of bone where they exert an exchanging role between blood and interstitial fluid that circulates in the lacunae and in canaliculi [Aubin, 1998].

Osteoclasts, large and multinucleated cells of the bone tissue involved in bone resorption. These cells originate from monocytes and are included in the mononuclear phagocyte system. They secrete the acid phosphatase enzyme which is involved in the erosion of the bony matrix determining the cavity formation known as Howship's lacunae.
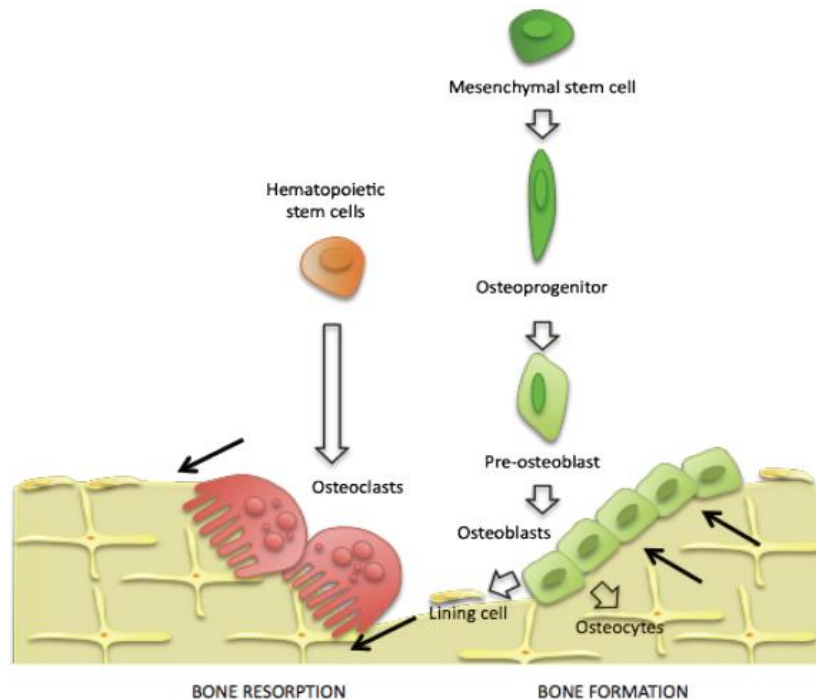
Figure 10. Overview of bone remodeling. During resorption phase osteoclasts degrade old bone matrix; after bone removal, osteoclasts undergo apoptosis and osteoblasts become activated and lay down new bone material in the trench. With the replacement of old bone by new one, the osteoblasts form resting flattened lining cells on the surface of bone, while the embedded in bone matrix one evolve to osteocytes.

2.2. BONE HEALING

The complex series of cellular events that lead to bone healing have been extensively studied in experimental models. Histologically is possible to distinguish an early inflammatory phase characterized by haematoma formation, inflammation and angiogenesis, a reparative phase, characterized by cartilage callus and immature bone tissue formation following by replacement of the callus with lamellar bone, and a late phase of remodeling, by restoring the original shape of the bone.

Inflammation. The interruption of skeletal integrity induces the destruction of bone architecture and it affects also the vascular structure and the supply of nutrients and oxygen to the lesion site. The haematoma represents a source of signaling molecules (growth factors and cytokines) for the recruitment of monocytes-macrophages and osteo-chondroblasts precursors. Macrophages and other recruited inflammatory cells, secrete fibroblast growth factor (FGF), tumor necrosis factor-α (TNF-α), PDGF, TGFβ, insulin-like growth factor I (IGF-I) and a variety of cytokines, including interleukin 1 (IL-1) and IL-6. In

turn, these have a chemotactic effect on inflammatory cells and osteoblasts precursors. During the early stage, the mesenchymal precursors proliferate and differentiate towards osteo-chondrogenic lineages (Figure 11); moreover, new blood vessels are formed from pre-existing vascular structures through a complex chain of events: enzymatic degradation of basement membrane, endothelial cell migration, proliferation, maturation and organization of endothelial cells in capillary tubes. This process is regulated by FGF, vascular endothelial growth factor (VEGF) and angiopoietin 1 and 2.
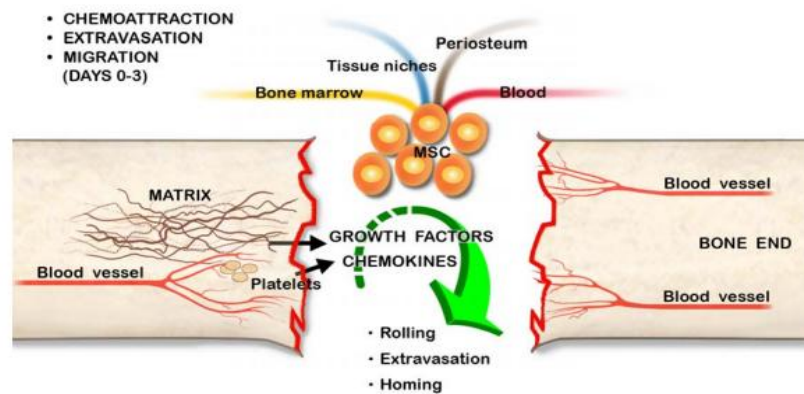
Figure 11. MSCs from blood, periosteum, bone marrow and other tissues, migrate to the site of bone fracture. Growth factors such as TGF-β, FGF, PDGF and IGF-I and the chemokine IL-1, IL-6 and TNF-α, released by ECM and platelets, promote the recruitment, migration, proliferation and the homing of MSCs to the site of the lesion.

Reparing. Intramembranous ossification begins few days after tissue damage, while enchondral ossification, which involves the adjacent tissues of the fracture site, spreads for more than a month. Subperiosteal and soft tissues, immediately surrounding the site of the fracture, formed the "hard callus" and directly create new bone tissue. In this process, mesenchymal precursors recruited to the site of injury, differentiate into osteoblasts and produce compact and trabecular bone, without inducing cartilage formation (Figure 12).
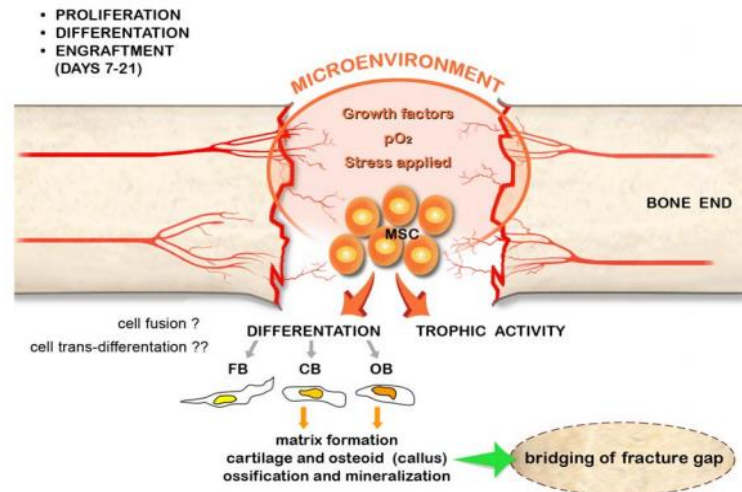
Figure 12. The site of fracture, micro-environmental factors, such as oxygen, mechanical stress and growth factors, induce MSCs differentiation in fibroblasts (FB), chondroblasts (CB) and osteoblasts (OB). These cells synthesize ECM that will undergo to a calcification process and then be converted into bone.

Chondrogenesis leads to the formation of a cartilaginous callus that fills and stabilizes the fracture site. Chondrocytes release calcium into the matrix and deposit collagen type II, type X and aggrecan. Subsequently, the partially mineralized membrane, is resorbed and replaced with collagen type I matrix. Chondrocytes release proteases and phosphatases to prepare the matrix to the next mineralization. After 4-5 weeks, chondroclasts, the multinucleated cells responsible of calcified cartilage degradation, are activated. During cartilage matrix resorption, the chondroclasts release signals that promote perivascular mesenchymal stem cells differentiation into osteoprogenitor cells. Endothelial cells promote vascular invasion, and the removal of residual cartilage structures.

Remodeling. The complete healing of the fracture is obtained during remodeling, in which osteoblasts and osteoclasts cooperate to convert the callus fracture in a bone structure able to bear physiological loads. Angiogenesis has a crucial role in the regulation of bone remodeling and fracture repair. Angiogenic factors such as VEGF and endothelin are regulators of osteoclasts and osteoblasts; moreover, blood vessels formation is important for the transport of osteogenic precursors at the site of bone remodeling. "Bone remodeling compartment" (BRC) consisting of bone lining cells expressing osteotrophic cytokines and growth factors, that regulate bone remodeling without interfering with the growth factors secreted by bone marrow cells.

2.3. MSCs AND MOLECULAR PATHWAYS INVOLVED IN OSTEOGENIC DIFFERENTIATION

The cells committed to the osteoblastic phenotype are called osteo-progenitors. Continuous recruitment, proliferation and differentiation of cells within bone tissue is regulated by the expression of genes providing the characteristics to the bone phenotype. A precise pattern of the expression of genes encoding the osteoblast phenotype has been shown [Heino et al., 2009; Lo Celso et al., 2009], which can be subdivided in three chronologically related distinct stages:

Proliferation phase: high mitotic activity that is accompanied by the expression of cell-cycle genes, including genes that encode for histones and cell growth genes (*c-Myc, c-Fos, and c-Jun*). During this period, genes associated with the formation of ECM, such as collagen type I, osteopontin (OPN) and fibronectin are actively expressed.

Matrix development phase: ECM composition and organization is widely modified, providing a favourable environment for the mineralization and an increase in alkaline phosphatase (ALP) activity.

Mineralization phase: coordinated by the osteoblast activity and by the deposition of calcium phosphate hydroxyapatite.

An overview of these modification is shown in Figure 13.
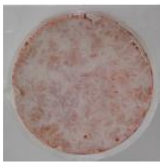
	early osteoblast	Pre-osteoblast	Differentiated osteoblast	Mature osteoblast
Markers	Runx2	Runx2 Col II Col IX	Osteopontin Col II Col IX	Osteopontin BspII
ALP activity	-	+	++	++
Mineralization				

Figure 13. Markers modification during MSCs differentiation through osteoblast lineage.

Osteoblast differentiation, recruitment, function and maturation is promoted and regulated by the secretion of lipid modified glycoproteins of the Wnt family, bone morphogenetic proteins (BMPs) and several transcriptional factors [Proff and Romer, 2009].

Wnt signaling pathway. Wnt proteins are secreted glycoproteins that bind the Frizzled transmembrane receptor (FZD), activating two distinct signal transduction pathways: the canonical and non-canonical Wnt pathway. The first involves the formation of a complex between the Wnt proteins, FZD, and the co-receptor LRP5 or LRP6. In the non-canonical pathways, Wnt binds the FZD receptor and activates heterotrimeric G proteins, inducing an increase of intracellular calcium by protein C-dependent mechanisms.

Wnt proteins regulate growth, differentiation, function and cell death, and have a key role in bone biology. The binding of Wnt proteins with the complex FZD/LRP5/6 induce a signal transduction, that involved Dishevelled, Axin and Frat-1 proteins causing the inhibition of glycogen synthase kinase 3β (GSK3). Thus, β-catenin phosphorylation and subsequent ubiquitin-mediated degradation are inhibited, and β-catenin translocates into the nucleus where it cooperates with factors T-cell transcription factor/lymphoid enhancer factor (TCF/LEF) in the regulation of target genes expression.

Canonical Wnt pathway is involved in bone formation and specific bone markers expression. It is likely that β-catenin activity is required for specific transcription factors activation such as Runx2, that plays a key role in osteogenic and chondrogenic differentiation [Day et al., 2005; Hu et al., 2005].

TGF-β signaling. Several members of the TGF-β superfamily, such as BMPs, have potent osteogenic effects. BMPs transmit signals thought Smad-dependent and Smad-independent pathway, including ERK, JNK and p38/MAPK transduction pathways. The BMPs-Smad pathway activates the expression of Distal-less homeobox 5 (Dlx5), which in turn induces the expression of Runx2 and Osterix (Osx) in osteoprogenitor cells.

Hedgehog (Hh) signaling. The protein Indian hedgehog (Ihh) is produced by hypertrophic chondrocytes and it has a direct effect on osteoblast progenitors. The signaling mediated by Ihh regulates the timing and spatial early osteoblastic commitment.

Notch signaling. Since Notch receptors and their ligands (Delta 1, 3, 4 and Jagged 1, 2) are transmembrane proteins, the signal transduction is activated upon cell-cell interaction. Notch 1 and Notch 2 are expressed into osteoblasts, while Notch 3 and Notch 4 were identified in subgroups of osteogenic lineage. Notch signaling is able to positively

regulate the expression of genes of osteoblastic differentiation, and also to suppress the osteoblasts maturation induced by BMPs, through Runx2 inhibition.

MAPK signaling. The MAPK are serine/threonine kinase proteins involved in cellular regulation. The MAPK pathway is activated by several growth factors, such as FGF, PDGF, IGF, and TGF-β involved into osteogenesis. Extracellular stimuli determine the activation of signal transduction consisting of MAP kinase, MAP kinase kinase (MKK or MAP2K) and MAP kinase kinase kinase (MAP3K or MKKK).

Transcription factors. A central regulator of bone formation is Runx2, also known as *Core-binding factor α1* (Cbf-α1), a member of the Runx (Runt-related factors) family of transcription factors. Runx2 is expressed in mesenchymal stem cells and it is important during the osteogenic differentiation by the activation of genes such as osteonectin, osteopontin and collagen type I [Komori, 2006]; moreover, Runx2 serves as an initial marker of osteogenic cell lineage [Franceschi et al., 2007]. During osteoblast differentiation, Runx2 and canonical Wnt signalling, play essential roles in the commitment of pluripotent mesenchymal cells to the osteoblastic lineage [Komori, 2006]: after commitment into the osteoblastic lineage, the osteoblasts express bone matrix proteins at different levels depending on the maturation grade of the cells.

Immature mesenchymal cells and pre-osteoblasts weakly express collagen type I, and its expression is up-regulated in immature osteoblasts [Inada et al., 1999]. Immature osteoblasts also express osteopontin (Spp1) and sialoproteins (Ibsp); maturate osteoblasts strongly express osteocalcin (bGlap) [Maruyama et al., 2007]. Mature osteoblasts are embedded into the bone matrix and finally become osteocytes, which express dentin matrix protein 1(Dmp1) [Toyosawa et al., 2001] (Figure 14).
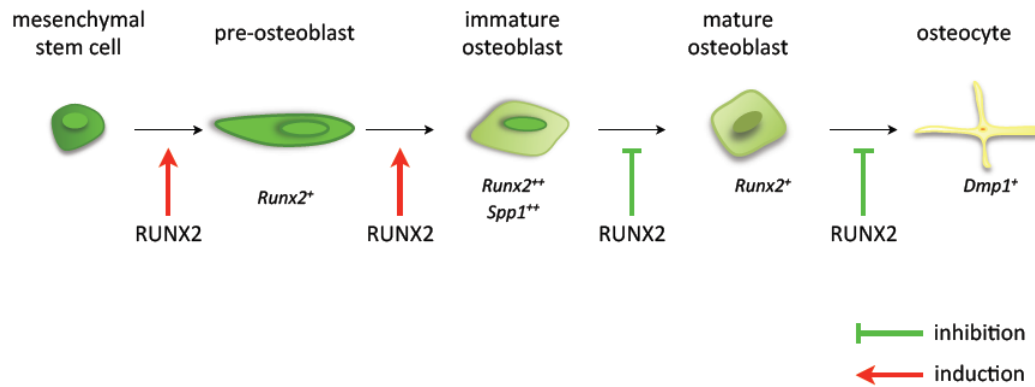
Figure 14. RUNX2 directs pluripotent mesenchymal cells to the osteoblast lineage, increases the number of immature osteoblast, but inhibits osteoblast maturation. Pre-osteoblasts express Runx2. Immature osteoblasts express Runx2 and Spp1. Mature osteoblast Runx2 expression is down-regulated. Osteocytes express Dmp1+. The transition of immature osteoblasts to osteocytes occurs at an early stage of bone development.

Targeted disruption of Runx2 results in the complete lack of bone formation by osteoblasts [Komori, 2008]. Runx2 has been designated as the most pleiotropic regulator of skeletogenesis [Karsenty and Wagner, 2002]; it functions as an inhibitor of proliferation of progenitor cells [Pratap et al., 2003], and it is also required for osteoblast function and differentiation [Ducy et al., 1999; Liu et al., 2001]. Other important transcription factors are Osx, involve into osteoblast differentiation from pre-osteoblast to immature osteoblasts, and Slug, or SNAIL-2, a transcriptional factor that plays a central role in different stages of development [Hemavathy et al., 2000; Nieto, 2002], but also involved in several biological functions, such as cell differentiation, cell motility, cell-cycle regulation, and apoptosis [Barrallo-Gimeno and Nieto, 2005]. Slug is also expressed in most normal adult human tissues, but little is still known about its potential functions. Recently, Lambertini et al have demonstrated that Slug is involved in osteoblast differentiation and maturation: Slug is positively correlated with osteoblast markers, such as Runx2, collagen type I, osteocalcin and osteopontin and Wnt/ β-catenin signaling and it is involved in osteoblast differentiation [Lambertini et al., 2009; Lambertini et al., 2010]. Other transcription factors involved in the process of osteoblastogenesis are ATF4 or CREB2 (*cAMP Response Elements Binding Protein 2*), which through the interaction with Runx2, regulates the transcription of osteocalcin [Xiao et al., 2005]; AP1, an important regulator of bone formation, and PPARγ (*Proliferation-activated Receptor γ*), known transcription factor involved in the differentiation of MSCs: an increased expression of PPARγ induces adipogenic

differentiation and reduces the osteogenic differentiation of MSCs [Lecka-Czernik et al., 1999].

Hormones and growth factors also play an important role in osteoblastogenesis. Estrogens, glucocorticoids, PTH and vitamin D, control bone tissue formation through the regulation of transcription factors in osteoblasts. PTH promotes bone formation through phosphorylation and activation of Runx2 resulting in gene activation [Krishnan et al., 2003]. In addition, PTH increases the expression of Osx and reduces the expression of PPARγ in the progenitor cells [Wang et al., 2006]. Estrogens and glucocorticoids support osteoblastogenesis promoting the differentiation of MSCs towards the osteogenic lineage through the activation of transcription factors such as Runx2 and Wnt/β-catenin pathway [McCarthy et al., 2003; Kousteni et al., 2007]. Growth hormones (GH) can modulate the transcriptional function of Runx2 in osteoblasts [Ziros et al., 2004], while vitamin D up-regulates the expression of Runx2 and simultaneously down-regulates the expression of PPARγ inducing osteoblastogenesis [Duque et al., 2004].

CHAPTER 3

3. TISSUE ENGINEERING AND REGENERATIVE MEDICINE

Diseases, injury and trauma can lead to a damage and the degeneration of tissues in the human body, which requires treatments to ameliorate their repair, replacement or regeneration.

The field of tissue engineering aims to regenerate damaged tissues by developing biological substitutes that may restore, maintain or improve tissue function [Atala, 2007]. The term "tissue engineering" was officially coined at a National Science Foundation workshop in 1988 to mean "the application of principles and methods of engineering and life sciences toward the fundamental understanding of structure-function relationships in normal and pathological mammalian tissues and the development of biological substitutes to restore, maintain or improve tissue function". The field of tissue engineering is highly multidisciplinary and it includes experts from clinical medicine, mechanical engineering, materials science, biology, biotechnology, genetics, and related disciplines from both engineering and life sciences. The field relies extensively on the use of porous 3D scaffolds to provide the appropriate environment for the regeneration of tissues and organs. These scaffolds essentially act as a template for tissue formation and are typically seeded with cells and occasionally growth factors, or subjected to biophysical stimuli by the use of bioreactors. These cell-seeded scaffolds are either cultured *in vitro* to synthesize tissues which can then be implanted into an injured site, or are directly implanted into the injured site, using the body's own systems, where regeneration of tissues or organs is induced *in vivo*. This combination of cells, signals and scaffold is often referred as a tissue engineering triad (Figure 15).
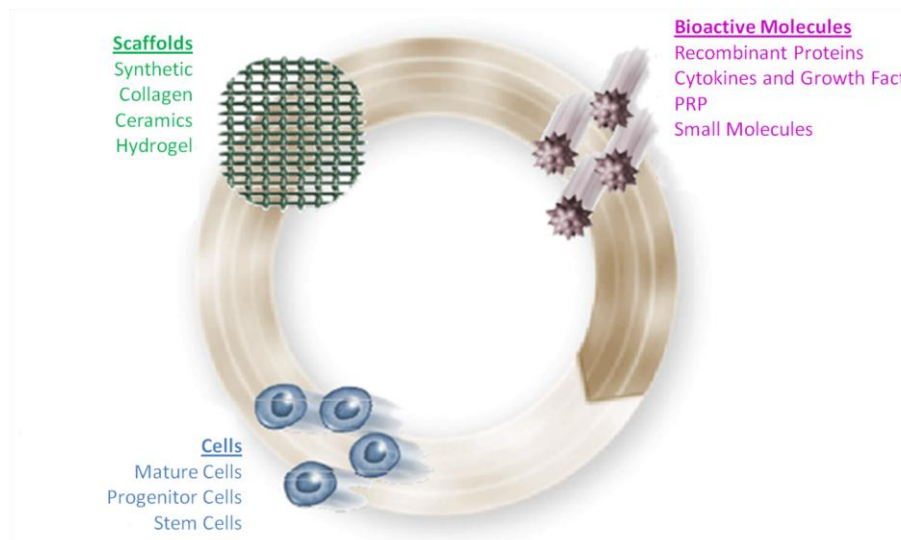
Figure 15. Player in tissue engineering [Boost et al., 2002].

These constructs must have the appropriate characteristics of mechanical function, strength and flexibility; in addition, an appropriate cell source for tissue engineering should be non-immunoreactive (unable to induce rejection and graft-versus-host disease, GvDH), has to possess a controlled proliferation rate and not to be tumorigenic. These populations should be available in large amount, expandable *in vitro* for many generations, possess or be able to acquire a specific protein expression patterns similar to that of the tissue to be regenerated, and finally, have adequate capacity to integrate within the surrounding tissues.

3.1. MSCs AND THERAPEUTIC APPLICATIONS

Mesenchymal stem cells are good candidates for applications in regenerative medicine: there are no limitations to their practical use related to ethical or religious considerations, and techniques of isolation and culture are simple to implement. Moreover, their phenotypic stability, multipotentiality and low immunogenicity give these cells a high therapeutic potential [Gimble, 2003]. The use of MSCs as therapeutic agents for the maintenance, regeneration or repair of damaged tissues, has been proposed in recent decades [Kirouac and Zandstra, 2008]. Stem cells are the basis for cell therapy: they are functionally undifferentiated cells with the ability to differentiate into different cell lineages and self-renewal, representing a potential inexhaustible cell source [Burns and Zon, 2002].

Therapeutic strategies using stem cells have been proposed in various clinical applications including Parkinson's and Alzheimer's disease, spinal cord injury, stroke, burns, arthritis, heart disease, diabetes, osteoarthritis and rheumatoid arthritis (http://stemcells.nih.gov) . Clinical studies show the success of the in situ injection of autologous MSCs in combination with suitable scaffolds for the treatment of critical bone [Lendeckel et al., 2004] and articular cartilage defects. In a recent study on 5 patients, autologous MSCs isolated from bone marrow and *in vitro* expanded were reimplanted in combination with a scaffold of fibrin glue and platelet rich plasma (PRP), in order to promote the repair of articular cartilage defects in the knee. Diagnostic investigations followed a year after treatment, showed an improvement of patients' outcome. Magnetic resonance imaging reveals in 3 of 5 patients a complete filling of the lesion and a complete compliance of the neo-formed cartilage surface [Haleem et al., 2010]. MSCs have also been used in a small number of patients with coronary heart disease. The injected cells were well tolerated and promoted functional recovery of patients. However, these results need to be confirmed by randomized clinical trials with larger numbers of patients [Lee and Makkar, 2004]. In a study it has also been investigated the effect of allogenic transplantation of systemic MSCs in a patient with osteogenesis imperfecta: the results showed the ability of homing of injected cells to the bone and their consequent ability to produce collagen [Kassem et al., 2004].

The therapeutic potential of ASCs was also used in the treatment of chronic ulcers: 20 patients undergoing chemotherapy and with functional impairment, were treated with autologous ASCs administered through a minimally invasive surgical procedure. In all the patients there has been a systematic improvement of the clinical outcome or remission of the symptoms [Rigotti et al., 2007]. In another recent study, a group of diabetic patients suffering of ulcer, were treated by traditional therapy associated with autologous ASCs transplantation, which have been able to promote neovascularisation and an acceleration of the healing process. However, further pre-clinical and clinical studies are required to better understand the therapeutic potential of ASCs and their possible future used in the treatment of diseases for which current medical and surgical therapies might be strongly improved.

3.2. MSCs AND BONE TISSUE REGENERATION

The repair of large bone defect remains a major clinical problem in orthopaedic the case of extensive bone loss due to pathological events such as trauma, inflammation, and tumor [Sarkar et al., 2006]. The biological processes involved in bone regeneration require an osteogenic potential able to provide cells directly into the graft site, osteoinductive factors able to promoting stem cells differentiation into mature osteoblasts, and osteoconductive scaffolds promoting the neovascularisation and cells infiltration [Miyazaki et al., 2009].

Actual therapeutic approaches include autologous or heterologous bone graft transplantation and implants of different bone substitutes. Autologous bone graft is considered a gold-standard for bone regeneration: it possesses a good characteristics of osteoconduction, osteoinduction and osteogenesis, and present a safe solution for the compatibility and absence of immune response. Although the percentage of success is high, complications, or non-unions are also common using bone grafts in the clinical practice. Moreover, the harvesting of autologous bone often results in significant donor site morbidity. Allografts, either from human cadaver or animal, present potential risks of infection, immune response, inadequate supply, difficulties in obtaining and processing tissue, and rapid resorption. In addition, the procedures for preparation and storage (freeze-drying and cryopreservation), performed in order to decrease the immunogenicity of the graft, result in a significant alteration of the osteoinduction and therefore a significant reduction in bone repair capacity [Giannoudis et al., 2005].

As alternative to transplantation is the use of implants made of metallic, polymeric or ceramic materials. These prostheses are not widely used (8% cases) since they have significant disadvantages. The main problem with prosthetic joints lies in their wear and corrosion during long-term use. The debris formed as a consequence of this wear results in tissue inflammation, osteolysis and finally loosening of the implant [Roy and Lee, 2007]. In order to reduce this phenomenon, new techniques of surface treatment and coating deposition have been developed to modify the biomaterials surface [Sharma et al., 2009]. There have been many studies during the last decade regarding innovative techniques to coat orthopaedic materials in order to obtain a hard and inert material to give an adequate protection to the implant and to decrease the wear rate of prosthetic devices.

Nowadays, for the treatment of bone diseases a valid alternative approach is the use of autologous cells able, alone or in combination with osteoconductive scaffold, to enhance the regeneration process of bone defect. Molecules or factors able to induce cell proliferation can be chemically conjugated to the material and can be released in the tissues at a controlled rate, by diffusion or fragmentation. These bioactive materials are able to induce locally a growth factors release, which in turn stimulates the cells involved in tissue regeneration.

Several types of approach are of particular interest in improving bone repair (Figure 16).
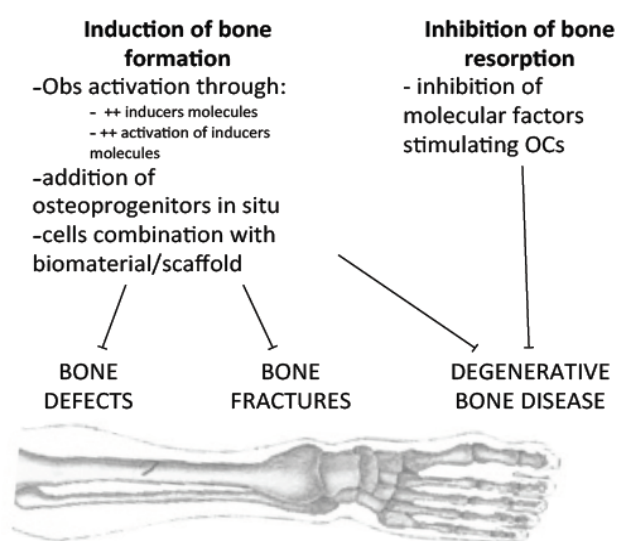
Figure 16. Different strategies can be used and combined to treat disease that weaken bones. Bone formation can be activated by (i) enhancing osteoblast (Obs) activation (ii) suppressing the activity of osteoclasts (Ocs) (iii) adding growth factors and hormones (inducers molecules). Osteoprogenitors cells (like MSCs) within bone defects can be added with or without the use of biomaterials (synthetic biomaterials, demineralized bone) (modified by [Deschaseaux et al., 2009]).

Scaffolds, cells and factors are the basic tools of tissue engineering and are distinguished according to their use of cell-free systems, cellular systems and factor-based therapies.

In cell-free systems, the chemistry and the structure of the scaffolds play a dominant role for the correct repair. With regard to skeletal tissue, bone substitutes should posses pores and interconnections and also be biodegradable in parallel to the *in situ* bone regeneration, without generate toxic products or induce a decrement of pH.

In a cell systems or cell-based therapies, are necessary stages from collection of cells from the donor site, their seeding on suitable scaffolds, their induction to proliferate and differentiate and finally the cells-scaffold constructs transplantation. In order to obtain an

effective and stable bone repair is necessary to isolate an adequate number of cells and maintain their correct phenotype. The cells should be organized within the three-dimensional structure of the scaffold and produce extracellular matrix, in order to achieve full integration with the local host tissue.

The factor-based therapies consist in the introduction in a cell-scaffold system of osteoinductive stimulus. BMPs, by binding to specific receptors on the surface of osteoprogenitor cells, activate signal transduction cascades, stimulating MSCs to differentiate into mature osteoblasts. In a prospective pilot study, BMP-2 has been applied in a specific device of collagen sponge in an anterior lumbar fusion. In this study, were found a total absence of adverse effects and 100% of fusion [Baskin et al., 2003]. A recent prospective randomized study has compared autologous bone graft with the administration of rhBMP-2 linked to a collagen, tricalcium phosphate and hydroxyapatite support, in the treatment of postero-lateral fusion. The results showed an increase in the rate of fusion for the group treated with rhBMP-2 [Dimar et al., 2006]. In many studies of bone regeneration have been used the centrifuged platelet-rich plasma (PRP), characterized by high levels of growth factors (PDGF and TGF-β) that promote chemotaxis and proliferation of MSCs: the combination of MSCs and PRP, significantly increases the osteogenesis of mandibular distraction [Hwang and Choi, 2010]. A more recent study conducted on 20 patients, has evaluated the efficacy of the combination of β-tricalcium phosphate and PRP in the treatment of periodontal defects, showing an improvement of the process of bone healing [Saini et al., 2011]. Moreover, autologous MSCs isolated from adipose tissue have been also used to promote bone regeneration in a 7 years paediatric patient suffering from a severe craniofacial injury. Autologous bone graft remains the gold-standard for the treatment of bone regeneration in craniofacial surgery, but this technique is difficult to implement in paediatric patients due to the limited amount of available autologous bone from the iliac crest. In this study, ASCs were isolated and immediately reimplanted in bone defects in combination with autologous fibrin glue and bone micro-fragment. The post-operative course did not present complications, and 3 months after the results demonstrated the complete bone regeneration at the defects areas [Lendeckel et al., 2004].

3.3. BIOMATERIALS

Several scaffolds produced from a variety of biomaterials have been used in attempts to regenerate different tissues and organs in the body. Regardless of the tissue type, a number of key considerations are important when designing or testing the suitability of a scaffold for their use in tissue engineering.

Biocompatibility. Cells must adhere, function, and migrate onto the surface and eventually through the scaffold and begin to proliferate before laying down new matrix. After implantation, the scaffold or tissue engineered construct must elicit a negligible immune reaction in order to prevent severe inflammatory response that might reduce healing or cause rejection by the body.

Biodegradability. Scaffolds and constructs, are not intended as permanent implants. The scaffold must therefore be biodegradable so it could allow cells to produce extracellular matrix. The products of degradation should also be non-toxic and able to be eliminated by the body without interfering with other organs. In order to allow degradation to occur in tandem with tissue formation, an inflammatory response combined with cells such as macrophages is required [Brown et al., 2009; Lyons et al., 2010].

Mechanical properties. Ideally, the scaffold should posses mechanical properties consistent with the anatomical site into which has to be implanted and, from a practical perspective, it must be stiff enough to allow surgical handling during implantation. While this is important in all tissues, it provides some challenges for cardiovascular and orthopaedic applications. Production of scaffolds with adequate mechanical properties is one of the great challenge in bone and cartilage repair. In these cases, the implanted scaffold should have sufficient mechanical integrity to function from the time of implantation to the completion of the remodeling process. A further challenge is the fact that the healing rates vary with age; for example, in young individuals, fractures normally heal to the point of weight-bearing in about six weeks, with complete mechanical integrity approximately at one year after fracture, but in elderly patients the rate of repair slows down. This should be considered when producing scaffolds for orthopaedic applications. However, as the field has evolved, many efforts have been placed on trying to develop scaffolds with mechanical properties similar to bone and cartilage. It is clear that a balance

between mechanical properties and porous architecture, sufficient to allow cellular infiltration and vascularisation, is the key to the success of any scaffold.

Scaffold architecture. The architecture of scaffolds used for tissue engineering is of critical importance. Scaffolds should have interconnected pores and high porosity to ensure cellular infiltration and adequate diffusion of nutrients to cells within the construct, and allow the diffusion of waste products out of the scaffold [Ko et al., 2007; Phelps and Garcia, 2009]. Another key component is the mean pore size of the scaffold. The pores thus need to be large enough to allow cells to migrate into the structure, but small enough to establish a sufficiently high specific surface, leading to a minimal ligands density to allow efficient binding of a critical number of cells to the scaffold [O'Brien et al., 2005]. Therefore, it exists a critical range of pore sizes [Murphy et al., 2010; Murphy and O'Brien, 2010] which may vary depending on the cell type used and the tissue to be engineered.

Manufacturing technology. The development of manufacturing processes to good manufacturing practice (GMP) is critically important in ensuring successful translation of tissue engineering strategies to the clinic [Hollister, 2009].

In the first Consensus Conference of the European Society for Biomaterials (ESB) in 1976, a biomaterial was defined as "a nonviable material used in a medical device, intended to interact with biological systems"; however, the ESB's current definition is a "material intended to interface with biological systems to evaluate, treat, augment or replace any tissue, organ or function of the body". This subtle change in definition is indicative of how the field of biomaterials has evolved. Biomaterials have moved from merely interacting with the body to influencing biological processes toward the goal of tissue regeneration.

Typically, three groups of biomaterials, ceramics, synthetic polymers and natural polymers, are used in the production of scaffolds for tissue engineering. Each of these groups have specific advantages and disadvantages, so the use of composite scaffolds made out of different phases is becoming increasingly common. Ceramic scaffolds, such as hydroxyapatite (HA) and tricalcium phosphate (TCP), have been widespread use in bone regeneration applications. These scaffolds are typically characterized by high mechanical stiffness, very low elasticity, and an hard brittle surface. They exhibit excellent biocompatibility due to their chemical and structural similarity to the mineral phase of native bone. The interactions of osteogenic cells with ceramics are important for bone regeneration [Ambrosio et al., 2001]. Various ceramics have been used in dental and

orthopaedic surgery to fill bone defects and to coat metallic implant surfaces to improve their integration with the host bone. However, their clinical applications for tissue engineering has been limited because of their brittleness, difficulty of shaping for implantation and new bone formed in a porous HA network cannot sustain the mechanical loading needed for remodeling [Wang, 2003]. In addition, although HA is a primary constituent of bone and might seem ideal as a bone graft substitute, some problems exist to control its degradation rate. Numerous synthetic polymers have been used to produce scaffolds including polystyrene, poly-l-lactic acid (PLLA), polyglycolic acid (PGA) and poly-dl-lactic-co-glycolic acid (PLGA). These materials can be produced with a specific architecture, and their degradation characteristics, controlled by modifying the polymer itself or the composition of each polymer [Lu et al., 2000; Rowlands et al., 2007]; however, they have also drawbacks including the risk of rejection due to reduced bioactivity. In addition, the degradation process of PLLA and PGA by hydrolysis, produce carbon dioxide that induces a local decrease of the pH resulting tissues necrosis [Liu et al., 2006]. Biological materials such as collagen, proteoglycans, alginate-based substrates and chitosan have all been used for the production of scaffolds. Unlike synthetic polymer-based scaffolds, natural polymers are biologically active and able to promote cell adhesion and growth. Furthermore, they are also biodegradable and so they allow host cells to produce extracellular matrix and replace the degraded scaffold. However, these scaffolds generally have poor mechanical properties, which limits their use in load-bearing orthopaedic applications. A number of groups have attempted to introduce ceramics into polymer-based scaffolds, while others have combined synthetic polymers with natural polymers in order to enhance their biological ability [Damadzadeh et al., 2010]. Moreover, metallic materials are also particularly suitable for the replacement of hard tissues such as bones and teeth and for the production of structures able to support loads without the risk of large elastic deformations. Biocompatibility is linked to the corrosive power of biological fluids on them; the corrosion may cause the release of metal ions *in situ* and their accumulation in other body districts. The metals used as biomaterials for the manufacture of prostheses are iron, cobalt, nickel, titanium, and tungsten. In particular, due to the characteristics of biocompatibility, corrosion resistance and excellent mechanical properties of titanium and titanium alloys, is suggested the use of these biomaterials in oral surgery, maxillofacial and orthopaedic surgery.

CHAPTER 4

4. MSCs AND CULTURE SYSTEMS

The main drawback in MSCs transplantation is sometimes the low number of MSCs. Since the biology of MSCs and their microenvironment are not totally understood, it is not easy to overcome this issue. *Ex vivo* expansion of MSCs became an alternative approach to increase the cell-dose available for transplants and to further understand MSCs [Zhai et al., 2004]. The differentiation of MSCs has been also extensively studied, using mainly well-established *in vitro* assays with culture-expanded MSCs. The data obtained *in vitro* are dependent on culture conditions for isolation and expansion of MSC populations, which unlikely correspond to the native cells which interact physically with the surrounding environment. The first line of interaction for MSCs is with the extracellular environment, be it plastic, a resorbable bio-scaffold, or a more rigid structure [Augello and De Bari, 2010]. Evidence of how the extracellular matrix can control stem cell fate, inducing seeded MSCs toward osteogenesis or chondrogenesis was reported [Engler et al., 2006]: these findings open up unexpected avenues for the regulation of MSC differentiation in regenerative medicine using physical factors, avoiding or combining these conditions with exogenous growth factors (Figure 17).

MSCs

Digestion
- Trypsin
- Collagenase

Ex-vivo
Expansion

Different culture conditions
- FBS
- Inductors

Different Devices
Physical and chemical modifications

Osteogenic Differentiation

Static Culture
- Nanotecnologies
- Biomolecules

Dynamic Culture
- Microgravity
- Bioreactor
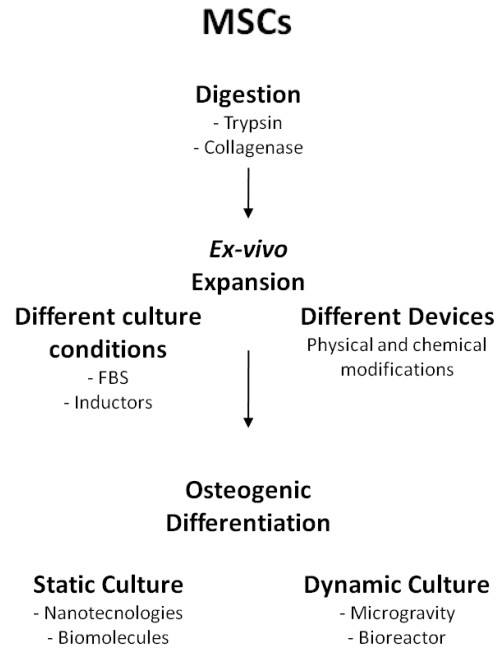
Figure 17. Modulation of cells phenotype could be reached at different levels through many different approaches, involving cell physical and biochemical environment modifications.

This knowledge leads to a new approach by researchers: to investigate all the possible conditions *in vitro* that can simulate or mimic the *in vivo* ones.

4.1. STATIC CULTURE

Static culture systems, such as polystyrene Petri dishes, multiwells, or flasks, have been the most widely used culture devices. MSCs are conventionally cultured in these containers, and put into a biological incubator, where two physical parameters are regulated: temperature and pH. Temperature is usually set at 37°C, whereas pH control is performed by maintaining an atmosphere at 5% CO_2 concentration, which corresponds to the physiological pH of 7.2. The main sources of variability among different culture protocols reside in medium composition, cell seeding density, and time intervals between cell dilutions, called cell passages, and medium changes. Conventional cultivation methods need of both optimized protocols and ad hoc technology [Cabrita et al., 2003].

Most investigators have used Dulbecco Modified Essential Media (DMEM) supplemented with animal or human serum and combinations of cytokines. Alternatively, serum-free and animal product-free media have been developed to avoid immunological issues affecting

transplantation [Andrade-Zaldivar et al., 2008]. Different cytokine cocktails aim the proliferation of undifferentiated MSCs and the maintenance of their engraftment capacity. The optimal combination and concentration of growth factors to preserve the stem state has not been yet established.

In normal conditions, after damage, bone formation begins when mesenchymal cells begin to respond to specific growth factors. Growth factors (GFs) are cytokines secreted by many cell types, which act as signaling molecules and that are essential for tissue formation. These proteins have pleiotropic effects: they play an important role in tissue engineering, since the link between growth factor and its receptor initiates a cascade of events such as the promotion or inhibition of cell adhesion, proliferation, migration and differentiation via up-regulation or down-regulation of specific proteins synthesis.

Like other tissues, bone responds to bone-specific soluble growth factors (Table 4).

TGF-β is able to affect cell growth and differentiation during the developmental processes such as embryogenesis and tissue repair, in particular modulating the expression of Runx2 and down-regulating the expression of PPARγ [Ahdjoudj et al., 2002]. In addition, several molecules belonging to the BMPs family, have been cloned and their involvement in the osteogenic differentiation was shown [Hay et al., 2004].

Additional growth factors also regulate bone development, and their role in MSCs differentiation is being investigated [Foster and Somerman, 2005].

FGF-2 or b-FGF (basic Fibroblast Growth Factor 2) is a growth factor involved in the proliferation of endothelial cells, in the process of bone remodeling, in the regulation and in the maintaining of the balance between bone formation and resorption [Kim et al., 2003]. Moreover, it also promotes angiogenesis, such as VEGF (Vascular Endothelial Growth Factor) and PDGF (platelet-derived growth factor), and has a role in the stimulation of osteogenic phenotype through the activation of the transcription complex Cbaf-1/Runx2

IGF-1 (Insulin Growth Factor 1 or somatomedin C) is an hormone with a quaternary structure very similar to that of insulin. It is produced mainly in the liver as an endocrine hormone, but also in its target tissues with paracrine/autocrine effect. IGF-1 is one of the most potent natural activators of the expression of Osterix, stimulating cell proliferation and inhibiting pro-apoptotic processes [Celil and Campbell, 2005]. Both IGF-1 and IGF-2 (or somatomedin A) seem to have a similar effect on bone metabolism. They are always found in the site of bone fracture: in fact, is known their role in the stimulation of collagen type I

synthesis, with an increase of bone matrix deposition. Moreover, PDGF, produced by osteoblasts, platelets and monocytes/macrophages, has also an important role in osteoblast progenitors migration toward the injury site.

The biological actions of growth factors are different, and have an important role in tissue regeneration, cell differentiation, embryonic development and regulation of the immune system. In particular, GFs regulate mesenchymal stem cells proliferation and the mitogenesis of fibroblasts, osteoblasts and endothelial cells, and they monitor the effects of other mitogenic growth factors [Everts et al., 2002].

BMPs are a group of growth factors well known for its ability to induce cartilage and bone tissue formation. They interact with specific receptors (Bone Morphogenetic Receptors, BMPRs,) and their activation induces signal transduction and activation of transcription factors, such as Cbfa-1, able of induce phenotype-specific genes pushing the cell to a complete differentiation. In addition, the BMPs, in association with their inhibitors, play a critical role in fetal development of specific organs like heart, central nervous system and cartilage, and, in the post-natal development, of bones.

The mechanism of action through which they act on MSCs has not yet been elucidated, but it is known, for example, that the BMP-2 plays a key role in the expression of some osteogenic markers, including alkaline phosphatase (ALP) and osteocalcin (OC). At the same time, BMP-2, together with BMP-7, is also involved in the expression of Cbaf-1/Runx2, the transcription factor responsible of the osteogenic differentiation and of the expression of osteocalcin and osteopontin. VEGF could also be potentially useful in bone tissue engineering due to its angiogenetic activity.

Due to the side effects of uncontrolled release of these factors in some culture conditions, like in static conditions, many researchers have studied appropriate delivery systems in form of nanoparticles, microspheres, and scaffolds. Although their design and composition are unique for each other, they share the same goal: how to deliver factors to the target and to meet their temporal and spatial need [Bae et al., 2010; Roger et al., 2010].

Among these candidates, biodegradable polymeric microspheres (PMs) have been widely utilized as a favourable vehicle in delivering various cytokines and proteins. The encapsulation of various drugs, bioactive proteins, or other molecules within degradable polymers has long been recognized an effective way to control the release profile of the retained substances [Bae et al., 2010]. Many efforts have been done to identify new drug

delivery systems able to enhance drug permeation and to control drug delivery release rate. In this context striking advantages can be given by nanotechnology [Civiale et al., 2009]. Pharmaceutical nanotechnologies including nanosuspensions, solid lipid nanoparticles, liposomes and polymeric micelles can allow to overcome some of the inconveniences of conventional drug delivery and sometimes improve water solubility of poorly soluble drugs and their chemical stability [Kayser et al., 2005].

GROWTH FACTOR	SOURCE	FUNCTION	ACTION ON BONE TISSUE
Bone Morphogenetic Proteins (BMPs)	Osteoprogenitor cell, osteoblast, chondrocyte, endothelial cells	Osteochondrogenesis, BMP2-7 and BMP9 are osteoinductive	Induction of chemotaxis, proliferation, differentiation and ECM synthesis; Angiogenesis
Transforming Growth Factor β (TGF-β)	Platelet, stromal cell, chondrocyte, endothelial cells, fibroblast	Immunosuppressor, pro-angiogenesis, cellular growth, differentiation and ECM synthesis	Induction of proliferation of undifferentiated MSCs, recruitment of osteoblast precursor, induction of osteogenic differentiation, ECM production
Fibroblast Growth Factor (FGF)	Macrophage, monocyte, stromal cell, chondrocyte, osteoblast, endothelial cell	Pro-angiogenesis	FGF-1 induce chondrocyte maturation; FGF-2 induce osteoblast proliferation and differentiation, inhibits apoptosis of immature osteoblast and stimulate apoptosis of osteocyte
Platelet-derived Growth Factor (PDGF)	Platelet, osteoblast, endothelial cell, monocytes, macrophage	Mitogen for connective tissue cells, chemotactic for monocytes, macrophages and smooth muscle cells, pro-angiogenesis	Induce osteo-progenitors proliferation and differentiation
Vascular Endothelial Growth Factor (VEGF)	Endothelial cell, osteoblast, platelet	Pro-angiogenesis, chemotactic for endothelial cells	Conversion from cartilage to bone tissue, osteoblast proliferation and differentiation, RANK induction in osteoclast precursor
Insulin-like Growth Factor (IGF)	Osteoblast, chondrocyte, hepatocyte, endothelial cell	Biological regulation of growth hormone	Induce osteoblast proliferation and ECM synthesis; bone resorption

Table 4. Growth factors and their role in bone repair.

Natural polymers, such as pectin and gelatin, can be used to produce biocompatible and biodegradable microparticles, obviating the toxicity or biodegradability problems (i.e., formation of localized granulomatous inflammation) related to the use of synthetic materials [Esposito et al., 2001]; [Civiale et al., 2009]. Alginate microspheres have been used for the encapsulation of a wide variety of biologically active agents, including proteins, antibodies, DNA and eventually cells [Capretto et al., 2010]. Recently, the production of alginate microbeads was also accomplished by microfluidic procedures [Choi et al., 2007].

All these strategies try to obtain controlled and predictable factors delivery, targeting sites or cells in a temporal and spatial optimized condition. However, in static conditions, the problem of the limited interactions of cells with the extracellular matrix or environment is not overcame yet.

4.2. DYNAMIC CULTURE

Despite static cultures have shown expansion of MSCs, the scaling-up represents a major problem because more volume means less oxygen flow and less nutrient availability in the system. Several dynamic models that incorporate gas flow have been used to overcome this problem [Andrade-Zaldivar et al., 2008]. Several bioreactors with specific characteristics have been designed for MSCs expansion since the 1990s. In addition, the latest designs have served as well to study the MSCs biology. Differences between tissues suggest that reactor design considerations and operating conditions can be different when dealing with a specific tissue. However, every type of tissue beneficiates from controlled shear stresses and optimal nutrient availability and wastes elimination [Martin and Vermette, 2005].

The term "bioreactor" has been frequently used. Bioreactors can be defined as devices in which biological and/or biochemical processes develop under closely monitored and tightly controlled environmental and operating conditions (ie. pH, temperature, pressure, nutrient supply, and waste removal). Different bioreactor systems matching this definition are currently being used in a wide range of biotechnological applications including industrial fermentation processing, wastewater treatment, food processing, and manufacturing of biopharmaceuticals. However, many systems encountered in the tissue-engineering

literature are composed of vessels of few millilitres, which, under many aspects, do not fit in the presented definition of a bioreactor [Martin and Vermette, 2005].

Dynamic bioreactor culture systems are essential for the *in vitro* cultivation and maturation of bone tissue engineering grafts, especially for larger grafts where the core of the scaffold is more than 200 mm from the surface [Chen and Hu, 2006]. Bioreactors improve the mass transport of nutrients and allow the diffusion limitation of traditional static culture, which is generally taken to be around 200 mm, to be overcome. In addition, the dynamic media flow applies a mechanical stimulus to the cells, enhancing cellular osteogenesis and mineralization through triggering of mechano-transduction signalling pathways [Gomes et al., 2003]. Currently, several types of bioreactors have been developed for bone tissue engineering applications, providing truly microgravity environment (Figure 18).
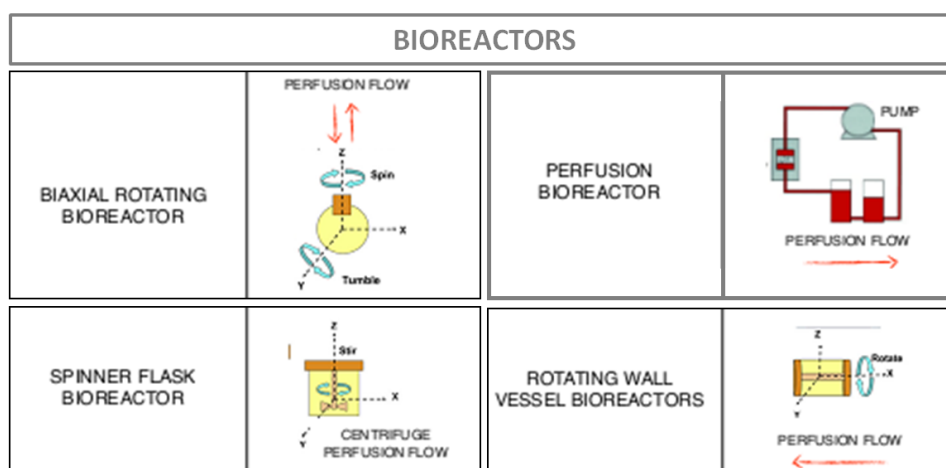

Figure 18. Designs of bioreactor systems.

CHAPTER 5

5. ANIMAL MODELS IN ORTHOPAEDIC RESEARCH

The development and modification of orthopaedic and dental implants has taken place for many years in an effort to create an optimal interaction between the body and the implanted material. The goal of achieving an optimal bone-implant interface has been approached by the alteration of implant surface topography, chemistry, energy and charge as well as bulk material composition. Schmidt et al. [Schmidt et al., 2001] defines an ideal bone implant material as having a biocompatible chemical composition to avoid adverse tissue reaction, excellent corrosion resistance in the physiologic environment, acceptable strength, a high resistance to wear and with a modulus of elasticity similar to that of bone to minimise bone resorption around the implant. The features relating to implant safety, such as avoidance of adverse tissue reaction and resistance to wear and corrosion are of high clinical significance for implants used in long-term clinical situations in both human and veterinary medicine, as there have been some links between prolonged exposure to non-biocompatible materials and neoplastic tissue responses. In order to determine whether a new material conforms to the requirements of biocompatibility and mechanical stability prior to clinical use, it must undergo rigorous testing under both initial *in vitro* and then *in vivo* conditions. *In vitro* testing is popular for the characterisation of bone-contacting materials, particularly as medical researchers embrace the principles of animal reduction. It is accepted that *in vitro* experiments must be used primarily as a first stage test for acute toxicity and cytocompatibility to avoid the unnecessary use of animals in testing cytologically inappropriate materials. These tests give information regarding cytotoxicity, genotoxicity, cell proliferation and differentiation [Hanks et al., 1996] and it is more easily standardised and quantifiable than *in vivo* testing. *In vitro* studies are also useful for screening new materials for product quality and the release of potentially harmful additives incorporated during the manufacturing process [Pizzoferrato et al., 1994].

However, *in vitro* characterisation is not able to demonstrate the tissue response to materials, instead being confined to the response of individual cell lines or primary cells

taken from animals. Moreover, no *in vitro* cell culture system is able to produce loading that simulates the *in vivo* situation and currently very few *ex vivo* systems are able to approach such physiological loading [Davies et al., 2006]. For these reasons animal models are essential for evaluating biocompatibility, tissue response and mechanical function of an orthopaedic material prior to clinical use in humans. Animal models allow the evaluation of materials in loading or unloading conditions over potentially long time durations and in different tissue qualities (i.e. normal healthy or osteopenic bone) and ages. While animal models may closely represent the mechanical and physiological human clinical situation, it must be remembered that it is only an approximation, with each animal model having unique advantages and disadvantages. Currently there are numerous models for testing implant materials *in vivo*, ranging in purpose from the assessment of protein adsorption and soft tissue adherence to the integration of bone and the dissemination of implant wear particles. For testing orthopaedic implants, it is necessary to use a model which is reproducible and in which implant dimensions are comparable to those used in humans. The number and size of implants to be tested will influence directly the species of animal chosen for a study and, regardless of the design, implants should have an appropriate size for the species chosen and for the bone implantation site. Guidelines are provided for the dimensions of implants for *in vivo* studies, based on the size of animal and bone chosen and on the implant design, in order to avoid pathological fracture of the test site. Moreover, these implants should be of a material already used in clinic (International Standard ISO 10993-6, 1994) and should allow outcome data to be related to existing products. Kirkpatrick et al. outlines three types of studies which yield data on factors influencing the biological response to materials implanted in bone [Kirkpatrick et al., 2002]. These are studies on explanted biomaterials, *in vitro* techniques and animal models. Desirable attributes of an animal model include demonstration of similarities with humans, both in terms of physiological and pathological considerations as well as being able to observe numerous subjects over a relatively short time frame [Liebschner, 2004; Egermann et al., 2005]. When deciding on the species of animal for a particular model there are several factors that should be considered: cost to acquire and care for animals, availability, acceptability to society, tolerance to captivity and ease of housing. Other factors include low maintenance care, ease of handling, resistance to infection and disease, inter-animal uniformity, biological characteristics analogous to humans, tolerance to surgery, adequate

facilities and support staff and an existing database of biological information for the species. In addition to this, the lifespan of the species chosen should be suitable for the duration of the study. More specifically, for studies investigating bone-implant interactions, an understanding of the species specific bone characteristics, such as bone microstructure and composition, as well as bone modelling and remodeling properties, are important when later extrapolating the results to the human situation. Finally the size of the animal must be considered to ensure that it is appropriate for the number and size of implants chosen [Schimandle and Boden, 1994].

The **rodent** are one of the most commonly used species in medical research and orthopaedic field (38% of preclinical studies) [O'Loughlin et al., 2008]. These animal models are the most commonly used for their low cost and easy handling. For their anatomy, they may be more easily subjected to surgery and biomechanical analysis. Several studies of biocompatibility involve them [Hoemann et al., 2005]. However, rodents have also been used in a limited number of studies of articular defects [Dausse et al., 2003] and in the field of bone tissue engineering: both mice that rats are often used to evaluate the bone healing process of the skull [Aalami et al., 2004]. In addition, both species can be manipulated to generate pathological situations that mimic the process of bone degeneration typical of human, such as osteoporosis.

The **rabbit** is one of the most commonly used animals for medical research, being used in approximately 35% of musculoskeletal research studies [O'Loughlin et al., 2008]. This is in part due to ease of handling and size. The rabbit is also convenient since it reaches skeletal maturity shortly after complete sexual development at around 6 months of age [Gilsanz et al., 1988]. A drawback with the rabbit used for the assessment of multiple implant materials is its size limitation. Despite this, the rabbit remains a very popular choice for testing of implanted materials in bone. Clearly there are gross differences in the bone anatomy between the rabbit and human both in size and shape of the bones and also in loading due to the differences in stance between the two species. While there is minimal literature on the differences between human and rabbit bone composition and density, some similarities are reported in the bone mineral density (BMD) [Wang et al., 1998]. Moreover, in comparison to other species, such as primates and some rodents, the rabbit has faster skeletal change and bone turnover [Castaneda et al., 2006]. This may make it difficult to extrapolate results from studies performed in rabbits onto the likely human

clinical response. However, rabbits are commonly used for screening implant materials prior to testing in a larger animal model.

The **dog** is one of the most frequently used large animal species for musculoskeletal and dental research. Unlike other animal species, there is a considerable amount of literature comparing canine and human bone with regard to the usefulness of the dog as a model for human orthopaedic conditions. The highly tractable nature of dogs can be beneficial during the post-operative healing phase where they may be trained to take an active part in recuperative protocols. However, there are increasing ethical issues relating to the use of dogs in medical research due to their status as companion animals. Depending on the size of dog, there may be some discrepancy in the size, shape and loading of canine bones in comparison to human bones. A study by Aerssens et al. [Aerssens et al., 1998] examines the differences in bone composition, density and quality between various species (human, dog, sheep and pig), finding that there is most similarity in bone composition between the dog and human. However, another difference between human and canine bone which may be important when assessing the effect of implant modifications, is the rate difference in bone remodeling between the species. The dog, like humans, do not possess the intrinsic ability to heal cartilage lesions [Cook et al., 2003], and suffer of problems such as osteochondrite and osteoarthritis as in human population. Canine models have also been used in studies of bone healing: the use of MSCs loaded on biomaterials were used in the treatment of bone defects with good results [Nakamura et al., 1998].

Most of the literature reports that the dog is a more suitable model for human bone from a biological standpoint than the **sheep**; however, adult sheep offer the advantage to be more similar to human for body weight and it has long bones of suitable dimensions for the insertion of human implants and prostheses [Newman et al., 1995], which is not possible in smaller species such as rabbits or dogs. Macroscopically, sheep bones may represent human bones enough closely, however, from the histology point of view, the bone structure is quite different, in particular considering its bone density. Moreover, several studies argue that the sheep is still a valuable model for human bone turnover and remodeling activity [den Boer et al., 1999].

Pigs are reported as the subjects of choice in a variety of studies including studies of osteonecrosis of the femoral head, fractures of cartilage and bone, bone ingrowths and studies evaluating new dental implant designs [Sun et al., 1999]. Commercial breeds of pig

are generally considered undesirable for orthopaedic research due to their large growth rates and excessive final body weight. However, the development of minipigs has overcome this problem to some extent. Nevertheless, pigs are often considered difficult to handle, noisy and aggressive and are therefore overlooked in favour of more amenable species such as the sheep and goat [Newman et al., 1995]. With regard to bone anatomy, morphology, healing and remodeling, the pig is considered to be closely representative of human bone and therefore a suitable species of choice [Thorwarth et al., 2005]. While having a denser trabecular network, the pig is described as having a lamellar bone structure which is similar to that of humans [Mosekilde et al., 1987]. When comparing the bone composition of various species, Aerssens et al. find that porcine bone mineral density and bone mineral concentration show similarities to human bone [Aerssens et al., 1997]. Moreover, the literature describes the pig as having bone remodeling processes similar to humans, for both trabecular and intracortical BMU based remodeling [Mosekilde et al., 1987].

The pig is widely used in various fields of tissue engineering: dental, maxillofacial and orthopaedic field [Wang et al., 2007; Ciocca et al., 2009]. Despite pig model has been widely used in the treatment of osteochondral defects [Chang et al., 2011], the use of **minipigs** is expanded, due to their docile and gentle behaviour, and also their body weight similar to that of an adult human (70-80 kg). The minipig bone reaches maturity 18-22 months of age, and does not have good self-healing capacity of chondral and osteochondral lesions [Gotterbarm et al., 2008]. Different studies have shown that, in these animal models the process of bone remodeling, bone structure, and cartilage thickness are quite similar to humans [Frisbie et al., 2006; Zelle et al., 2007]. Different studies of chondral and osteochondral defect healing were performed using this animal model [Harman et al., 2006], showing promising results in the field of tissue engineering.

Preclinical studies are crucial before proceeding to human trials, but the transition from preclinic to clinic requires a large number of significant statistically data.

RABBIT ADIPOSE-DERIVED STEM CELLS

AND TIBIA REPAIR

The aim of this study conducted during my PhD course, was to evaluate the effect of the administration of adipose-derived stem cells to repair or regenerate loss bone tissue. For this purpose, in collaboration with the Faculty of Veterinary Medicine of the University of Milan and the IRCCS Galeazzi Orthopaedic Institute of Milan, we have performed an experimental study on 12 adult New Zealand White rabbits (*Oryctolagus Cuniculus,* 2.5-3 kg) with the aim to evaluate the ability of autologous rabbit Adipose-derived Stem Cells (rbASCs) in association with clinical-grade hydroxyapatite disks (HA), to repair a critical size bone defect.

All the animals were treated in accordance with both policies and principles of laboratory animal care and with the European Union guide-lines (86/608/ECC) approved by the Italian Ministry of Health (Law 116/92).

MATERIALS AND METHODS

1. Adipose Tissue Harvesting

Adipose tissue was collected from interscapular region of six rabbits (group C and D). Anaesthesia was induced by intramuscular injection of a combination of ketamine (44 mg/kg) and xylazine (6-8 mg/kg) and maintained via inhalation of a mixture of oxygen and isofluorane. Sagittal incision of about 2-3 cm of length was performed in the interscapular skin region and subcutaneous adipose tissue was harvested, being careful to separate vessels from skin. After harvesting the minimum required amount of adipose tissue, the small wound was sutured and rabbits were treated with marbofloxacin (5 mg/kg) every 24 hours for 7 days. To reduce pain, rabbits were administered with flunixin (1 mg/kg) every 12 hours for 5 days. Adipose tissue was collected in a sterile jar with PBS 1X (NaCl 137 mM, KCl 2.7 mM, $Na_2HPO_4 \cdot 7H_2O$ 4.3 mM, KH_2PO_4 1.4 mM, pH 7.4) supplemented with 300 U/ml penicillin, 300 µg/ml streptomycin and 0.75 µg/ml amphotericin B (Sigma-Aldrich, Milano, Italia) (Figure 1).
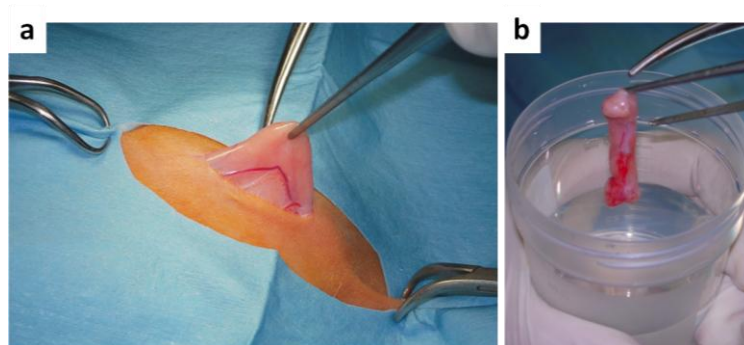

Figure 1. Adipose tissue harvesting (a) and carrying in a sterile refrigerate jar in the lab (b).

2. Isolation of Rabbit Adipose-derived Stem Cells (rbASCs)

After adipose tissue harvesting, the tissue was finely minced and washed with PBS 1X supplemented with 300 U/ml penicillin, 300 µg/ml streptomycin and 0.75 µg/ml amphotericin B and centrifuged at 1200 g for 2 minutes to remove erythrocytes and cellular debris. Samples were then digested in a shaking water bath for 60 minutes at 37°C by 0.1% collagenase type I (225 U/mg; Worthington, Lakewood, NJ) in PBS 1X supplemented with 300 U/ml penicillin, 300 µg/ml streptomycin and 0.75 µg/ml amphotericin B. After digestion, the collagenase type I was neutralized by adding an equal volume of control medium (CTRL) made up of DMEM (Sigma-Aldrich) supplemented with 10% (v/v) FBS (Fetal Bovine Serum, Sigma-Aldrich), 2 mM L-glutamine (Sigma-Aldrich), 100 U/ml penicillin (Sigma-Aldrich), 100 µg/ml streptomycin (Sigma-Aldrich) and 0.25 µg/ml amphotericin B (Sigma-Aldrich). The samples were centrifuged for 10 minutes at 1200 g to separate the Stromal Vascular Fraction (SVF) from adipocytes, cellular debris and undigested tissue (Figure 2). The SVF was filtered through sterile medication lint, the cellular suspension was centrifuged for 4 minutes at 320 g and the pellet was resuspended in CTRL medium. Cell number and viability were determined by trypan blue exclusion. Rabbit Adipose-derived Stem Cells (rbASCs) derived from SVF were plated in CTRL medium at a density of 10^5 cells/cm^2 and maintained at 37°C in a humidified atmosphere with 5% CO_2. After 48-72 hours, non-adherent cells were discarded by washing with PBS 1X.
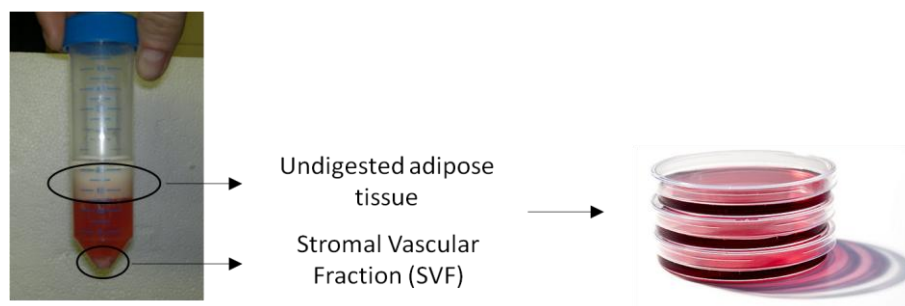

Figure 2. Rabbit Adipose-derived Stem Cells (rbASCs) isolation protocol.

3. In Vitro Culture of rbASCs

During all the period of culture the medium was changed three times a week and after reaching of 80-90% of confluence, cells were detached by incubation with 0.5% Trypsin/ 0.2% EDTA (Ethylene Diamine Tetra Acetic acid, Sigma-Aldrich) for 3 minutes at 37°C. Cell

number and viability were determined by trypan blue exclusion and rbASCs were plated at a density of 5×10^3 cells/cm^2 for further expansion and experiments.

3.1. Cryopreservation and Defreezing of rbASCs

The aim of cryopreservation is to enable stocks of cells to be stored to prevent the need to have all cell lines in culture at all times, to reduce the risk of microbial contamination or cross contamination with other cell lines or to reduce the risk of genetic drift and morphological changes. The basic principle of successful cryopreservation is a slow freeze and quick thaw. Cultures should be healthy with a viability of > 90% and should be in log phase of growth. 10^6 of rbASCs were resuspended in 1 ml of freezing medium made up of 90% FBS and 10% DMSO, a cryopreservant to help protect the cells from rupture by the formation of ice crystals. rbASCs suspension was put in cryovials and placed in a jar (Nalgene) containing 100% isopropanol (Fluka) at -80°C; this permit that cells were cooled at a rate of -1°C to -3°C per minute. Important is also that the cells were thawed quickly by incubation in a 37°C water bath for 2-3 minutes. When defrozen, cellular suspension was diluted with CTRL medium to neutralize DMSO and centrifuged at 300 g for 3 minutes. The pellet was resuspended and plated in a Petri dish that was placed in incubator at 37°C with 5% CO_2.

3.2 In Vitro rbASCs Characterization

3.2.1. MTT Cell Proliferation Assay

The MTT cell proliferation assay measures the cell proliferation rate and conversely, when metabolic events lead to apoptosis or necrosis, the reduction in cell viability. The yellow tetrazolium MTT [3-(4, 5-dimethylthiazolyl-2)-2, 5-diphenyltetrazolium bromide] is reduced by metabolically active cells, by the action of dehydrogenase enzymes in the mitochondria, to generate reducing agents such as NADH and NADPH. The resulting intracellular purple formazan can be solubilized and quantified by spectrophotometric means [Denizot and Lang, 1986]. From passage 1 to 4 in culture, rbASCs were trypsinized and plated at a density of 5×10^3 cells/cm^2 in control medium. rbASCs viability was monitored at various time points (1, 6, 10 or 14 days) by addition to the culture medium of MTT at a final

concentration of 0.5 mg/ml and further incubation for 4 hours at 37°C. The resulting formazan precipitate was then solubilised by using 100% DMSO and the absorbance was read at 570 nm with a Wallac Victor II plate reader.

3.2.2. Fibroblast and Osteoblast Colony-Forming Unit Assay

A colony forming unit-fibroblast assay (CFU-F) was performed as previously described [Castro-Malaspina et al., 1980] with minor modifications with the aim to identify the percentage of stem cell precursor in a primary cell culture. rbASCs were plated in six-well plates at low density (50 cells/cm^2, 25 cells/cm^2 and 12.5 cell/cm^2) and cultured at 37°C in a humidified atmosphere with 5% CO_2 in CTRL medium supplemented with 20% FBS. At day 7, the medium was changed and, at day 14 cells were fixed with 100% methanol (Sigma-Aldrich) and stained with 2 mg/ml Crystal Violet (Fluka, Buchs, Switzerland). A colony forming unit-osteoblast assay (CFU-O) was performed by plating cells in six-well plates by limiting dilution (100 cells/cm^2, 50 cells/cm^2 and 25 cell/cm^2) and culturing at 37°C in osteogenic medium (as described below) for 14 days. Colonies were fixed with 70% cold ethanol and stained with 40 mM Alizarin Red S (ARS, pH 4.1 - Sigma Aldrich). The frequency of the CFU-F and CFU-O was established by scoring individual colonies (consisting of at least 20-30 cells) respect to the number of seeded cells.

3.2.3. Haematoxylin-Eosin Stain

Haematoxylin and eosin stain is a popular staining method in histology. The staining method involves application of hemalum, which is a complex formed from aluminium ions and oxidized haematoxylin. This colours nuclei of cells blue. The nuclear staining is followed by counterstaining with an aqueous or alcoholic solution of eosin, which colours eosinophilic structures in various shades of red, pink and orange.
10^5 rbASCs were seeded on a polylysine coverslips (Polysine[TM] 25 mm x 75 mm x 1 mm) and left adhere overnight. The day after, the cells were fixed with 100% methanol (Fluka) for 5 minutes and then stained for 2-3 minutes with a solution of haematoxylin-eosin (Sigma-Aldrich), washed with deionized water and mounted with Pertex mountat (Bio-Optica, Milano, Italia).

3.3. Osteogenic Differentiation and Evaluation of Differentiation Markers

From passage 1 to 4, rbASCs were differentiated towards the osteogenic lineage by using a specific inductive medium (OSTEO) supplemented with 10 nM dexamethason (Sigma-Aldrich), 10 mM glycerol-2-phosphate (Sigma-Aldrich), 150 µM L-ascorbic acid-2-phosphate (Sigma-Aldrich) and 10 nM cholecalciferol (Sigma-Aldrich) (Table 1) [de Girolamo et al., 2007].

	BASAL MEDIUM	SUPPLEMENT
CTRL MEDIUM (CTRL)	DMEM + 10% FBS 2 mM L-glutamine 100 U/ml penicillin 100 µg/ml streptomycin 0.25 µg/ml amphotericin B	
OSTEOGENIC MEDIUM (OSTEO)	DMEM + 10% FBS 2 mM L-glutamine 100 U/ml penicillin 100 µg/ml streptomycin 0.25 µg/ml amphotericin B	150 µM L-ascorbic acid-2-phosphate 10 nM dexamethason 10 mM glycerol-2-phosphate 10 nM cholecalciferol

Table 1. Control (CTRL) and osteogenic (OSTEO) medium composition

Differentiation was performed in monolayer, cells being seeded at a density of 5×10^3 cells/cm^2. Cells were cultured at 37°C in a humidifier atmosphere (5% CO_2) for various periods (7 and 14 days), the medium being changed three times a week. At the appointed time, differentiated rbASCs were photographed to document morphological changes. After 7 and 14 days in culture, the expression of specific markers of osteogenic differentiation such as alkaline phosphatase activity, calcified extracellular matrix deposition and the expression of collagen type I, osteocalcin and osteonectin, was evaluated.

3.3.1. Immunofluorescence

7×10^4 rbASCs differentiated for 7 days on coverslips were rinsed and fixed with 3% paraformaldehyde and incubated with the first-step primary antiserum, rabbit α-actin (1:200 dilution) (Abcam, Cambridge, USA) for 24 hours and subsequently treated with the Avidin-Biotin blocking kit solution (Vector Laboratories Inc., USA). The samples were incubated with a solution of 10 µg/ml goat biotinylated α-rabbit IgG (Vector Laboratories

Inc.) in TBS for 1 hour and then treated with Fluorescein-avidin D (Vector Laboratories Inc.), 10 μg/ml in NaHCO3, 0.1 M, pH 8.5, 0.15 M NaCl for 1 hour. For the second step of the double immunofluorescence procedure, the slides were treated with either α-collagen type I (Coll I, 1:200 dilution) (Chondrex Inc, USA) or α-osteopontin (OPN, 1:100 dilution) (Santa Cruz Biotecnology, USA) antisera, blocked as described above and incubated with 10 μg/ml goat biotinylated α-mouse IgG (Vector Laboratories Inc.) for 1 hour. The samples were then treated with Rhodamine-Avidin D (Vector Laboratories Inc.), 10 μg/ml in $NaHCO_3$, 0.1 M, pH 8.5, with 0.15 M NaCl for 1 hour, and finally they were embedded in Vectashield Mounting Medium (Vector Laboratories Inc.) and observed by a confocal laser scanning microscope (FluoView FV300, Olympus, Italy). All reactions were performed at 18-20°C; the absence of cross-reactivity with the secondary antibody was verified by omitting the primary antibody during the first incubation.

3.3.2. Cellular Lysis

At passage 4, rbASCs were plated in 12-multiplate at $5x10^3$ cells/cm^2 in CTRL and OSTEO medium, replacing the medium twice a week. At day 7 and 14 of the culture, cells were washed with PBS 1X and lysed in non-denaturant conditions using 60 μl of 0.1% Tryton X-100 (Sigma-Aldrich) in distilled H_2O, to induce osmotic shock and cellular lysis without altering the biochemical properties of alkaline phosphatase (ALP). The lysates were collected in 1.5 ml tube and were placed on ice for 30 minutes, vortexing every 10 minutes. After incubation were performed 3 cycles of freezing/ thawing to facilitate the breaking of the cell membrane. Finally, the samples were centrifuged at 14000 g for 10 minutes (4°C) and supernatants recovered and frozen at -20°C until use.

Western Blot samples were prepared lysing 10^6 rbASCs in 100 μl of 50 mM Tris-HCl pH 8, 150 mM NaCl, 1% Nonidet P40, 0,1% Sodium Dodecyl Sulfate (SDS) supplemented with protease inhibitor cocktail (104 mM AEBSF, 1.4 mM E-64, 4 mM bestadin, 2 mM leupeptin, 80 μM aprotinin, 1.5 mM pepstatin A, Sigma-Aldrich) and 1 mM Phenyl Methane Sulfonyl Fluoride (PMSF, Sigma-Aldrich) for 30 minutes on ice followed by centrifugation at 14000 g for 10 minutes (4°C).

3.3.3. Protein Assay

Protein concentration was determined using the BCA[TM] Protein Assay Kit (Pierce, Rockford, IL, USA) optimized with the use of 96-multiplate. This assay is a detergent-compatible formulation based on bicinchoninic acid (BCA) for the colorimetric detection and quantification of total protein. This method combines the reduction of Cu^{2+} to Cu^{1+} by protein in an alkaline medium (the biuret reaction) with the highly sensitive and selective colorimetric detection of the cuprous cation (Cu^{1+}) using a unique reagent containing bicinchoninic acid. The purple-coloured reaction product of this assay is formed by the chelation of two molecules of BCA with one cuprousion.

In each well, 3 µl of cellular lysates were dosed adding 200 µl of solution obtained mixing two reagents ($CuSO_4$ and bicinchoninic acid) following the manufacturing instruction. The plate was incubated at 37°C for 30 minutes to allow the reaction and the samples were read by measuring the absorbance at 550 nm using a microplate reader Wallac VictorII-1420. The protein concentrations of samples were obtained interpolating the absorbance data on a standard curve of Bovine Serum Albumine (BSA, Sigma-Aldrich) at known concentrations (range 125 µg/ml - 2 mg/ml).

3.3.4. Alkaline Phosphatase Activity (ALP)

ALP activity is performed on cellular lysates using a colorimetric assay in which *p*-nitrophenyl phosphate (*p*NPP), a colourless phosphatase substrate, is converted into *p*-nitrophenol (*p*NP) when dephosphorilated by ATP, producing a yellow product (λ = 405 nm) (Figure 3).
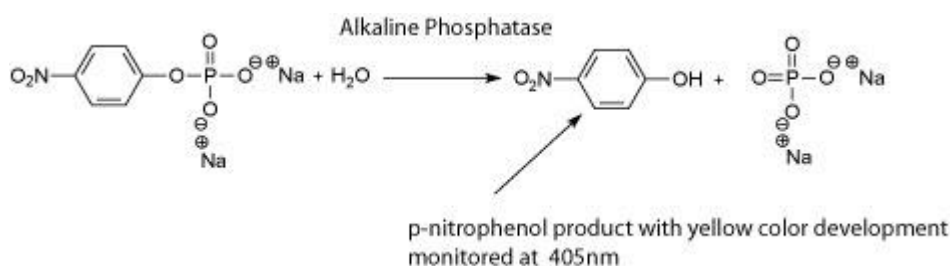

Figure 3. Alkaline phosphatase reaction with substrate *p*NPP

Experiments were performed as previously described with minor modifications to be applicable in 96-well plates [Bodo et al., 2002]. 20 μl of lysate were assayed (each sample is assayed in duplicate to calculate a statistical variability) and in each well were added 100 μl of substrate solution (10 mM pNPP diluted in 100 mM diethanolamine buffer (Fluka)/ 0.5 mM MgCl$_2$•6H$_2$O, pH=10.5). Samples were incubated at 37°C for the time necessary to develop the reaction. At the end of the incubation period, the reaction was stopped with 50 μl NaOH 1N and the absorbance was read using a microplate reader Wallac VictorII-1420. The absorbance values of samples were interpolated with a standard curve of pNP (range 6.25-200 μM) (Sigma-Aldrich). Enzymatic activity was calculated in Unit (U), where 1U is the amount of enzyme required to hydrolyze 1 μmol of pNPP according to the formula: U= μM/ min * 1000 → 1000 nM / min.

Alkaline phosphatase activity were then normalized to protein concentration of each samples and percentage increase was calculated comparing treated to control samples.

3.3.5. SDS-PAGE and Western Blot Analysis

SDS-PAGE, sodium dodecyl sulfate polyacrylamide gel electrophoresis, is a technique widely used in biochemistry, genetic and molecular biology to separate proteins according to their electrophoretic mobility (a function of length of polypeptide chain or molecular weight). Samples were boiled at 90°C for 5 minutes in 4X sample buffer (250 mM Tris-HCl pH 6.8 supplemented with 40% Sucrose, 6% SDS, 20% β-mercaptoethanol e 0.04% bromophenol blue). A total of 20 μg of proteins were loaded in each wells and an electric field was applied across the gel (80 V in the stacking gels and 120 V in the resolving gel), causing the negatively-charged proteins to migrate across the gel towards the positive electrode. Depending on their size, each proteins moved differently through the gel matrix.

The proteins are then transferred to a membrane of nitrocellulose (Amersham Bioscences, Milan, Italy) in the transfer buffer (20% methanol, 20 mM Tris-HCl, 150 mM glicin, 0.05% SDS) for 2 hours at 80V (4°C). The uniformity and the effectiveness of protein transfer from the gel to the membrane was checked by staining the membrane with Ponceau S dyes (0.1% Ponceau S, 5% acetic acid in distilled H$_2$O) for 5 minutes. Ponceau S is sensible and water soluble dye and can subsequently destain using TBS-Tween 0.1% (200 mM Tris-HCl, 15 mM NaCl, 0.1% Tween 20). Blocking of non-specific binding was achieved by placing the

membrane in a solution of 5% nonfat dry milk in TBS-Tween for 1 hours at room temperature. Membrane was then incubated at 4°C overnight with either mouse anti-osteonectin (1:200 dilution; Santa Cruz Biotecnology, Santa Cruz, Calif., USA) and mouse anti-collagen type I (1.1000 dilution, Chondrex Inc. USA) and mouse anti-β-actin (1:3000 dilution, Sigma-Aldrich). Specific proteins were revealed by horse-radish peroxidase (HRP)-conjugated secondary antibodies (GE Healthcare).

The pattern of primary and secondary antibodies used for this study is described in Table 2.

PRIMARY ANTIBODY	SPECIES	ORIGIN	DILUTION	
α-collagen type I	Mouse	Monoclonal	1:1000	Chondrex Inc. USA
α-osteonectin	Mouse	Monoclonal	1:200	Santa Cruz Biotecnology Inc.
α-β tubulin	Mouse	Monoclonal	1:5000	Sigma-Aldrich

SECONDARY ANTIBODY	DILUTION	
Horseradish peroxidase (HRP) anti mouse	1:3000	Ge Healthcare

Table 2. Primary and secondary antibody

After incubation the membrane was washed 3 times with TBS-Tween 0.1% in order to remove the excess of secondary antibody and the signal was detected using ECL Western Blotting Analysis System Kit (GE Healthcare) according to the manufacturer's protocol. Proteins expression was then quantified by using ImageJ software. The osteo-specific proteins content was normalized to that of β-actin.

3.3.6. Collagen Production

Osteogenic differentiation was also evaluated by collagen deposition assay. This method is based on the ability of Sirius Red compound to selectively bind to fibrillar collagens (types I to V), specifically to the {Gly-X-Y]n helical structure. Collagen type I, produced by osteoblast, represents about 90% of total collagen. This assay is performed as previously described [Tullberg-Reinert and Jundt, 1999; Bosetti et al., 2003; Sandrini et al., 2005] with minor modifications.

Undifferentiated rbASCs were plated in 12-multiplate at $5x10^3$ cells/cm^2 and osteo-differentiated for 14 days in culture. The cells were fixed with Bouin's solution (Sigma-Aldrich) for 1 hour at 37°C. The total collagen was evaluated by using 0.1% Sirius Red F3BA in saturated picric acid (Sigma-Aldrich) (w/v) for 1 hour at room temperature and the non-specific stain was removed by washing with 10 mM HCl (Sigma-Aldrich). Sirius Red was then resolubilized with 600 μl 0.1 M NaOH (Sigma-Aldrich) for 5 minutes. After extraction, absorbance was read at 550 nm using a microplate reader Wallac VictorII-1420. The amount of secreted collagen was calculated based on a standard curve of known concentration of calf skin type I collagen (Sigma-Aldrich, range 5-80 μg) and their optical density measurements, and percentage increase was calculated comparing treated to control samples.

3.3.7. Extracellular Calcified Matrix Deposition

Alizarin Red-S (AR-S) staining has been used to evaluate calcium-rich deposits by cells in culture. It is particularly versatile and the dye can be extracted from the stained monolayer and assayed. To evaluate extracellular calcified matrix deposition, $5x10^3$ rbASCs/cm^2 were plated and maintained in culture in CTRL or OSTEO medium for 14 days. After fixation in 70% ice-cold ethanol (Sigma-Aldrich), the cells were stained with 40 mM Alizarin Red-S for 1 hour at room temperature and the quantification of mineral deposition was performed by incubating the samples with 600 μl 10% w/v cetylpyridinium chloride (CPC, Sigma-Aldrich) in 0.1 M phosphate buffer (pH 7.0) for 15 minutes to extract AR-S. Absorbance was read at 550 nm with a Wallac Victor II plate reader [Halvorsen et al., 2001], and percentage increase was calculated comparing treated to control samples.

3.4. In Vitro rbASCs–Hydroxyapatite Constructs

Granules of the same clinical-grade HA ($Ca_{10}(PO_4)_6(OH)_2$, 70-80% of porosity, pore size <10μm, ≈3% vol; 10-150 μm, ≈11% vol; >150 μm, ≈86% vol, kindly provided by Finceramica S.p.A., Italy) used for the *in vivo* experiments were seeded with undifferentiated rbASCs at passage 4 ($2x10^5$ cells/scaffold – $7.5x10^6$ cells/cm^3), to evaluate their ability to grow and differentiate in a 3D environment. Cells were let adhere overnight to HA in 1.5ml-tubes at

37°C in a 5% CO_2 humidified incubator and the following day the seeded scaffolds were transferred into a 24-well plate and cultured for 14 days in non inductive medium (CTRL).

4. Surgical Technique and Constructs Implantation

At passage 2, undifferentiated ASCs from each rabbit (1.5×10^6 cells/80 µl) were loaded on clinical-grade HA ($Ca_{10}(PO_4)_6(OH)_2$; Finceramica S.p.A., Faenza, Italy) cylindrical scaffolds (8 mm diameter × 4 mm height). The seeded scaffolds were maintained overnight in the incubator in cryovials to let rbASCs adhere to the disk. The following day, an 8-mm diameter full-thickness bone defect was created bilaterally in the proximal epiphysis of the medial facet of the tibia in all the rabbits (Figure 4a), inducing anaesthesia as previously described. HA scaffold constructs were implanted into the defect through "press-fit" technique in groups B and D (Figure 4b and 4d). The same number of rbASCs (1.5×10^6 cells/40 µl) in semi-liquid suspension was directly injected in the bone defects of group C just before the last suture stitch of the periostium (Figure 4c). After surgery rabbits were allowed free movement and again administered with marbofloxacin and with flunixin as described for the post-surgical recovery treatment after the adipose tissue harvesting.

Eight weeks after implantation, animals were sacrificed under general anaesthesia (44 mg/kg ketamine, 6-8 mg/kg xilazine followed by an overdose of 50 mg/kg thiopental and 60 mEq KCl); tibia specimens were explanted, and evaluated by gross examinations, radiography, bone mineral density (BMD) measurements, histology and immunocytochemical analysis, histomorphometric and biomechanical tests.

Figure 4. Surgical technique and constructs implantation. Creation of a critical size tibia defect using a trephine (a), implantation of HA scaffold alone (b) or in association with rbASCs (d) into defect through "press-fit" technique, and filling of the lesion site with a semi-liquid suspension of rbASCs (c).

5. Radiographic Analysis

Lateral radiographs were taken immediately after the surgical treatment (T_0), 6 weeks after intervention (T_6) and post-tibia removal (8 weeks, T_8). The scoring system (Table 3) included an evaluation of bone integration in terms of good repair for the group treated without scaffold, or integration of the HA scaffolds.

6. Gross Analysis

Eight weeks after implantation, rabbits were euthanized under anaesthesia with an overdose of pentothal sodium (50 mg/kg) and potassium chloride (60 mEq) and left and right proximal tibiae were dislocated from each rabbit and dissected free of soft tissue. Filling of the lesions and stiffness of the new regenerated tissue were evaluated, using a modified version of Wakitani scale, adapted to the description of bone defects (Table 3) [Wakitani et al., 1994].

MACROSCOPIC ANALYSIS		RADIOGRAPHIC ANALYSIS
Filling	*Stiffness*	*Bone integration*
Same level = 3	Same stiffness = 3	Good repair/integration = 3
Overgrowth = 2	Softer = 2	Overgrowth = 2
Undergrowth >1 mm = 1	Very soft = 1	Undergrowth >1 mm = 1-0

Table 3. Morphologic and radiographic scoring system for the evaluation of the bone regeneration process.

7. Bone Mineral Density (BMD)

Measurement of Bone Mineral Density (BMD) was conducted using a Hologic QDR 1000/Plus DXA instrument (70 kVp/l40 kVp), localized at the section of Veterinary Radiology of the Faculty of Veterinary Medicine at the University of Milan. BMD is a medical term referring to the amount of matter per cubic centimetre of bones, that is used in clinical medicine to evaluate the mineral content (hydroxyapatite) in the bone tissue and is considered an indirect indicator of osteoporosis and fractures risk. There were analyzed three different areas for each tibiae, as seen in the scheme (Figure 5): R1 (0.25 cm^2), R2 (0.25 cm^2), and R3 (0.09 cm^2), where R2 represented the lesion site. Pure scaffold density

(HA cylindrical scaffold inserted in explanted rabbit tibia) and normal tibia density were also measured as control. BMD was expressed in grams for cm^2 (g/cm^2).
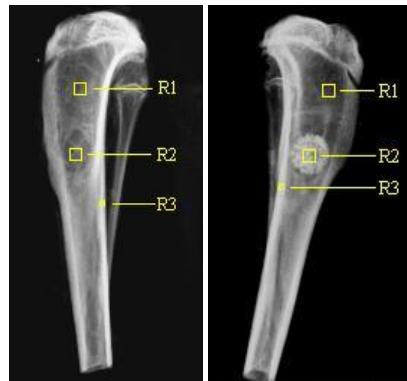

Figure 5. Three different BMD areas, for each tibia were analyzed, where R2 represented the lesion site.

8. Histological Analyses

The removed tibiae (8 weeks) were dissected free of soft tissue and fixed for 3 days in 10% buffered formalin and decalcified in a formic acid-sodium citrate solution. The solution was changed daily until it was calcium free; at this time point decalcification was considered complete [Donath and Breuner, 1982]. After decalcification procedure, samples were embedded in paraffin, cut into 5 μm-thick sections and stained with haematoxylin and eosin (HE) sequential stain for ascertaining structural details with light microscope (Olympus BX51, Olympus, Italy). The sections were also analyzed with a polarized light microscope (LeicaDM LP; Leica Microsystems, Wetzlar, Germany) in order to investigate the tissue organization of the newly formed structures.

9. Immunohistochemistry

Explanted tibiae were prepared for immunohistochemical evaluation as previously described. 5 μm-thick decalcified sections were rehydrated and then a heat-induced antigen retrieval was performed (5 minutes at 500 W). To block endogenous peroxidase activity, sections were incubated in an aqueous solution of 1% H_2O_2 for 30 minutes at room temperature. Sections were then incubated overnight with either mouse anti-collagen type I antibody (1:500 dilution) (Chondrex Inc) or osteopontin (1:250 dilution) (Santa Cruz Biotechnology). Antigen-antibody complexes were detected with a peroxidase-conjugated

polymer which carries secondary antibody molecules directed against mouse immunoglobulins (EnVisionTM+, DakoCytomation, Italy) applied for 60 min at room temperature. Peroxydase activity was detected with diaminobenzidine (DAB, DakoCytomation) as the substrate. For both the immunohistochemical procedures the sections were weakly counterstained with Mayer's haematoxylin, dehydrated, and permanently mounted. The specificity tests for the collagen type I or osteopontin antisera were carried out. Microphotographs were taken using Olympus BX51 microscope (Olympus, Italy) supplemented by a digital camera.

10. Histomorphometric Analysis

Explanted specimens were fixed in 10% formalin/0.1M phosphate buffer saline solution (PBS, pH 7.4) at RT for 48 hours and then processed for undecalcified light microscopy [Donath and Breuner, 1982]. Bone cores were dehydrated using increasing concentrations of ethanol (from 70 to 100%), infiltrated for 30 days and embedded in Kulzer Technovit 7200 VLC (Bio-Optica, Italy). Each resin block was sliced perpendicularly to the long axis of the tibia using a diamond saw (Micromet Remet, Italy). The two longitudinal sections passing through the center of the critical defect area were grounded and polished (Micromet & LS2, Remet, Italy) to a final thickness of about 40 mm. The sections were stained with Toluidine blue/Pyronine Y (Sigma-Aldrich). Histomorphometric measurements of tissue fractions (newly formed bone, non mineralized connective tissue and HA in the scaffold-treated samples) in the defect area were performed by a computer-assisted differential standard point-counting technique. Briefly, a 100 test points grid was placed over the defect area of each 40 μm-thick histological section and photographed at a total microscopic magnification of 40X. The tissue underlying each grid intersection was recorded as either new bone, residual HA or bone marrow spaces and expressed in percentage values representing the volume density of these 3 components.

11. Biomechanical Tests

Mechanical tests consisted in nanoindentation experiments conducted using a NanoTest Indenter System (Micro Materials Ltd., UK) with a diamond Berkovich indenter tip. Both the

tip area function and the machine compliance were calibrated on a fused silica reference sample. An automatic preliminary thermal drift correction was applied at all indentation data.

Nanoindentation tests were performed on sections obtained from non-decalcified samples (thickness ~ 40 μm) treated with both empty HA disk and HA seeded with ASCs. Three different maximum loads (1mN, 5mN, and 50mN) were chosen as to acquire knowledge of the mechanical properties of the tissue at multiple length-scales. 4x4 indentation matrices were carried out for each load on three different locations for each sample. Some care was taken to conduct experiments in regions with mature bone tissue, which was found primarily along the walls of the scaffold pores.

The classical Oliver-Pharr method [Oliver et al., 1992] was employed to obtain the reduced modulus Er, which represents a measure of the stiffness of the tissue and is directly related to its elastic properties (Young's modulus E), and the hardness H, which is related to the strength of the tissue.

12. Statistical Analysis

Data are expressed as mean ± standard deviation and statistical analysis (Two-way ANOVA) were performed using GraphPad Prism v5.00 (GraphPad Software, USA). * p<.05; ** p<.01; *** p<.001.

RESULTS

The aim of my PhD work has been to assess *in vitro* the use of autologous rbASCs in association with hydroxyapatite (HA), in the regeneration of a critical-size bone defects in the tibial crest of a small size animal such as the rabbit. This has been possible by a tight collaboration with the Faculty of Veterinary Medicine of the University of Milan, the Centre for Research and Biotechnological Applications in Cardiovascular Surgery (CRABCC) of Milan and the IRCCS Galeazzi Orthopaedic Institute of Milan.

The study was conducted on 12 New Zealand White rabbits (2.5-3 kg). All animals were maintained and treated according to the rules dictated by the European Union relating to care of laboratory animals (86/609/ECC). The study was divided into the following phases:

1. Withdrawal of adipose tissue from the rabbit interscapular region
2. Isolation and culture of rbASCs
3. rbASCs osteogenic differentiation and *in vitro* evaluation of specific osteo-markers
4. Surgical creation of critical-size bone defect and its treatment
5. Radiographic analysis immediately after surgery and at 6 weeks from intervention
6. Macroscopic and radiographic analysis after tibia removal (8 weeks)
7. Evaluation of Bone Mineral Density (BMD)
8. Histological and immunohistochemical analyses of the newly formed bone tissue
9. Histomorphometric analysis
10. Bio-mechanical tests by nanoindentation experiments

Withdrawal of Adipose Tissue from the Rabbit Interscapular Region

Collection of adipose tissue was performed with particular attention to the mini-invasiveness of the procedure, to ensure animals' survival.

Rabbits have a large adipose tissue pouch with a definite location and easy access: these rabbits have an H-shaped deposit of adipose tissue located along the dorsomedial line, nearly 5 cm from the skull in the craniocaudal direction (Figure 6a).

The adipose tissue is accessed through a sagittal incision of 2- to 3-cm in the dorsomedial line over the tissue location (Figure 6b).
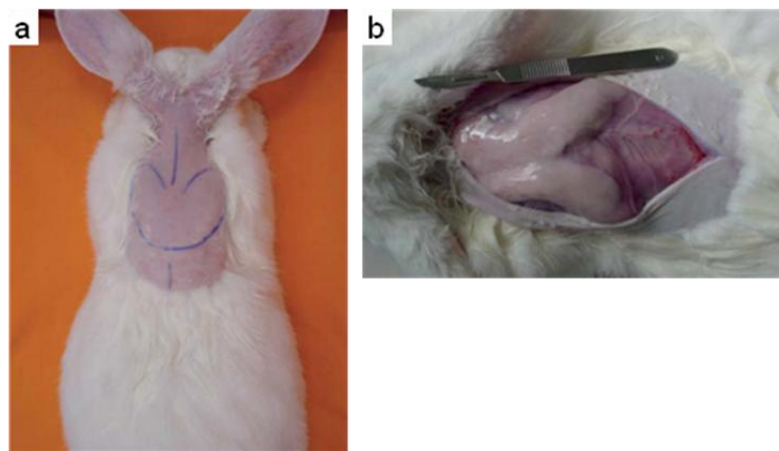

Figure 6. Adipose tissue localization. Label on the anatomic region in which the adipose tissue pouch is located (a). Pouch of adipose tissue (b) [Torres et al., 2007].

The tissue was collected from the interscapular region of 6 rabbits, under general anaesthesia, and after the removal of the minimum amount of fat the wound was sutured. The amount of collected adipose tissue varied according to the animal mass: we have obtained from a minimum volume of 3 ml of raw adipose tissue from rabbit #3, to 8 ml of adipose tissue from rabbit #2 (Table 4).

Isolation and Culture of rbASCs

rbASCs were isolated from six rabbits with an average of $2.8 \times 10^5 \pm 1.9 \times 10^5$ cells/ml of adipose tissue. The highest cell number was obtained from rabbit #4 (Table 4).

	Adipose tissue (ml)	rbASCs/ ml of raw adipose tissue
rbASCs1	5.5	1.64×10^5
rbASCs2	8	4.38×10^4
rbASCs3	3	4.33×10^5
rbASCs4	5	5.60×10^5
rbASCs5	5	2.80×10^5
rbASCs6	5	2.00×10^5
MEAN ± SD	5.2 ± 1.6	$2.8 \times 10^5 \pm 1.9 \times 10^5$

Table 4. Cellular yield of rbASCs per ml of adipose tissue

One week later, all the rbASCs rapidly started to proliferate and, at passage 1, the variability in terms of cell number among the 6 different derived rbASCs, was reduced, reaching, in 30 days, $2.6 \times 10^8 \pm 9.9 \times 10^7$ cells starting from 1.5×10^5 rbASCs. These cells showed the characteristic fibroblast-like morphology that was maintained during culture, without any sign of cellular senescence (Figure 7).
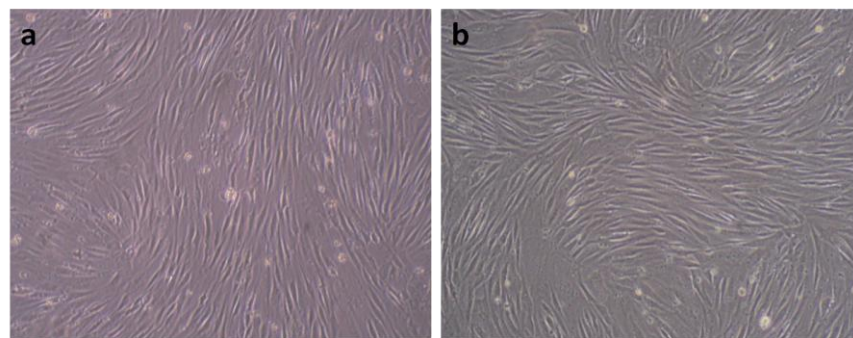

Figure 7. Microphotographs of rbASCs2 (a) and rbASCs3 (b) maintained in undifferentiated culture conditions (100X magnification).

To maintain rbASCs in culture, usually cells were seeded at 5×10^3 cells/cm^2 reaching 80-90% of confluence every 7 days: their doubling time was 56.9 ± 14.8 hours, quite constant from passage 2 to 6 (Figure 8a), to drastically decrease at late passages in culture, reaching at passage 9, a doubling time of 115.96 ± 39.02 hours (data not shown).

By MTT cell viability assay we confirmed that all the rbASCs maintained a similar trend of vitality when monitored for 7 days in culture (Figure 8b).
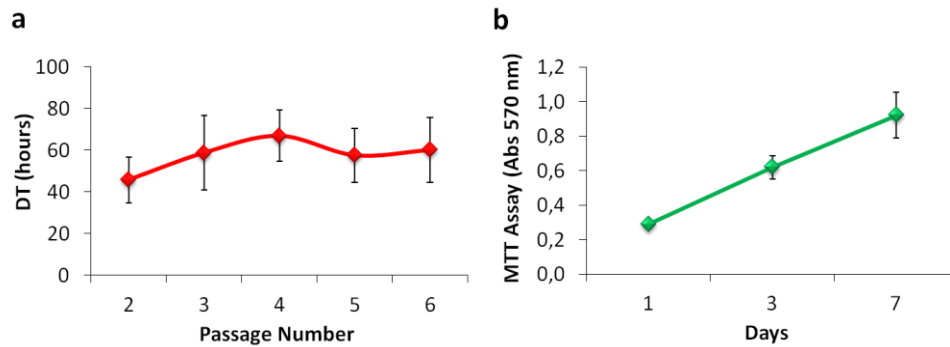
Figure 8. Proliferation trend at early passages assessed by cell counting at different passages in culture and expressed as doubling time [DT= t ×ln(2)/ln(N /N_0), t: time in culture, N: final number of cells, N_0 initial number of cells] (a) and viability of rbASCs maintained for 1 week in undifferentiated condition (b) (mean ± SD) (n=6).

rbASCs were able to produce fibroblast (CFU-F) and osteoblast (CFU-O) colonies. From passages 1 to 4, clonogenic abilities were quite similar among the six-cell populations, with an average value of 3.0±1.6% (range: 2.0-5.2%) and 4.3±1.9% (range: 3.5-6.9%), for CFU-F and CFU-O, respectively (Figure 9). Surprisingly, rbASCs-2 cells showed a reduced clonogenic ability respect to the other cell populations.

Furthermore, cryopreservation did not affect rabbit stem cells features, as we have previously shown for human cells (hASCs). Despite the fact that it has been observed a brief lag phase after thawing, the DT was similar to that of fresh cells maintained in culture at the same passages (data not shown).
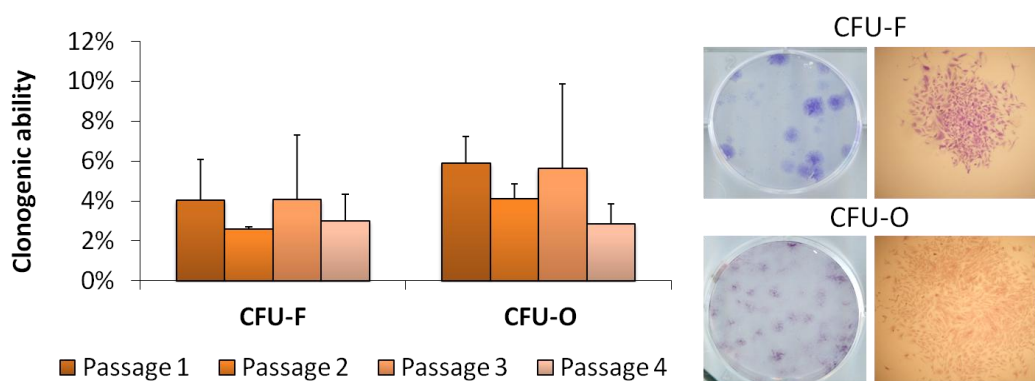

Figure 9. CFU-F and CFU-O frequencies expressed as percentage of number of colonies/number of plated cells (mean ± SD) (n=6) (left panel); microphotographs of CFU-F and CFU-O by rbASCs stained with Crystal Violet and Alizarin Red-S, respectively (right panel).

rbASCs Osteogenic Differentiation

Osteogenic differentiation was obtained maintaining rbASCs in osteo-inductive medium (OSTEO) for 7 and 14 days.

As early as 7 days in culture, all of the cells exhibited some morphological modifications compared to cells maintained in undifferentiative medium (CTRL): differentiated cells lost their fibroblast-like morphology (Figure 10a and 10c), assuming a more rounded/cubical shape (Figure 10b and 10d).

To determine the induced modifications, specific osteogenic proteins have been checked over time: alkaline phosphatase (ALP) and OPN for early osteogenesis , collagen type I (Coll I) and osteonectin (ONC) for the intermediate phase, and osteocalcin (OC) and bone mineralization for late osteogenesis.
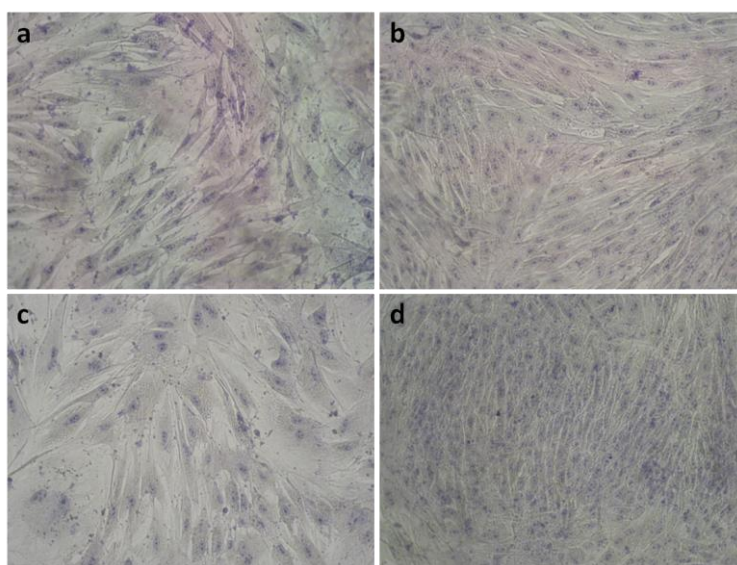

Figure 10. Morphological analysis of rbASCs maintained in CTRL and osteo-inductive medium (OSTEO). Microphotographs of 7-days undifferentiated (a, c) and differentiated cells (b, d) (100X magnification).

As shown in Figure 11, rbASCs, in the presence of osteogenic stimuli, efficiently differentiate into osteoblast-like cells: indeed, already after 7 days, ALP activity is abundant in osteo-differentiated cells respect to undifferentiated ones, and the average increase was about 28.9% (range 7.2-85.4%) (Figure 11a). Moreover, the expression of OPN is up-regulated in rbASCs, and it is possible to appreciate its cytoplasmic localization (Figure 11b).
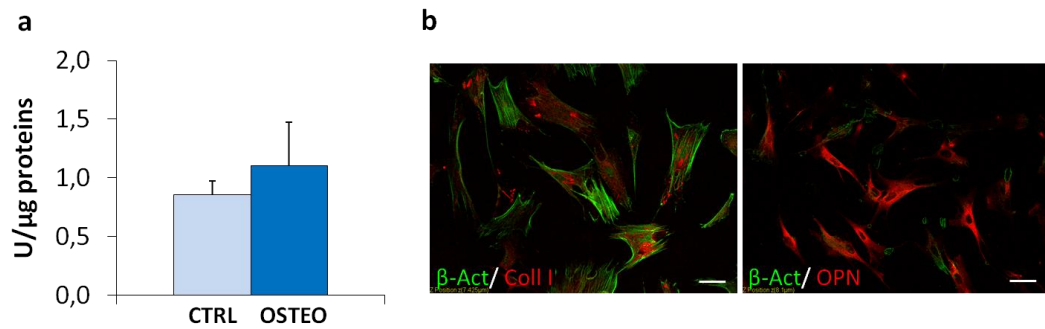
Figure 11. 7 days of differentiation: ALP activity (means ± SD) of rbASCs (mean ± SD) (n=6) (a); Double immunofluorescence of osteo-induced rbASCs for either collagen type I (Coll I) or osteopontin (OPN) (red fluorescence) and β-actin (β-Act) (green fluorescence) (scale bar 50 μm) (b).

Similar, osteo-rbASCs early expressed ONC (+157.6%), even if its expression was more evident after 14 days (+1193.7%) in comparison to undifferentiated cells (Figure 12). The kinetic of expression was similar for collagen type I (Figure 12): indeed, densitometric analysis of collagen I expression quantified a significant increase in Coll I/ β-Act protein ratio in osteo-differentiated rbASCs compared to undifferentiated ones with a significant increase 432.2% and 1233.9% after 7 and 14 days, respectively (Figure 12).

These data were also confirmed by Sirius Red assay. Osteogenic differentiated cells produced a significantly increased level of collagen I, of 105.9% respect to the same cells maintained in CTRL medium (range 23.3-159.4%) (Figure 13b). Despite a great inter-donor variability, in rbASCs5 (+159.4%) then in rbASCs1 (+109.9%), in rbASCs4 (+100.4%) and then rbASCs6 (+23.3%) populations, the collagen production was always more abundant in differentiated cells respect to the undifferentiated ones (Figure 13a).
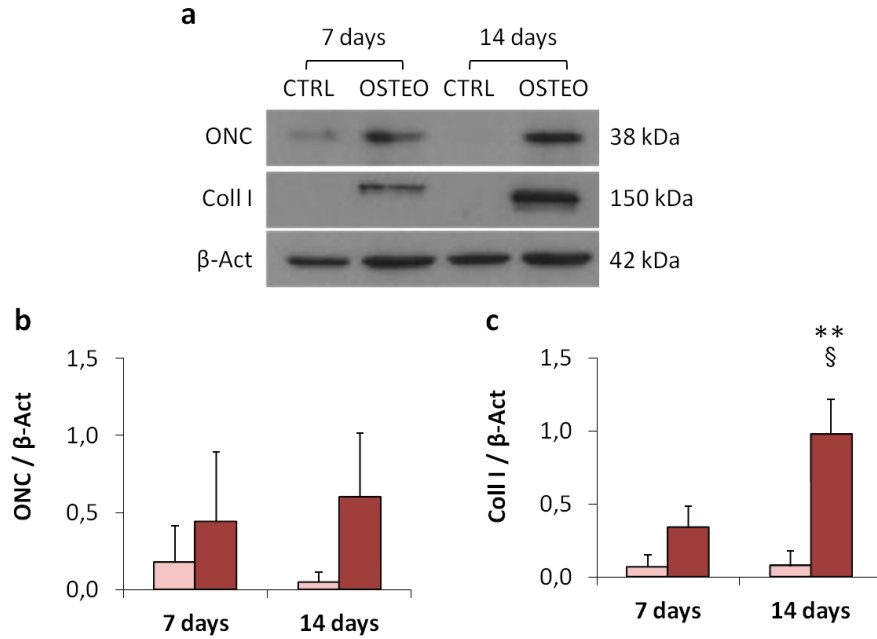
Figure 12. Western blot analysis of osteonectin (ONC) and Coll I expression at 7 and 14 days in undifferentiated (CTRL) and osteogenic differentiated (OSTEO) rbASCs (a) and densitometric analysis of ONC (b) and Coll I (c) normalized on β-Act expression (means ± SD) (n=2).

CTRL vs OSTEO: **p<.01; 7 days vs 14 days: §p<.05.
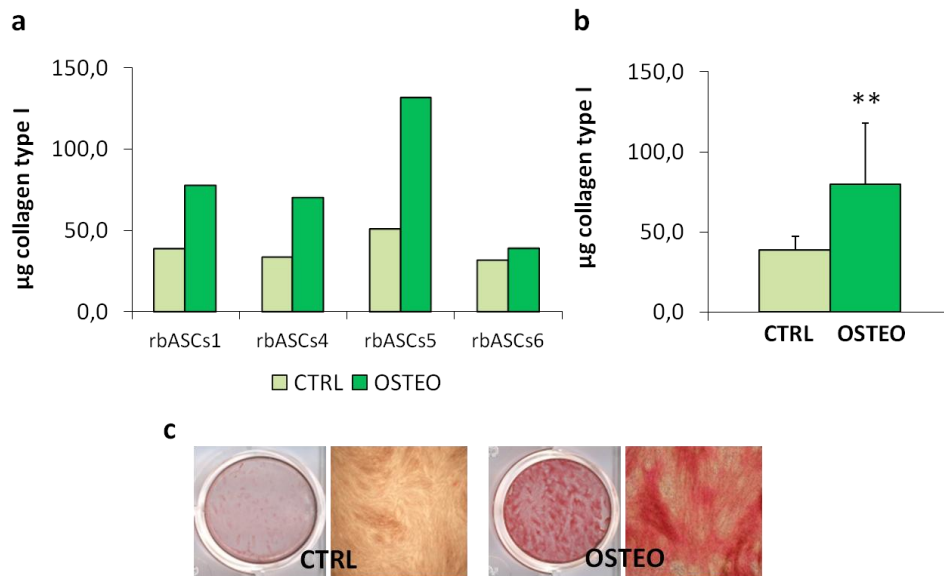
Figure 13. Collagen production by rbASCs cultured for 14 days in undifferentiated and osteogenic conditions (a): average collagen production (means ± SD) (n=4) (b). Pictures of rbASCs stained with Sirius Red and maintained in CTRL or OSTEO medium (c). CTRL vs OSTEO: **p<.01.

Moreover, adipose progenitor cells produced an abundant amount of calcified extracellular matrix with a significant increase of 168.1% respect to undifferentiated rbASCs (range 69.5-

324.4%) after 2 weeks (Figure 14b). In particular, osteo-differentiated rbASCs5 showed the greatest increment of calcium deposition in comparison to the undifferentiated cells (+324.4%). Osteo-differentiated rbASCs4 and rbASCs3 showed a significant increase of 204.3% and 143.1%, respectively, compared to the same cells maintained in non-inductive medium. Finally, differentiated rbASCs1, rbASCs2 and rbASCs6 produce 124.8%, 91.9%, and 69.5% more calcified matrix than the same cells maintained in control medium (Figure 14a).
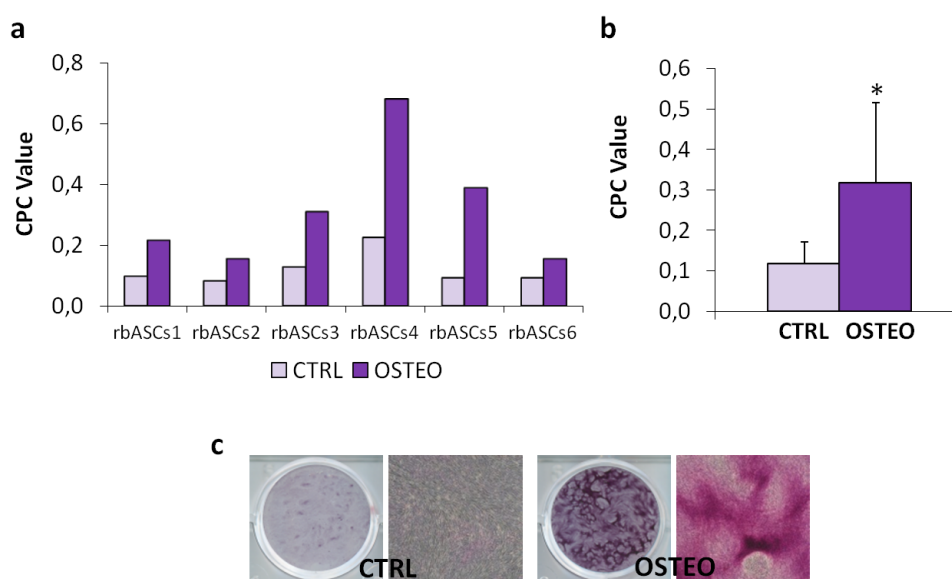

Figure 14. Extracellular calcified matrix quantification produced by rbASCs cultured on polystyrene for 14 days in undifferentiated and osteogenic conditions (CPC, cetylpyridinium chloride extraction) (a); average of extracellular calcified matrix deposition (mean ± SD) (n=6) (b). Pictures of rbASCs stained with Alizarin Red-S maintained in CTRL or OSTEO medium (c). CTRL vs OSTEO: *p<.05.

In vitro rbASCs - hydroxyapatite constructs

In the orthopaedic field, the efficacy of hydroxyapatite as a bone substitute has been already established. Hydroxyapatite (HA) is a biocompatible and bioactive material that can be used to restore or repair damaged bone tissue. Moreover, this scaffold exhibits strong bonding to the bone, and possesses suitable mechanical properties and interconnecting pores which allow cellular infiltration, graft integration and vascularisation. Other important features of this scaffold are its osteoinductive and osteoconductive properties and its high grade of resorbability. To confirm all of these characteristics in our experimental setting, and to assess if rbASCs respond to the physical stimuli produced by HA, undifferentiated rbASCs were seeded in the presence of HA and they showed a great

ability to finely adhere to the scaffold (Figure 15) and to produce a marked production of collagen type I, respect to the same cells grown on monolayer (PA, plastic adherence). The average increase was 48.2% (range 17.8-100.7%) (Figure 15).
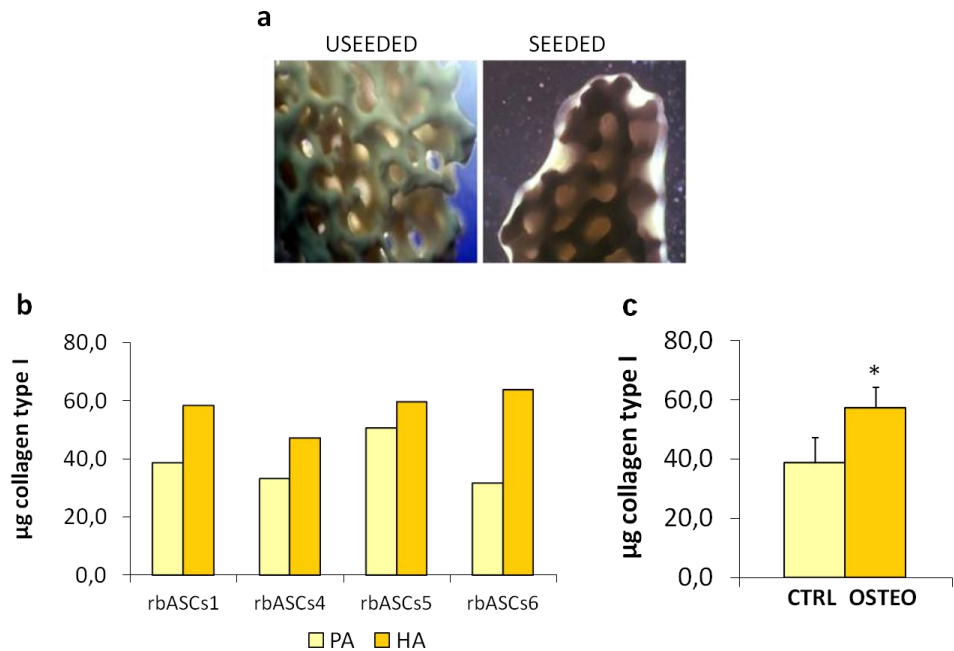

Figure 15. rbASCs - hydroxyapatite interaction. Light microscopy and SEM pictures of HA granules unseeded or seeded with rbASCs (a). Collagen quantification produced by each rbASCs population cultured on polystyrene (PA) or on hydroxyapatite (HA) for 14 days in undifferentiated conditions (b); average collagen production (mean ± SD) (n=4) (c). HA vs PA: *p<.05.

Surgical Creation of critical-size bone defect and its treatment

About 15 days of cell culture, 1.5×10^6 of undifferentiated passage 2 rbASCs from each rabbits, were resuspended in 80 µl of fresh control medium, loaded on HA disks (Figure 16a), and maintained at 37°C - 5% CO_2 overnight.

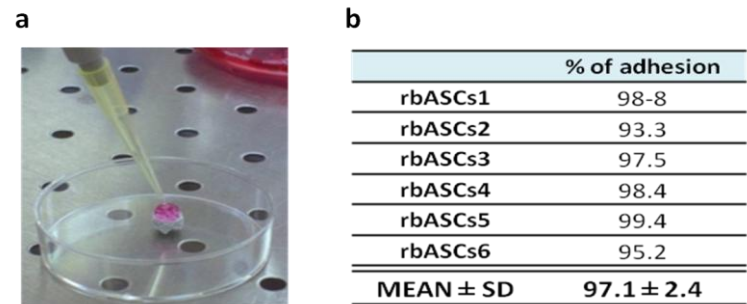|	% of adhesion
rbASCs1	98-8
rbASCs2	93.3
rbASCs3	97.5
rbASCs4	98.4
rbASCs5	99.4
rbASCs6	95.2
MEAN ± SD	97.1 ± 2.4

Figure 16. Loading of 1.5×10^6 undifferentiated rbASCs on hydroxyapatite disks (a). Percentages of cell adhesion after 16 hours of contact of rbASCs with the HA disk (b).

An average of 97.1±2.4% of cells finely adhered to the disks that were then implanted in the bone defect (Figure 16b).

All the animals were underwent surgery under general anaesthesia. A critical lesion of 8 mm of diameter was bilaterally created in the proximal tibia of each animal by the use of a dental trephine. The animals were previously divided into four groups, as shown in Table 5.

Group	Defect treatment	Side	n
A	Untreated	Right	6
B	HA	Left	6
C	rbASCs	Right	6
D	rbASCs-HA	Left	6

Table 5. Experimental Scheme of the Bone Defects Treatment.

For group A, the lesion was left untreated as a control, whereas in the left tibia (group B) the defect was filled with just HA disks. In group C, a semi-liquid suspension of 1.5×10^6 autologous rbASCs in 40 µl of medium was directly inoculated in the lesion site, before the last stitches. At last, in group D, the combination of autologous rbASCs and HA disks was implanted.

All the rabbits survived during the experimental study without any complications during the surgical procedures and the follow up. No bone resorption, abnormal bone callous formation, fractures, extrusions, infections, or severe inflammatory reactions were observed. The next day after surgery, all the rabbits could move regularly in their cages.

Radiological Assessment and Gross Appearance Analyses

The surgical outcome and the state of bone healing during the study were evaluated by lateral radiographs immediately after the surgical treatment (T_0), 6 weeks after intervention (T_6) and post-tibia removal (8 weeks, T_8). At T_0, we observed that all the scaffolds were correctly placed and no bone fracture was present at the lesion site (Figure 17, T_0). The second radiographic analysis evaluated the status of the bone regeneration process, and no signs of osteolysis, fracture, or osteopenia were observed and all the lesions showed a quite advanced bone remodeling process (Figure 17, T_6).
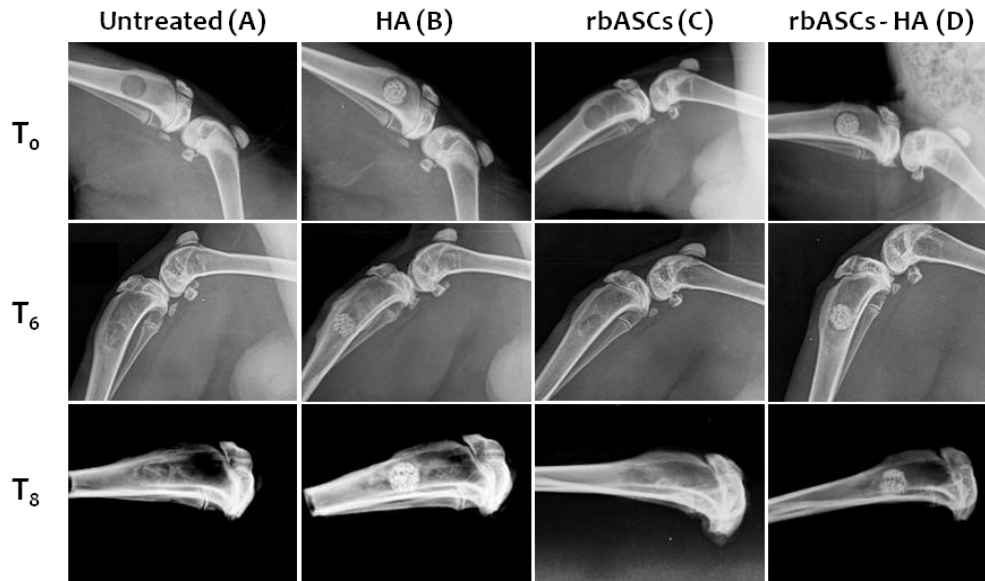
Figure 17. Rabbits were X-rayed immediately after surgical treatment (T_0), after 6 weeks from intervention (T_6), and post-tibia removal (8 weeks, T_8) Untreated group (group A), treated with hydroxyapatite scaffold (group B), semi-liquid suspension of rbASCs (group C) and with the combination of rbASCs loaded on hydroxyapatite (group D).

8 weeks later, the animals were sacrificed and the tibia explanted. In order to evaluate bone integration, we applied the scoring system showed in Table 6.

Gross Appearance Analyses		Radiographic Analyses
Filling	*Stiffness*	*Bone Integration*
Same level = 3	Same stiffness = 3	Good repair / integration = 3
Overgrowth = 2	Softer = 2	Overgrowth = 2
Undergrowth > 1 mm = 1	Very soft = 1	Undergrowth > 1 mm = 1-0

Table 6. Morphologic and radiographic scoring system for the evaluation of the bone regeneration process.

In all the four groups bone defects were satisfactorily filled and, according to the modified Wakitani scale, the stiffness was considered good. Indeed, no significant differences were observed between the control and rbASCs treated group (Figure 18). The same observation was made for scaffold-implanted cells, where no significant differences have been observed between empty or seeded scaffolds (Figure 18). Only in one defect of group D, we observed a modest mobilization of the scaffold.
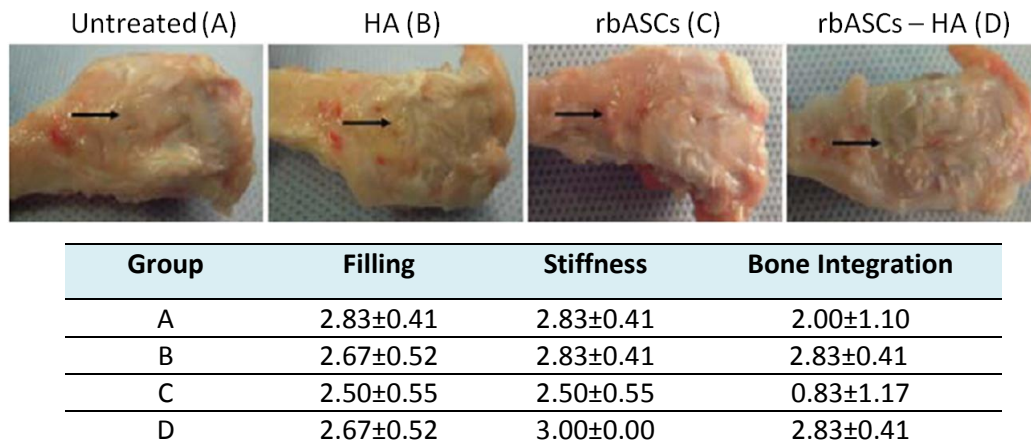
Group	Filling	Stiffness	Bone Integration
A	2.83±0.41	2.83±0.41	2.00±1.10
B	2.67±0.52	2.83±0.41	2.83±0.41
C	2.50±0.55	2.50±0.55	0.83±1.17
D	2.67±0.52	3.00±0.00	2.83±0.41

Figure 18. Morphological appearance of untreated group (group A), treated with hydroxyapatite scaffold (group B), semi-liquid suspension of ASCs (group C) and with a combination of ASCs loaded on hydroxyapatite (group D) at 8 weeks of follow-up (upper panel). Analyses of the tibia explanted from the 4 animal groups. No significant differences have been depicted. A, untreated; B, HA; C, rbASCs; D, rbASCs - HA (lower panel).

Bone integration was also checked by radiographic analysis. Bone defects of group A, seemed to be partially filled in a non-homogeneous way, showing a mild periosteal reaction, whereas the use of just rbASCs (group C) allowed a more complete and homogeneous filling of the lesion. In both groups B and D, the scaffolds showed signs of good osteointegration, even if a conspicuous amount of HA was not reabsorbed and still clearly evident (Figure 17, T_8).

Evaluation of Bone Mineral Density (BMD)

The amount of mineral matter per square centimetre of new bones in the lesion site was evaluated by bone mineral density (BMD) analysis. The BMD of R1 and R3 regions resulted very homogeneous among all groups and not significantly different from normal tibia values. R1 BMD mean values were 0.31±0.01, 0.27±0.04, 0.29±0.05, and 0.28±0.05 g/cm^2 for groups A, B, C, and D, respectively; R3 BMD mean values were 0.81±0.15, 0.77±0.01, 0.58±0.12, and 0.70±0.12 g/cm^2. The group A's mean R2 BMD value (just lesion) was not significantly different from those of group C (just ASCs) too, with values of 0.46±0.03 and 0.40±0.08 g/cm^2, respectively. For scaffold-treated groups, R2 mean BMD's value was 0.73±0.05 g/cm^2 for group D, showing an increase of 15% respect to those of group B (0.66±0.05), even if this difference was not statistically significant. Normal tibial density was 0.34±0.01, 0.48±0.01, and 0.60±0.01 g/cm^2 for R1, R2, and R3, respectively .

Histological and Immunohistochemical Analyses

The untreated defects (group A) showed little or no new bone formation; just a periosteal reaction participated in the defect repair (Figure 19a). The semi-liquid suspensions directly injected in the lesions of the animals of group C revealed that newly formed bone was present to fill the defect and that it had a distinct woven matrix conformation (Figure 19c). In the scaffold-implanted defects (groups B and D, Figure 19b and 19d, respectively), analyses revealed variable amounts of newly formed bone. Both in the absence and in the presence of rbASCs, the new bone formation was observed within the scaffold pores in all the implants, as well as a small number of multinucleated giant cells. In the cell-free scaffolds, bone formation did not occur at a uniform rate within the pores: the new bone was always in a direct contact with the walls of the pores, whereas the central part of the pores was commonly filled with bone marrow (Figure 19b). In particular, most of the larger pores were filled with adipocytes, suggesting the presence of poorly differentiated bone marrow. The rbASCs-HA constructs showed a lower rate of pores filled with adipocytes respect to those of group B. Moreover, in the cell-seeded scaffolds, pores were filled more homogeneously (Figure 19d): along the walls we observed new mature bone and in the inner part connective fibrous tissue, indicating an ongoing maturation process of bone tissue. In both groups, osteoblasts were observed in conjunction with bone trabecules, located at the periphery of the scaffold pores, which displayed a lamellar matrix.
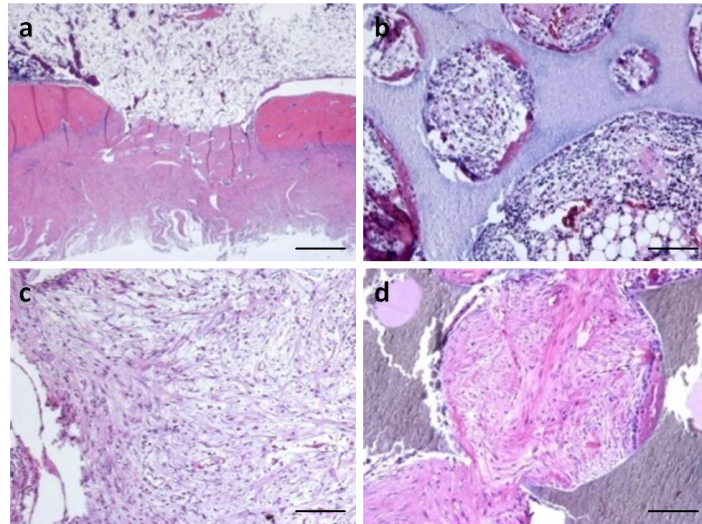
Figure 19. Histological analyses of sections of decalcified tibial samples. Periosteal reaction in the defect reparation site of group A (a). Newly formed tissue at the lesion site of group treated with hydroxyapatite scaffold (b), semi-liquid suspension of rbASCs (c) and with the combination of rbASCs loaded on HA (d). Haematoxylin-eosin staining (a, scale bar - 500 μm; b, scale bar – 100 μm; c-d, scale bar - 200 μm).

The expression of specific proteins of bone tissue was also detected on tissue sections by immunohistochemical analysis. In particular, it was analyzed the expression of collagen type I (Coll I) and osteopontin (OPN). Immunohistochemistry confirmed the results of histological analysis, in fact, a variable amount of newly formed bone tissue was observed within the pores of the scaffold either in the presence and in the absence of rbASCs.

The expression of two markers of osteogenic differentiation was absent in 75% of the untreated tibia samples (group A) and was extremely weak in the remaining (Figure 20a and Figure 21a). The same result was obtained when the defect was treated by rbASCs injection (Figure 20c and Figure 21c).

Strong immunopositivity of new bone tissue for Coll I and OPN proteins were observed in conjunction with bone trabecules located at the periphery of the scaffold pores both in group B and D, even if bone formation did not occur at a uniform rate within the pores themselves (Figure 20b,c and 21b, c). In particular, in all rbASCs-scaffold implanted defects, several positive osteoblasts and new mature lamellar bone matrix, strongly positive for Coll I and OPN, were observed, all along the walls of the pores; however, also in the inner part, immunostaining revealed the positivity of the connective fibrous tissues for these markers (Figure 20d and Figure 21d). In contrast, the defects treated with not seeded HA presented positive osteoblasts only along the wall of the pores, whereas the inner part

is filled by less mature fibrous tissue, with some residual bone marrow, faintly positive for Coll I and OPN (Figure 20b and Figure 21b).

Figure 20. Expression of collagen type I in sections of tibiae. Untreated group (a), group treated with just autologous rbASCs (b), scaffold alone(c, arrow) and group treated with autologous rbASCs in combination with HA (d, arrow) (scale bar 100 μm).
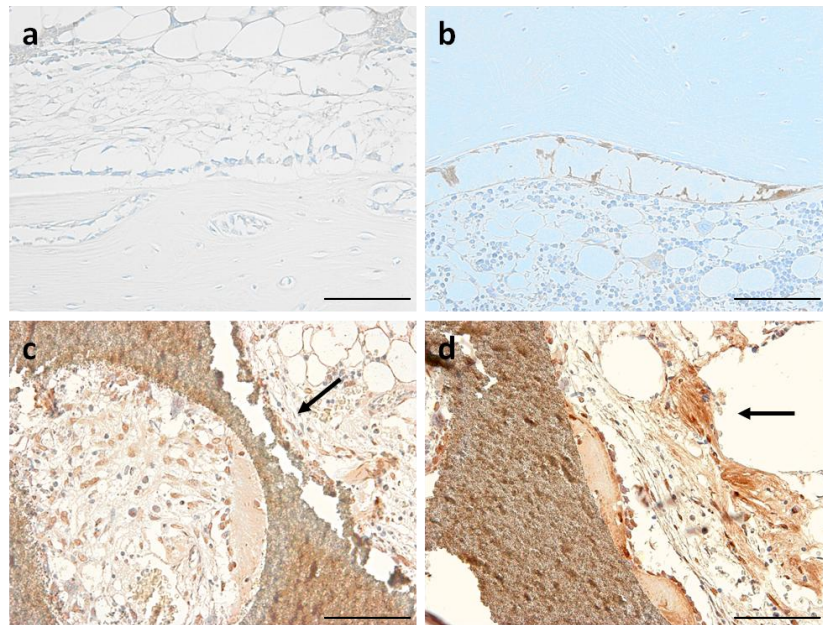

Figure 21. Expression of osteopontin in sections of tibiae. Untreated group (a), group treated with just autologous rbASCs (b), scaffold alone(c, arrow) and group treated with autologous rbASCs in combination with HA (d, arrows) (scale bar 100 μm).
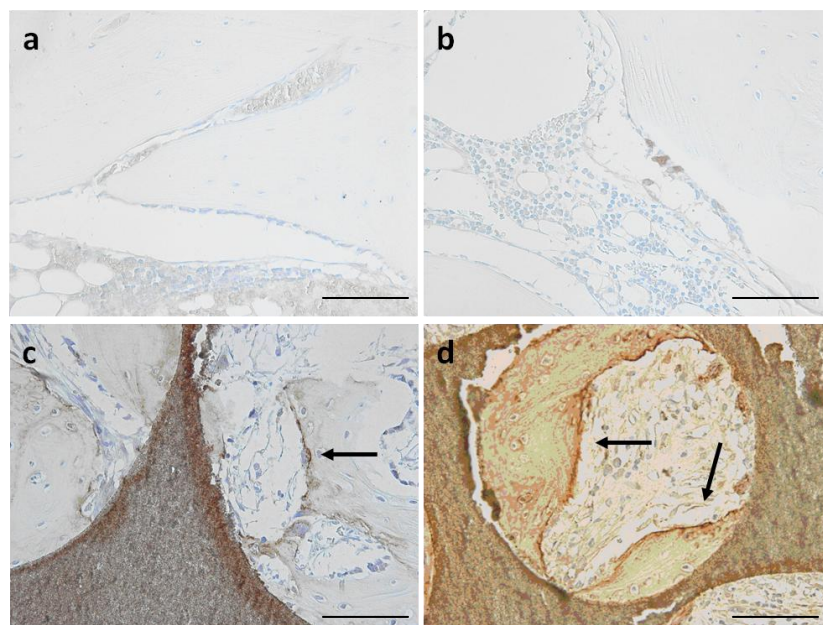
Inside the pores of the scaffold and in the presence of rbASCs was also observed the presence of plurinucleate giant cells and osteoclasts that are responsible of bone resorption and are able to destroy the mineral component of bone and enzymatically digesting the organic ones (Figure 22).
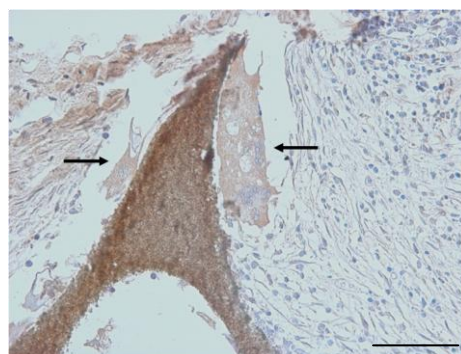

Figure 22. Bone resorption performed by osteoclasts (arrows) located in the proximity of the pores of the scaffold (scale bar 200 μm).

Histomorphometric Analyses

Histological examination of the explanted specimens (5 μm thick sections), stained with Toluidine blue/Pyronine Y (Figure 23a), showed an important formation of new bone without inflammatory infiltrate.

In both scaffold-implanted defects with or without rbASCs, similar amount of HA was still detectable: 30.3±5.6% and 29.2±4.1% of the new tissue filling the defects was composed by HA for group D and group B, respectively. No Howship's lacunae with resorption activity were visible next to the walls of the scaffold pores. Considering the overall area of the defect, also similar quantities of new bone were found between the two samples with a percentage of 21.9±4% for group D and of 20.4±4.3% in group B, with some differences in its spatial distribution (Figure 23 and 24). Indeed, in the unseeded scaffold, the new bone filled in almost all the pores at the level of the walls (Figure 23b, c), but only few regenerated areas were present in the inner portion of the defect where a poorly cellular adipose tissue was prevalent (Figure 23c). In contrast, in the cell-seeded scaffold the new bone formation seemed to proceed from the periphery to the centre of the defect and remarkable amount of new bone was present within the pores localized in the cancellous part of the tibia (Figure 23d, e). In particular, the HA pores of small dimensions were filled

by new bone for about one third, while the larger pores contained variable amounts of regenerated bone at their boundary (Figure 23e). The new bone consisted of immature tissue with a prevalent woven bone structure. In the regenerated areas, the surface of mineralized tissue was surrounded by osteoid matrix covered by a layer of osteoblast-like cells. Bone marrow spaces were filled by undifferentiated mesenchymal cells, adipocytes and several blood vessels with erythrocytes; the proportion of adipose tissue increased in the deeper part of the defect (Figure 23e).
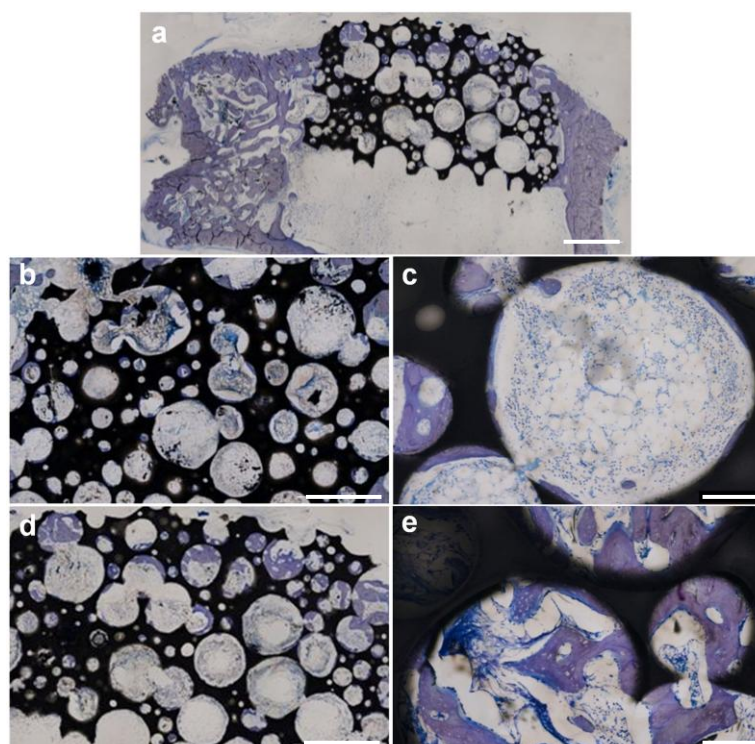
Figure 23. Representative thick section of undecalcified tibia stained with Toluidine blue/Pyronine Y (~40 mm of thickness, 4X magnification - scale bar 500 µm) (a). Group B - HA (b, c) and group D - rbASCs-HA (d, e) defect area in which histomorphometric analyses were performed using a standard point-counting technique (4X magnification - scale bar 500 µm) (b, d). Microphotographs of hydroxyapatite pores of each experimental groups (10X magnification - scale bar 100 µm) (c, e).
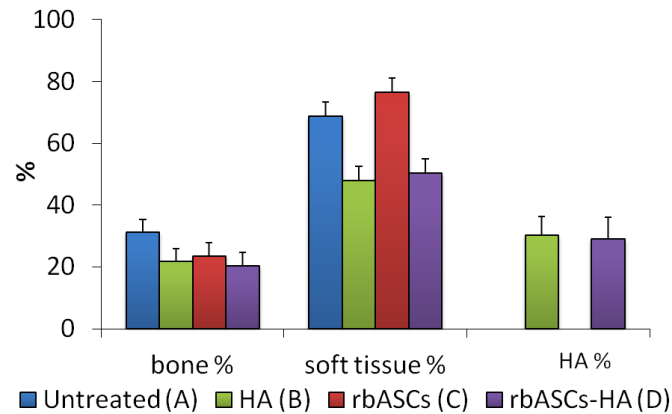
Figure 24. Graphic representation of the percentage of new formed bone tissue, soft tissue and not resorbed HA in the four experimental groups.

Biomechanical Tests

Nanoindentation is derived from the classical hardness test, but it is carried out on a much reduced scale. 4x4 indentation matrices showed a good reproducibility of the experiments in terms of loading-unloading curves repeatability and in terms of reduced modulus (*Er*) and hardness (*H*), where a ratio between standard deviation and mean value lower than 10% was obtained. These measurements involve applying a small force (1mN, 5mN, and 50mN) to a sample using a sharp probe and measuring the resultant penetration depth. The measured values are used to calculate the contact area and hence the particular property of the sample material. Residual indents left by the nanoindentation testing at a maximum force of 50 mN were clearly visible (Figure 25a, b).

A comparison of the reduced modulus *Er* and the hardness H of the two analyzed groups at the three investigated loads was reported as a function of the mean penetration depth with the purpose to show how the mechanical properties of the tissue were in fact evaluated over characteristic lengths spanning one order of magnitude.

Defects treated with rbASCs-HA show improved mechanical properties, suggesting that these constructs have an improved capability to bear mechanical loading. This is quite evident at low forces (1mN, corresponding to 200 nm of penetration depth), where it is possible to observe an increase of 19.8% in stiffness and 31.6% in hardness for rbASCs-HA treated group with respect to HA-group (Figure 25). In contrast, at the highest depth the

opposite outcome has been found; i.e. the empty scaffold treated group is slightly stiffer and harder than the other one (Figure 25).

The obtained reduced moduli Er and the hardness H are summarized in Table 7.
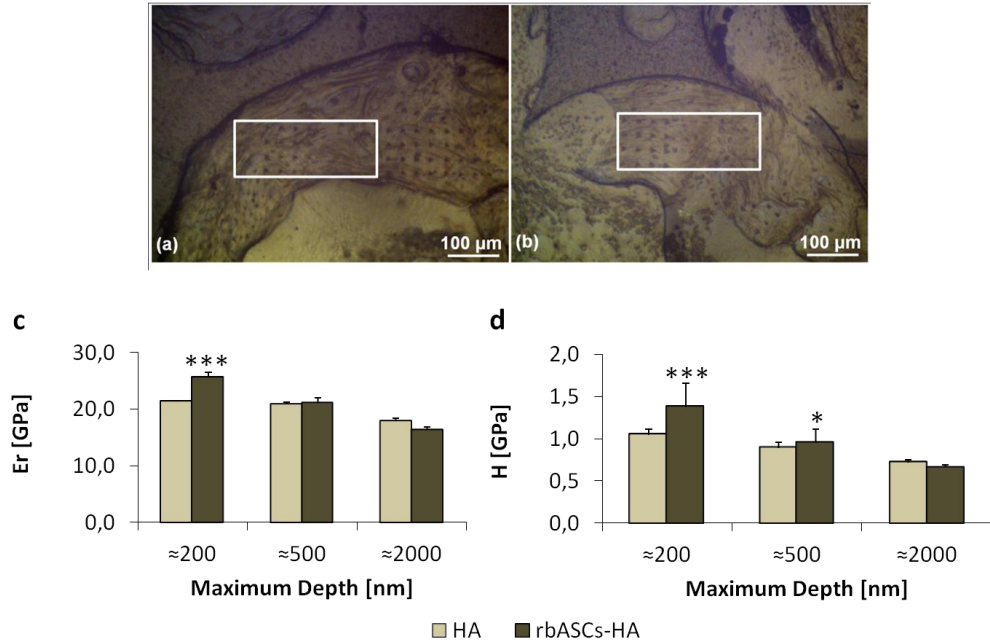
Figure 25. Locations of the indentation experiments for the empty hydroxyapatite disk group B - HA (a) and for the hydroxyapatite disk (group D - rbASCs-HA) (b). The white boxes approximately include the specific regions where the tests were carried out. Residual indents at a maximum force of 50 mN are clearly seen. Reduced moduli Er (c) and hardness H (d) of the two analyzed groups at the three investigated loads (1mN, 5mN and 50mN, corresponding to ≈200 nm, ≈500 nm, and ≈2000 nm maximum depths, respectively) are reported (mean ± SD) (n=44).

Er [GPa]	Load		
	1mN	*5mN*	*50mN*
HA	21.39±2.48	20.84±1.99	17.93±1.80
rbASCs-HA	25.71±3.55	21.16±1.46	16.35±1.23

H [GPa]	Load		
	1mN	*5mN*	*50mN*
HA	1.08±0.09	0.87±0.08	0.70±0.04
rbASCs-HA	1.40±0.31	0.96±0.11	0.65±0.04

Table 7. Reduced moduli Er and hardness H of samples from group B - HA and group D - rbASCs-HA. Data are expressed as mean ± SD.

...BEFORE MOVING TO THE CLINIC...

On the basis of their regenerative properties, hASCs could become important tools for cell-mediated therapy in bone diseases. Preclinical applications for hASCs in muscle-skeletal tissue engineering are reported [Abdallah and Kassem, 2008; de Girolamo/ Arrigoni et al., 2011; Arrigoni et al., submitted], but, there are several aspects that have to be considered before moving to the clinic.

✓ If autologous cellular therapy will be chosen, may the ability of human ASCs to osteo-differentiate be affected by the donor's physio/pathological conditions?

✓ May the use of selected pharmacological treatment, such as Reversine, enhance the cellular plasticity?

✓ If autologous or heterologous cellular application will be applied, may the use of immunoselected CD34+ and L-NGFR hASCs be advantageous in the field of skeletal-muscle tissue regeneration?

MATERIALS AND METHODS

1. Isolation of Human Adipose-derived Stem Cells (hASCs)

Adipose tissue used in these studies was collected by the surgeons at the IRCCS Galeazzi Orthopaedic Institute of Milan. Subcutaneous fat aspirates were obtained from donors, after written consent and Institutional Review Board (IRB) approval. Primary cultures of the stromal vascular fraction (SVF) were established as previously described with minor modification. Briefly, the matrix was digested with 0.075% type I collagenase in a shaking water bath at 37°C for 30 minutes and then centrifuged for 10 minutes at 1200 g to separate the SVF from adipocytes, cellular debris and undigested tissue. Cells derived from the SVF were plated in control medium, at 10^5 cells/cm^2. The cells were maintained at 37°C in a humidified atmosphere with 5% CO_2. After 24 to 48 hours, non-adherent cells were discarded and the medium was changed twice a week [Zuk et al., 2001]. Once they reached 80-90% of confluence, cells were detached by 0.5% trypsin/0.2% EDTA (Sigma-Aldrich) and plated at a density of 10^4 hASCs/cm^2 for further expansion and experiments.

2 . Positive Selection of CD34+ and L-NGFR+ hASCs

hASCs obtained from liposuction has been divided into three fractions: one of these fractions, obtained simply by adherence to plastic, representing the total cell population (PA, Plastic Adherence) and two fractions selected by immunomagnetic sorting by the expression of markers CD34 or L-NGFR.

hASCs were positively selected for CD34+ and L-NGFR+ using the Direct CD34 Progenitor Cell Isolation Kit and the CD271 Microbead Kit, respectively (Miltenyi Biotech, Calderara di Reno, Italy), according to the manufacturers' instructions.

Briefly, using the Direct CD34 Progenitor Cell Isolation Kit, the cell suspension was centrifuged at 300 g for 10 minutes and resuspended in 300 µl of buffer (PBS supplemented

with 0.5% BSA, and 2 mM EDTA). Starting from 10^8 cells, 100 µl of FcR Blocking Reagent were added to prevent non-specific binding of cells to the microspheres. 100 µl of CD34 MicroBeads were then added to the cell suspension and the samples were incubated for 30 minutes at 4°C. After incubation, hASCs were washed with 5-10 ml of buffer, centrifuged at 300 g for 10 minutes and resuspended in 500 µl of buffer. Cell suspension was loaded onto a MACS® Column which was placed in the magnetic field of a MACS Separator. The magnetically labeled CD34+ cells were retained within the column. The unlabeled cells run through; this cell fraction is thus depleted of CD34+ cells. After removing the column from the magnetic field, the magnetically retained CD34+ cells can be eluted as the positively selected cell fraction.

In CD271 Microbead Kit, cells were firstly labeled with CD271 (LNGFR)-PE, and then with Anti-PE MicroBeads. The cell suspension was then loaded onto a MACS® Column placed in the magnetic field of a MACS Separator. The magnetically labeled CD271 (LNGFR)+ cells were retained on the column. The unlabeled cells run through; this cell fraction is thus depleted of CD271 (LNGFR)+ cells. After removing the column from the magnetic field, the magnetically retained CD271 (LNGFR)+ cells can be eluted as the positively selected cell fraction.

CD34+ and L-NGFR+ cells were then counted and assessed for viability; their purity was determined by flow cytometry.

3. Flow Cytometry

Flow cytometry is the technique most commonly used for the detection of cell membrane antigens. Cell suspensions are incubated with specific antibodies directed against membrane antigens, directly or indirectly labelled with a fluorescent dye. UV exposure of these samples causes the emission of fluorescence from the dye. The individual cells in the suspension is passed through a laser and analyzed for fluorescence emission using special tools (Fluorescence Activated Cell Sorter, or FACS).

hASCs ($3X10^5$ per sample) were washed in PBS supplemented with 10% FBS, 0.01% NaN_3 (FACS Buffer, FB) to remove the growth medium. All the procedures were performed on ice to increase the antigen-antibody binding and to prevent the antibodies internalization. Cells were centrifuged and the pellet were resuspended in 100 µl FB with the primary antibody

(Table 1) and incubated for 30 minutes on ice. After incubation, samples were washed 2 times with FB and primary antibodies were revealed with secondary antibody either with Streptavidin-PE or FITC conjugated sheep anti-mouse Ab for 20 minutes at 4°C. Samples were then washed with FB, resuspended in 500 µl of FB and analyzed using FACS (FACSCalibur flowcytometer - BD Biosciences Europe, Erembodegem, Belgium) and data was analyzed using CellQuest software (BD Biosciences Europe).

PRIMARY ANTIBODY	FUNCTION	SPECIES	TYPE	COMPANY
CD13	Aminopeptidase N - Zinc-binding metalloproteinase	Mouse	Monoclonal FITC	Ancell
CD14	LPS/LBP receptor	Mouse	Monoclonal FITC	Ancell
CD29	VLA-1/4 subunit (β1 Integrin)	Mouse	Monoclonal Byotinilated	Ancell
CD34	Stem cell marker	Mouse	Monoclonal Byotinilated	Ancell
CD44	H-CAM - Adhesion	Mouse	Monoclonal FITC	Alexis
CD45	LCA - Leukocyte common antigen	Mouse	Monoclonal FITC	Ancell
CD49d	VLA-4 subunit (α4 Integrin)	Mouse	Monoclonal Byotinilated	Ancell
CD54	ICAM-1 - Adhesion	Mouse	Monoclonal Byotinilated	Ancell
CD71	T9 - Transferrin receptor	Mouse	Monoclonal Byotinilated	Ancell
CD90	Thy-1 - stem cell and neuron differentiation	Mouse	Monoclonal Byotinilated	LabVision
CD105	Endoglin - TGF-β1 receptor	Mouse	Monoclonal Byotinilated	Ancell
CD106	VCAM-1 - Adhesion	Mouse	Monoclonal Purified	LabVision
CD271	Neurotrophin-receptor - L-NGFR	Mouse	Monoclonal PE	Santa Cruz

SECONDARY ANTIBODY	SPECIES	LABEL	COMPANY
Sheep anti-mouse	Sheep	FITC	Boheringer
Streptavidin (SA)		PE	Ancell

Table 1. Primary and secondary antibodies used in FACS experiments.

4. MTT Cell Proliferation Assay

10^4 cells/cm^2 of hASCs were plated in control medium and MTT assay was performed as previously reported.

5. Fibroblast Colony Forming Unit (CFU-F) Assay

A colony forming unit - fibroblast assay was performed as previously described, with minor modifications. hASCs were plated in 6-well plates at low density by limiting dilution (starting from 48 cells/cm^2, ending dilution 1 cell/cm^2) and cultured at 37°C in a humidified atmosphere with 5% CO_2 in CTRL medium supplemented with 20% FBS. After 6 days the medium was replaced, and 10 days after cells were fixed with 100% methanol (Sigma-Aldrich) and stained with 2 mg/ml Crystal Violet (Fluka). The frequency of CFU-F was established by scoring the individuals colonies and expressed as a percentage relative to the seeded cells.

6. Osteogenic Differentiation

10^4 cells/cm^2 were induced to differentiate on monolayer in osteogenic medium (OSTEO), as previously reported. After 14 and 21 days, alkaline phosphatase activity and extracellular calcified matrix deposition were determined as previously described.

7. Adipogenic Differentiation

10^4 cells/cm^2 were induced to differentiate into the adipogenic lineages using a pulsed induction comprising 48 hours in control medium supplemented with 1 µM dexamethason (Sigma-Aldrich), 10 µg/ml insulin (Sigma-Aldrich), 500 µM 3-isobutyl-1-methyl-xanthine (IBMX, Sigma-Aldrich) and 200 µM indomethacin (Sigma-Aldrich), followed by 48 hours maintenance in CTRL medium supplemented only with 10 µg/ml insulin. After 14 and 21 days, the medium was removed and cells were rinsed, fixed in 10% neutral buffer formalin for 1 hour and stained with fresh 2% w/v Oil Red O in 60% isopropanol (ORO, Sigma-Aldrich) for 15 minutes. Oil Red O is a neutral lipid-soluble dye used to detect the presence of triglycerides and non-polar lipids, due to its partition coefficient that allows it to

concentrate in the polar phase. After incubation the dye was removed and the excess dye was removed by washing with distillate H_2O, and the samples were then photographed. To quantify the lipid vacuole content, the dye was extracted with 100% isopropanol and absorbance was read at 490 nm using Wallac Victor II plate reader. Adipogenic differentiation was also evaluated analyzing PPAR-γ expression by Western Blot analysis as previously described. 15 μg of proteins were loaded on 10% SDS-PAGE and electrotransferred onto Hybond-ECL[TM] extra nitrocellulose membrane (Amersham Bioscience). After blocking in 5% non-fat dry milk in TBS and 0.1% Tween-20 for 1 hour at room temperature, the membrane was incubated with rabbit anti-PPAR-γ (Santa Cruz Biotecnology Inc) and mouse anti-β-actin (Sigma-Aldrich), diluted 1:500 and 1:3000, respectively. This was followed by incubation with horseradish peroxidise (HRP)-conjugated secondary antibodies (GE Healtcare) for 1 hour at room temperature. Protein visualization was performed using the ECL[TM] Western blotting analysis kit (GE Healtcare) according to the manufacturing protocol. The images were analyzed using ImageJ software.

8. Chondrogenic Differentiation

Chondrogenic differentiation was induced in pellet culture conditions: 5×10^5 hASCs were centrifuged (500 g , 5 minutes) in a 15-mL centrifuge tube, the pellets were resuspended either in control or in chondrogenic medium consisting of DMEM supplemented with 1% FBS, 50 U/mL penicillin, 50 μg/mL streptomycin, and 2 mM L-glutamine, 1 mM sodium pyruvate (Sigma-Aldrich), 0.15 mM L-ascorbic acid-2-phosphate (Sigma-Aldrich), 1× ITS (Sigma-Aldrich), 0.1 μM dexamethason (Sigma-Aldrich), and 10 ng/mL TGF-β1 (Biosource-Invitrogen, Camarillo, CA) and then centrifuged again (500 g, 5 minutes). After 21 days, micromasses were digested overnight at 56°C by proteinase K (50 μg/ml in 100 mM K_2HPO_4, pH 8.0, final digestion volume 100 μl; Sigma-Aldrich). The next day, the digestion was blocked by incubating the samples at 90°C for 10 minutes to inactivate the proteinase K [Calabro et al., 2000]. Sulphated glycosaminoglycans (GAGs) were then quantified according to a modified version of the dimethylmethylene blue (DMMB; Sigma-Aldrich) assay [Barbosa et al., 2003]. 50 μl of each sample were incubated for 30 minutes with 400 μl of DMMB Complexation Solution to allow the DMMB to form an insoluble complex with glycosaminoglycans. Briefly, DMMB Complexation Solution was made of 3.2 mg DMMB

dissolved in 5 ml ethanol and filtered through filter paper. 40 ml of 1 M GuHCl, 0.25 g sodium formate, and 0.4 ml 98% formic acid were then added to the DMMB ethanol solution, and the final volume was completed to 200 ml with distilled H_2O. After incubation, the samples were centrifuged at 12000 g for 10 minutes and the supernatant was removed. The pellets were then resuspended in 350 µl of Decomplexation Solution: 50 mM sodium acetate solution buffer (pH 6.8) containing 10% 1-propanol was prepared and used to solubilise powdered GuHCl to a final concentration of 4 M; this solution consist of an high salt concentration to prevent the maintenance of the link between glycosaminoglycans and DMMB. Absorbance was read at 655 nm and the GAGs content, expressed as µg GAGs/micromass, was determined using bovine trachea chondroitin-4-sulfate (Sigma-Aldrich) as standard. GAGs content of each sample was normalized with respect to DNA measured by Hoechst 33258 fluorescence assay (355 nm excitation - 460 nm emission, Wallac Victor II plate reader). For each micromass lysate were assayed 5 µl of sample adding 5 µl of TNE buffer (10 mM Tris, 200 mM NaCl, 1 mM EDTA, pH 7.4) to obtain a final volume of 10 µl. In each well were added 200 µl of a solution 0.2 µg/ml Hoechst 33258 (Sigma-Aldrich) in TNE buffer; the samples were incubated 1 minute and the fluorescence was read using the microplate reader Wallac Victor-1420. Data were interpolated in a standard curve of salmon sperm DNA (range 1.25-40 µg/ml).

9. hASCs-Scaffold Constructs

10^5 undifferentiated hASCs were seeded on porous (60%) hydroxyapatite blocks (HA) (Finceramica, Faenza, Italy) and silicon-carbide-plasma-enhanced chemical vapour deposition (SiC-PECVD) fragments. Cells were allowed to adhere overnight to scaffolds in polypropylene vial, then transferred to a 24-well plate and cultured in static conditions for 14 and 21 days. The SiC-PECVD samples were assessed for ALP activity after 14 days of differentiation and for calcium deposition after 21 days; ALP activity at 14 and 21 days was evaluated for HA samples.

10. Reversine Treatment

Reversine was synthesized in the laboratories of Dr. Anastasia according to the published procedure [Chen et al., 2004], and its purity ($\geq$ 98%) was checked by HPLC and LC-MS analysis. All Reversine treatments were conducted 24 hours after cell seeding in CTRL medium and maintained for 72 hours. Control cells were incubated with DMSO at the same concentration used for dissolving Reversine (0.05% w/v).

10.1. MTT Cell Proliferation Assay

hASCs were plated at a density of 5×10^3 cells/cm^2 in control medium in 96-well plate. hASCs viability was monitored at various time points (1-3 days during Reversine treatment; 1-3-7 days after Reversine treatment), using different Reversine concentration (50-250-750 nM, 1.5-5 µM), and MTT assay was performed as previously reported.

10.2. Osteogenic Differentiation

4×10^3 control or Reversine 50 nM and 5 µM pre-treated cells/cm^2 were induced to differentiate on monolayer in osteogenic medium (OSTEO). Osteogenic differentiation of hASCs was assessed by evaluating morphological changes, alkaline phosphatase staining, expression by Real Time PCR, and enzymatic activity. For ALP staining cells were fixed with 4% paraformaldehyde at room temperature for 10 minutes and stained with ALP staining according to the manufacturer's procedures (Sigma-Aldrich). ALP expression was also determined by Real Time PCR (Table 2). Total RNA was isolated with RNeasy Mini kit (Qiagen, Milan, Italy) and cDNA was synthesized starting from 0.8 µg of RNA, with the iScript cDNA Synthesis kit (Bio-Rad Laboratories) according to the manufacturer's instruction. Briefly, 10 ng of total RNA was used as template for real-time PCR performed using the iCycler thermal cycler (Bio-Rad Laboratories). PCR mixture included 0.2 µM gene-specific primers for human ALP or human UBC (Ubiquitin), which was used as housekeeper gene, 50 mM KCl, 20 mM Tris/HCl, pH 8.4, 0.8 mM dNTPs, 0.7 U iTaq DNA Polymerase, 3 mM MgCl$_2$, and SYBR Green (iQ SYBR Green Supermix from Bio-Rad Laboratories) in a final volume of 20 µl. Amplification and real-time data acquisition were performed using the

following cycle conditions: initial denaturation at 95°C for 3 minutes, followed by 40 cycles of 10 seconds at 95°C and 30 seconds at 57°C.

10.3. Smooth Muscle Cells Differentiation

Control or Reversine 50 nM and 5 µM pre-treated hASCs were plated at the concentration of $4x10^3/cm^2$ and induced to differentiate to smooth muscle cells using DMEM supplemented with 1% FBS and 0.2 µl/ml TGF-β1 (Millipore) for 7 days. Cells were then fixed with 4% (w/v) paraformaldehyde at room temperature for 10 minutes and permeabilized with 0.1% (w/v) Triton X-100 and 1% (w/v) BSA in PBS for 30 minutes. Immunostaining was carried out with anti smooth muscle α-actin (α-SMA) monoclonal antibody (Sigma-Aldrich) at 1:200 dilution. After incubation with primary antibody cells were washed three times in PBS and incubated with FITC-conjugated secondary antibodies 1 hour at room temperature. After washing in PBS, cells were analyzed under a fluorescent microscope. Cell nuclei were counterstained with Hoechst 33342 (1:500) for 15 minutes. Smooth muscle α-actin expression was determined by Real-Time PCR, as described before for ALP, but using the primer showed in Table 2.

10.4. Skeletal Muscle Cells Differentiation

After 50 nM Reversine (or DMSO) treatment for three days, hASCs were washed twice with PBS and twice with DMEM containing 10% FBS. C2C12 myoblasts were then added to stem cells containing plates in a ratio of 4:1, C2C12 being prevalent. The following day co-cultures were shifted in DMEM supplemented with 2% horse serum HS (Sigma-Aldrich) and differentiation was carried out for 7 days. Cells were then fixed with 4% (w/v) paraformaldehyde at room temperature for 10 minutes and then permeabilized with 0.1% (w/v) Triton X-100 and 1% (w/v) BSA in PBS for 30 min. Cells were incubated for 1 hour at room temperature with the following primary antibodies: anti-human nuclei antibody (Millipore) at 1:400 dilution, anti-myosin heavy chain (MF20) monoclonal antibody (Sigma-Aldrich) at 1:100 dilution. After incubation cells were washed three times in PBS and incubated with the appropriate FITC- or TRIC-conjugated secondary antibodies (Sigma-Aldrich) 1 hour at room temperature. After washing in PBS, cells were analyzed under a

fluorescent microscope (Olympus IX51). Cell nuclei were counterstained with Hoechst 33342 (1:500) for 15 minutes.

10.5. Stem cell markers expression

The expression of Klf-4, c-Myc, Nanog and Oct4 was determined by Real-Time PCR, as described before for ALP, but using the primers Klf-4, c-Myc, Nanog, and Oct4, as shown in Table 2.

NAME	PRIMER FORWARD	PRIMER REVERSE
ALP	CGCACGGAACTCCTGACC	GCCACCACCACCATCTCG
ACTA2	CTGTTCCAGCCATCCTTCAT	TCATGATGCTGTTGTAGGTGGT
Klf-4	GACTTCCCCCAGTGCTTC	CGTTGAACTCCTCGGTCTC
c-Myc	AGGAGGAACAAGAAGATGAGG	GTTGTGCTGGATGTGTGGAGA
Nanog	GGTCCCAGTCAAGAAACAGA	GAGGTTCAGGATGTTGGAGA
Oct-4	AGGAGAAGCTGGAGCAAAA	GGCTGAATACCTTCCCAAA

Table 2. List of primer used in the Real-Time PCR experiments.

RESULTS

Influence of Physiological Conditions on hASCs' Donors

In this study we evaluated the influence of age of female healthy donors, on proliferation, clonogenic ability and differentiation potential of mesenchymal stem cells isolated from human adipose tissue (hASCs).

hASCs were isolated from liposuction of subcutaneous adipose tissue from 26 female donors. We determined the progenitor cell numbers and clonogenic potential of hASCs derived from healthy-young-females under 35 years old (hASCs<35 y/o, n=12, mean age 31±4 years, BMI=23.5±1.6), and middle-age ones (hASCs>45 y/o n=14, mean age 56±7 years, mean BMI=28.4±1.8). We isolated an average of $2.7±1.3x10^5$ hASCs<35 y/o per ml of raw tissue, and $6.1±4.0x10^5$ from the older donors, as shown in Table 3. Despite the large fluctuations among samples derived from the over 45-years/old group, the cellular yield turned out to be significantly different in comparison to the younger group.

	n	Age	BMI	hASCs / ml of raw adipose tissue
hASCs<35 y/o	12	31±4	23.5±1.6	$2.7±1.3x10^5$
hASCs>45 y/o	14	56±7	28.4±1.8	$6.1±4.0x10^{5}$ **

Table 3. Comparison of cell number of hASCs derived from three groups of female. Cellular yield is expressed as the average of hASCs/ml of raw adipose tissue ± standard deviation.

After an initial lag phase of about one week, cells isolated from donors belonging both groups started to growth and presented a homogeneous fibroblast-like shape without any differences among the donors (Figure 1).
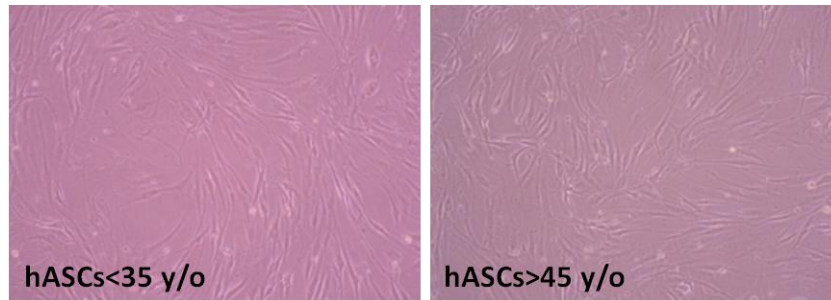
Figure 1. Morphology of two representing samples of cells isolated from donors under 35 years of age and over 45 years of age. Optical microscope photographs of hASCs grown in CTRL medium for 2 weeks after isolation (40X magnification).

hASCs cells isolated from young and elderly women reached 80-90% confluence about every 7 days: the doubling time (DT) was 123.9±10.6 and 148.2±14.6 hours for hASCs<35 y/o and hASCs>45 y/o, respectively. Donor's age did not influence the proliferation rate of hASCs, although a high inter-donor variability is observed (Figure 2).
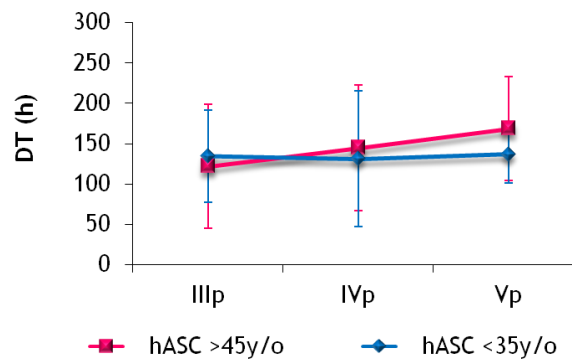

Figure 2. Average doubling time (DT) of different population of hASCs<35 y/o and hASCs>45 y/o; DT= t ×ln(2)/ln(N /N_0), where t is the time in culture (in hours), N is the final number of cells and N_0 is the initial number of cells (mean ± SD).

The clonogenicity of these cells has been compared by CFU-F assays (Figure 3). At earlier passages, hASCs from both younger and older groups produced colonies, although cells from younger donors showed a statistically significant increase in clonogenic activity (15±4% and 7±3%, respectively). This trend was maintained during passages, even if a slight decreased was observed in hASCs<35 y/o (data not shown).
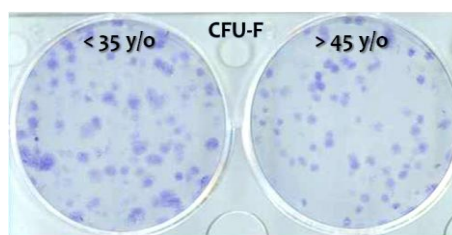
Figure 3. Microphotographs of colonies at passage 1 stained with Crystal Violet of hASCs isolated from younger and older donors, respectively.

By FACS analysis, no significant variations related to donor age were observed between hASCs isolated from younger and older donors. These cells expressed high levels of CD13, CD90, CD105 and CD44, whereas they did not express hematopoietic markers such as CD14, CD45 and CD71 (Figure 4). hASCs<35 y/o expressed more CD49d in comparison to hASCs>45 y/o; moreover, in hASCs<35 y/o, the expression of CD34 was variable (30.8±29.4%), whereas hASCs isolated from older donors were CD34 low.
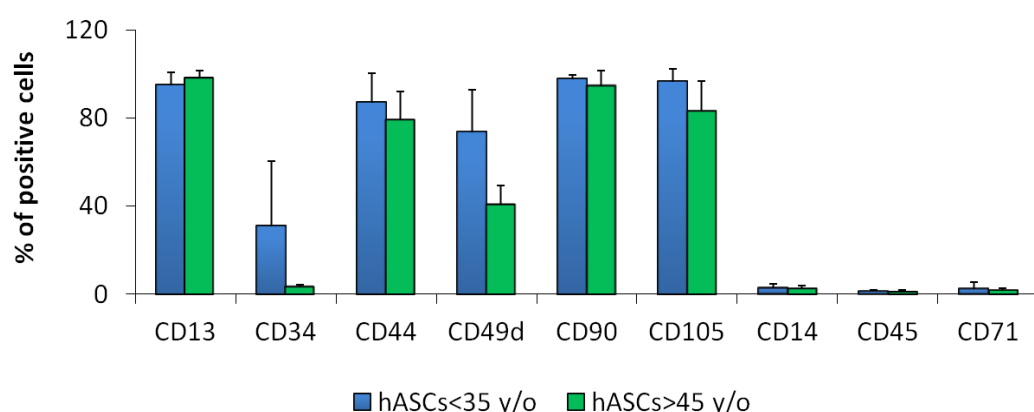

Figure 4. Immunophenotype of fresh human adipose-derived stem cells (hASCs) deriving from younger and older donors (hASCs<35 y/o and hASCs>45 y/o, respectively) (mean ± SD).

hASCs induced to differentiate towards adipocytes and osteoblast-like cells for two weeks, showed a significant morphological changes compared to undifferentiated hASCs (Figure 5a). The typical fibroblast-like morphology of undifferentiated hASCs was progressively lost when cells were maintained in adipogenic and osteogenic media; hASCs became large, with a cytoplasm full of lipid vacuoles, or less outstretched, with an indented cellular membrane, respectively. We did not observed any relevant morphological variations among all the older and younger females.

We have evaluated the hASCs adipocytes differentiation potential by comparing the amount of lipid vacuoles produced by several samples of adipogenic-differentiated hASCs, as shown in Figure 5. The *in vitro* adipogenic differentiation potential of younger and older donors was not statistically different, although the increase in lipid content of differentiated hASCs was 140 and 360% for cells derived from under 35 and over 45 years old donors, respectively.
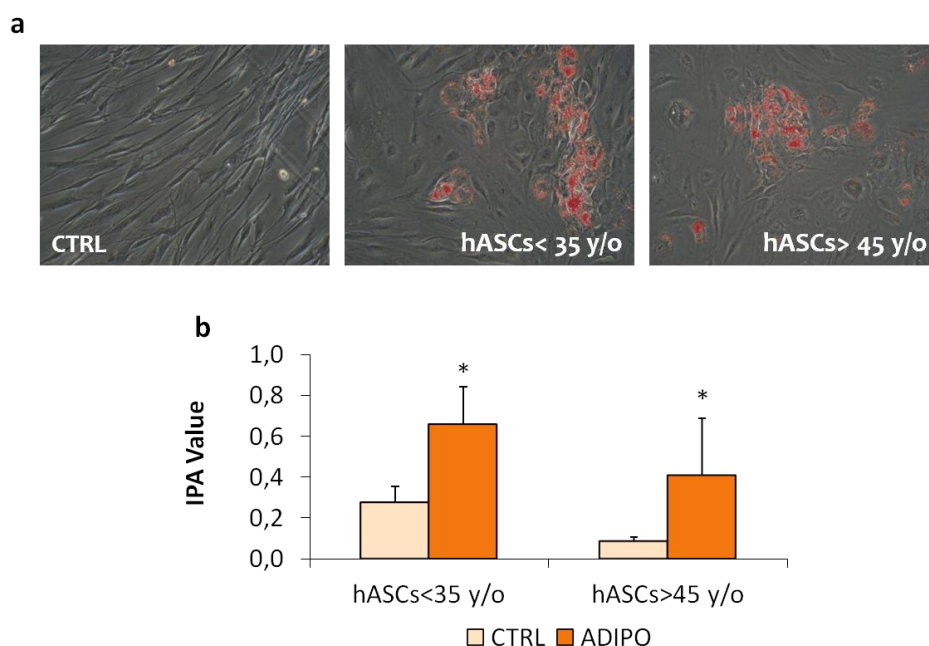

Figure 5. Microphotographs of hASCs<35 y/o and hASCs>45 y/o in CTRL medium and differentiated towards adipogenic lineage stained with Oil Red O after 14 days in culture (40X magnification) (a). Quantification of lipid deposition in undifferentiated (CTRL) and adipogenic-differentiated hASCs for 14 days (ADIPO) in both age groups. Data are expressed as mean ± SD (n=5) (IPA, isopropanol) (b). ADIPO vs CTRL: *p<.05.

PPAR-γ expression in undifferentiated and adipogenic differentiated hASCs was also analyzed (Figure 6). PPAR-γ (Peroxisome Proliferator-Activated Receptor gamma) is a member of the super-family of nuclear receptors and regulates the transcription of several genes involved in adipogenic differentiation and fatty acids metabolism. PPAR-γ was expressed in undifferentiated cells and up-regulated in adipogenic-differentiated cells, after 14 days of culture, of about 40 and 52% in hASCs<35 y/o and hASCs>45 y/o, respectively. However, the difference of PPAR-γ expression in differentiated hASCs was not significant.
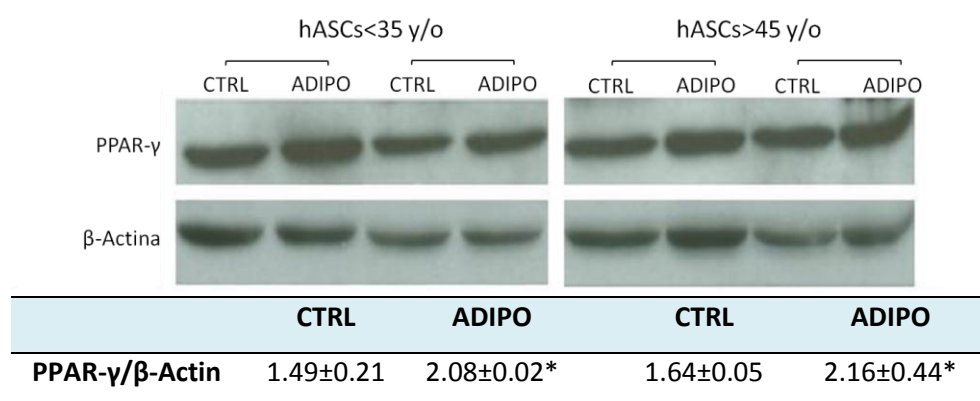
	CTRL	ADIPO	CTRL	ADIPO
PPAR-γ/β-Actin	1.49±0.21	2.08±0.02*	1.64±0.05	2.16±0.44*

Figure 6. PPAR-γ expression in younger and older donors. Western blot analysis of two populations for each group (upper line) and quantification of PPAR-γ expression standardized on β-Actin content; data are expressed as mean ± SD (n=4). ADIPO vs CTRL: *p<.05.

When hASCs isolated from younger and older donors were induced to differentiate towards osteogenic lineage, after one week of differentiation, both hASCs lost their fibroblast-like shape assuming a more rounder and cubical morphology, characteristic of osteoblast cells (Figure 7a). hASCs from younger donors cultured in osteogenic medium for 14 days showed a higher ALP activity compared with cells from older donors (Figure 7b). Indeed, differentiated cells from the younger groups showed an increase in ALP activity of 280% with respect to undifferentiated ones, whereas the increase was just 40% for hASCs derived from the over 45 years old group. Osteo-differentiated hASCs<35 y/o showed also a significant increase of about 771% in comparison to osteo-hASCs>45 y/o; moreover, hASCs>45 y/o when induced to osteo-differentiate did not produce ALP levels significantly higher in comparison to undifferentiated ones (+39%) (Figure 7b). Moreover, the ALP basal level in undifferentiated hASCs derived from younger donors was 3-fold higher than from older donors (55 U/µg vs 17 U/µg).
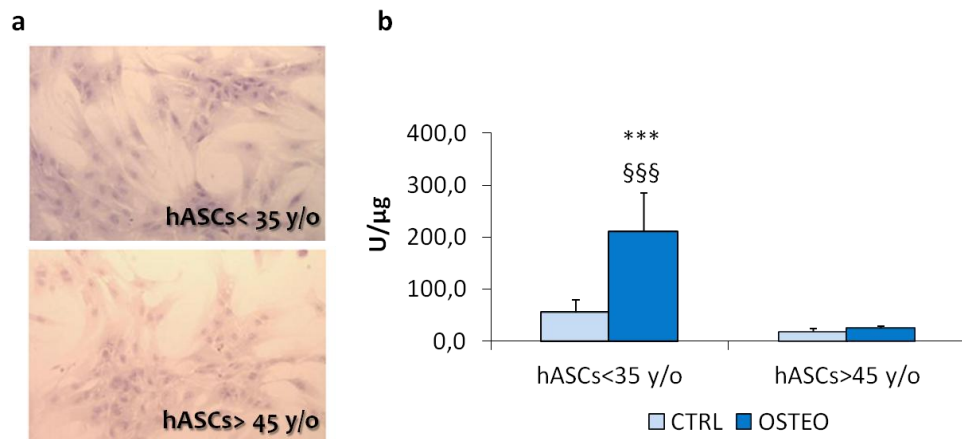
Figure 7. Microphotographs of hASCs<35 y/o and hASCs>45 y/o differentiated towards adipogenic lineage stained with haematoxylin-eosin after 14 days in culture (40X magnification) (a). ALP activity, in undifferentiated hASCs and osteogenic-differentiated hASCs for 14 days. Data are normalized with respect to protein content and expressed as mean ± SD (n=5) (b). OSTEO vs CTRL: ***p<.001; hASCs<35 y/o vs hASCs>45 y/o: §§§p<.001

These observation were partially confirmed by quantification of calcium deposition: after 21 days of culture, cells isolated from the under 35 y/o group produce a greater amount of calcium deposits compared with cells from the over 45 y/o group (+110%) (Figure 8a,b). However, a great variability among donors meant no significant difference between the two groups. The increase in extracellular matrix deposition by differentiated hASCs was 220 and 73% from younger and older donors, respectively.
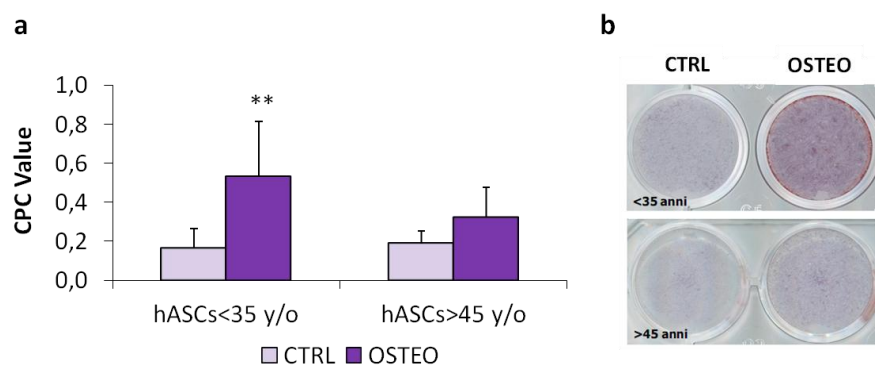

Figure 8. Quantification of calcium deposits in undifferentiated and osteogenic-differentiated hASCs for 21 days. Alizarin Red S-stained samples were extracted with CPC; data are expressed as mean ± SD (n=5) (a). Alizarin Red S staining of extracellular calcified matrix of CTRL and OSTEO hASCs<35 y/o and hASCs>45 y/o cultured for 21 days (b). OSTEO vs CTRL: **p<.01.

Moreover, due to it is known that cells-scaffold construct play an important role in the field of bone regeneration, we have compared the osteogenic potential of hASCs<35 y/o and hASCs>45 y/o in the presence of hydroxyapatite granules (HA) and fragment of silicon carbide plasma enhanced chemical vapour deposition (SiC-PECVD).

hASCs of both groups cultured on scaffolds well adhered on HA, colonizing the pores of its 3D structure (Figures 9a). Their osteoblastic differentiation ability in the presence of HA scaffolds was monitored after 14 and 21 days of culture, by ALP assay only, as the amount of calcium produced by cells could be masked by the calcium released by HA. As shown in Figure 9b, even when cultured on HA, the ALP activity of hASCs from younger and older donors produced significant levels of ALP activity in comparison to the same cells maintained on plastic (PA) in CTRL and OSTEO medium, showing and confirming the osteoinductive properties of HA. Osteo-differentiated hASCs<35 y/o cultured for 14 days on plastic or in the presence of HA, showed a significant increase of ALP activity of 303.5 and 290.7%, respectively (Figure 9b). These data were also maintained after 21 days of culture. hASCs>45 y/o were also able to osteo-differentiate: after 14 days of differentiation both hASCs cultured on plastic or on HA, produce significant level of ALP activity (+27.5 and +31.4%, respectively), respect to CTRL cells (Figure 9c). After 21 days of differentiation, hASCs significantly differentiate, even if the basal level of ALP was reduced in comparison to the values at 14 days. Moreover, ALP activity of hASCs isolated from younger donors was significantly higher compared with the one determined in cells from older donors, with an increase of about 10-fold (Figure 9b, c).
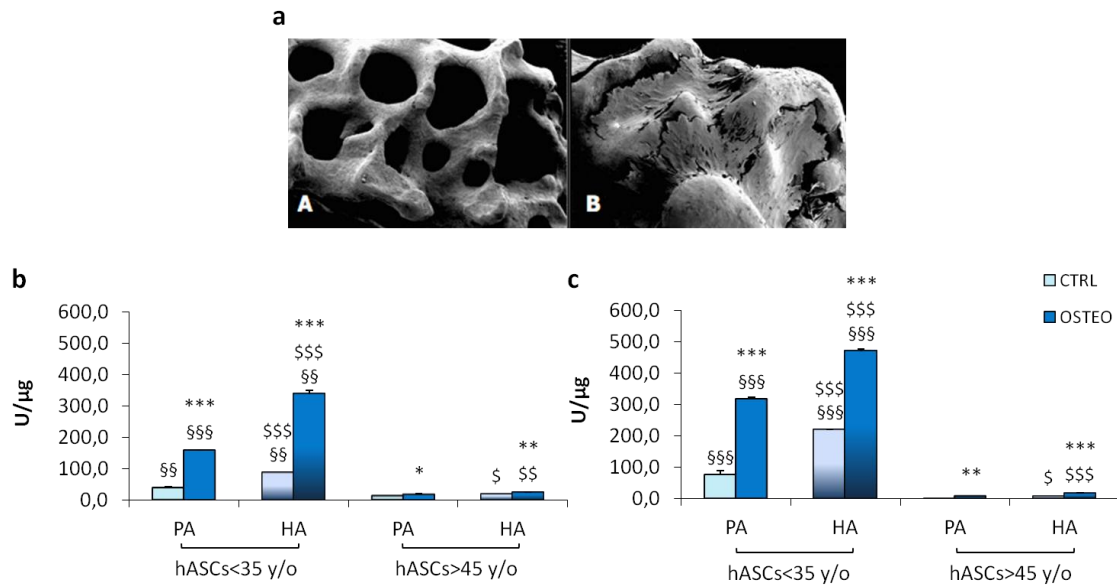
Figure 9. SEM picture of unseeded (A) and seeded hydroxyapatite granules (B) maintained in osteogenic medium for 14 days (a). Influence of HA on *in vitro* osteoblastic differentiation of hASCs belonging to the two age groups. ALP activity, in undifferentiated hASCs, from hASCs under 35 year-old and the over 45 year-old groups cultured for 14 (b) and 21 days on PA and HA (c). Data were standardized with respect to protein content and expressed as mean ± SD (n=3). OSTEO vs CTRL: *p<.05, **p<.01, ***p<.001; HA vs PA: §p<.05, §§p<.01, §§§p<.001.

As shown in Figure 10a, undifferentiated and osteogenic differentiated hASCs were able to adhere on the surface of SiC-PECVD. The influence of this scaffold on the osteoblastic differentiation ability of hASCs was analyzed evaluating ALP activity at 14 days of differentiation, and extracellular calcified matrix deposition after 21 days. SiC-PECVD did not show any particular osteoinductive property: no significant difference in ALP activity was detected from cells derived from both groups cultured on PA and SiC-PECVD (Figure 10b), even if hASCs<35 y/o showed higher level of ALP activity in comparison to hASCs from older donors. Indeed, these cells produce significant increases of ALP activity and calcium deposition both on plastic (+303.5 and +321.7%, respectively) and in the presence of SiC-PECVD (+231.6 and +358.3%, respectively) (Figure 10 b, c). Also, donor age negatively influenced the osteoblastic marker expression analyzed (Figure 10 b, c).
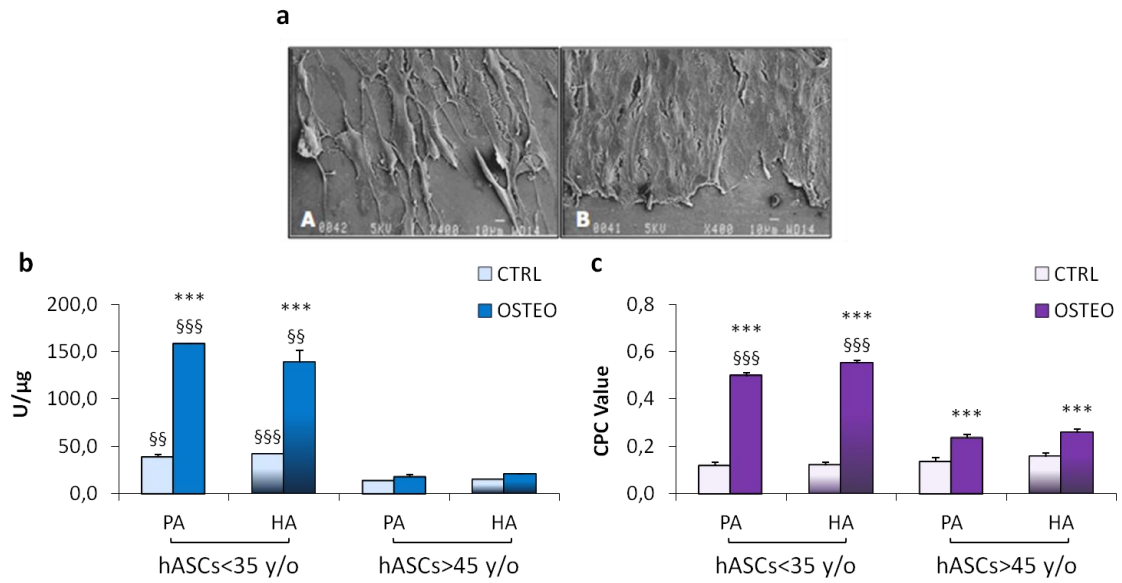
Figure 10. SEM picture of unseeded (A) and seeded SiC-PECVD fragments (B) maintained in osteogenic medium for 14 days (a).). ALP activity, in undifferentiated (CTRL) and osteogenic differentiated (OSTEO) hASCs cultured for 14 days on PA and SiC-PECVD. Data were standardized with respect to protein content and expressed as mean ± SD (n=3) (b) Quantification of calcium deposits in undifferentiated and osteogenic-differentiated hASCs cultured for 21 days on PA and SiC-PECVD. Alizarin Red S-stained samples were extracted with CPC (c). OSTEO vs CTRL: ***p<.001; SiC-PECVD vs PA: §§p<.01, §§§p<.001

Treatment with Reversine to Increase hASCs Plasticity

We have also explored the possibility to increase hASCs plasticity by pre-treatment with the purine Reversine before differentiation toward osteoblasts, smooth and skeletal muscle cells (Figure 11).
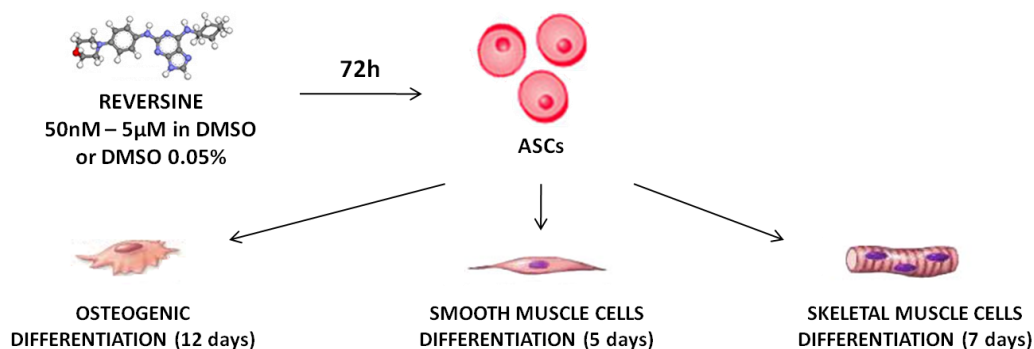
Figure 11. Schematic experimental protocol.

At first we have treated hASCs for 3 days with different doses of Reversine (range 50 nM - 5 µM), to determined its cytotoxicity. As shown in Figure 12a, the vehicle (DMSO 0.05%) did not reduced cells viability. Reversine, from 50 nM to 1.5 µM, was not cytotoxic, however, cells viability was reduced increasing Reversine concentration (Figure 12b). Reversine 5 µM was cytotoxic for hASCs (Figure 12b).

Figure 12. Viability of hASCs treated with different doses of Reversine. Comparison of hASCs untreated or treated with the vehicle DMSO 0.05% (a); hASCs treated with different doses of drug (b) (mean ± SD) (n=3).

Then we worked with 2 concentration of Reversine 50 nM and 5 µM.

50 nM Reversine, did not cause appreciable changes in cell morphology and maintained a normal proliferation rate (Figure 13). In contrast, 5 µM Reversine caused drastic morphological changes: cells became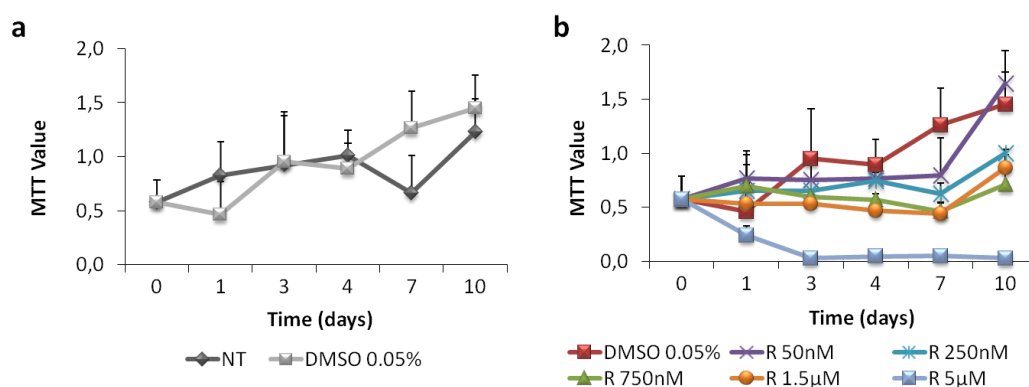 larger in size and more sticky to the culture plates. Moreover, this treatment caused an average of 25.3% of cell death.
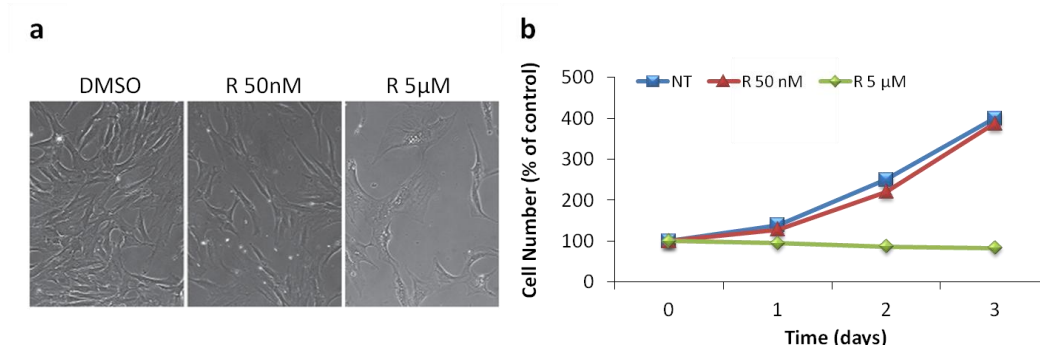
Figure 13. Phase-contrast microphotographs of hASCs after 3 days of treatment with DMSO 0.05% and Reversine 50 nM and 5 µM (100X magnification) (a). Control and Reversine-treated cell proliferation rate (b).

After a three-days Reversine pre-treatment at 50 nM or 5 µM, hASCs were cultured in osteogenic medium for 12 days. Alkaline phosphatase (ALP) staining revealed the presence of several osteoblasts-like cells in all Reversine-treated and untreated cells, with a significant increase in the number of ALP-positive cells at 50 nM, while a slight reduction could be observed at 5 µM (Figure 14).
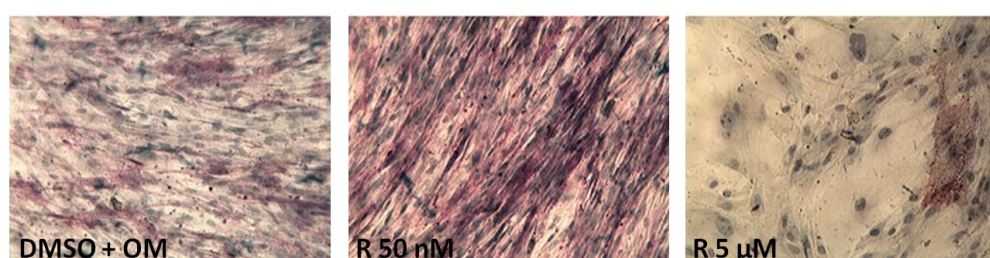
Figure 14. Reversine effects on osteogenic differentiation of hASCs after three-days of Reversine treatment at 50 nM or 5 µM stained with alkaline phosphatase (ALP). In purple osteoblast-like cells (100X magnification).

To confirm the osteogenic Reversine pre-treatment effect, we have also tested ALP gene expression and ALP activity (Figure 15a, b). As known, osteogenic medium significantly up-regulate ALP gene expression, with an increase of 429.1, 349.6 and 663.9% in DMSO, 50 nM and 5 µM Reversine pre-treated hASCs respect to undifferentiated ones (Figure 15a).

Similar results were obtained evaluating ALP activity (+126.7, +86.4 and + 37.0% of DMSO, 50 nM and 5 μM Reversine pre-treated hASCs, respectively respect to CTRL ones) (Figure 15b). Moreover, ALP gene expression and ALP activity increased in 50 nM Reversine pre-treated and osteo-differentiated hASCs, with an average of 45.8 and 44.2%, respectively, in comparison to untreated osteo-differentiated ones. On the other hand, 5 μM Reversine pre-treatment did not cause any significant change after osteo-differentiation induction.
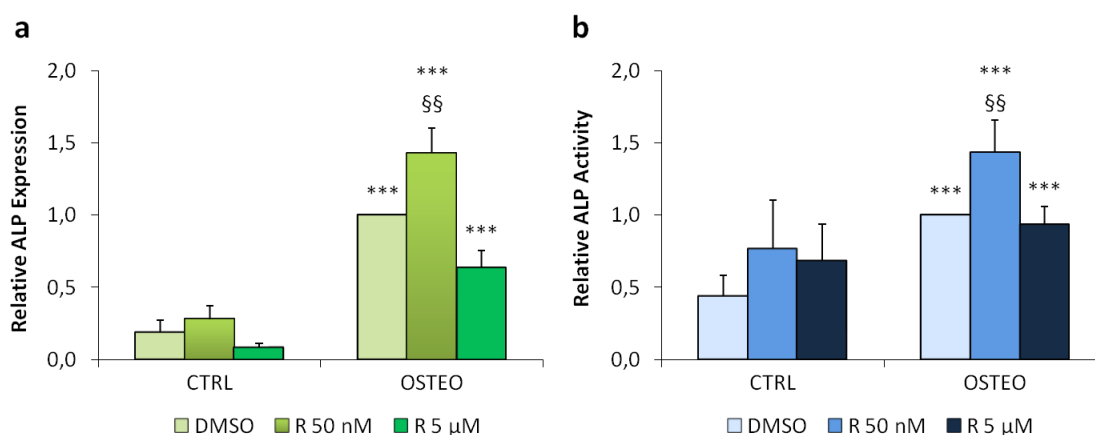
Figure 15. ALP gene expression by Real-Time PCR (a) and ALP enzymatic activity of undifferentiated and osteo-differentiated, untreated and Reversine pre-treated hASCs (b) Both quantitative data are expressed as relative values respect to control group DMSO OSTEO (mean ± SD) (n=4).
OSTEO vs CTRL: ***p<.001; Reversine vs DMSO: §§p<.01.

hASCs were also induced to differentiated into muscle cells lineages.

Cells were cultured in smooth-muscle medium for 5 days and treated as previously described. Immunofluorescence with smooth muscle α-actin (α-SMA) antibody revealed stem cell differentiation toward smooth muscle cells. Qualitative analysis of α-SMA staining revealed a substantial fluorescence increase in 50 nM Reversine pre-treated hASCs (Figure 16a). Instead, an appreciable reduction in signal intensity could be observed in 5 μM Reversine pre-treated cells. Next, to quantify Reversine-induced changes in the differentiation potential of mesenchymal cells toward smooth muscle cells, we tested α-SMA gene expression by Real-Time PCR. Inductive media induce an increased expression of 189.9, 339.5 and 162.6% of DMSO, R 50 nM and 5 μM treated cells in comparison to undifferentiated ones (Figure 16b). Moreover, α-SMA gene expression showed an average increase of 89.0% in Reversine pre-treated hASCs at 50 nM, while 5 μM Reversine caused a 30% decrease (Figure 16b).
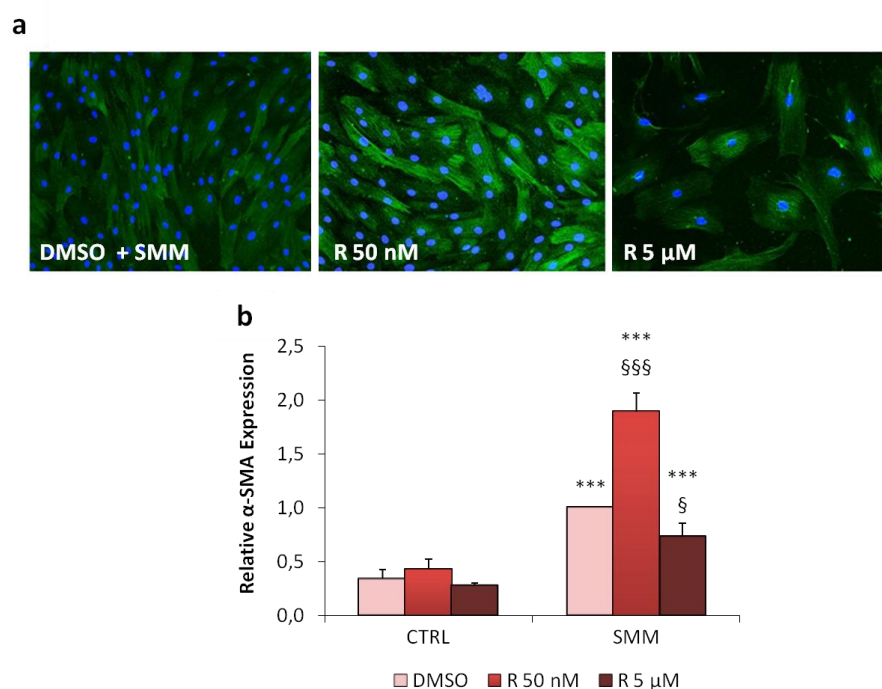
Figure 16. Immunofluorescence analysis of hASCs stained with smooth muscle α-actin (α-SMA) antibody (a) and α-SMA gene expression by Real-Time PCR in undifferentiated and smooth mesce-differentiated, untreated and Reversine pre-treated hASCs (mean ± SD) (n=4) (b). SMM vs CTRL: ***P<0.001; Reversine vs DMSO: §p<.05, §§p<.01.

Moreover, to test whether Reversine pre-treated hASCs would acquire myogenic competence to differentiate into skeletal muscle, which they normally do with very low yield, cells were pre-treated with 50 nM Reversine for 3 days, and then co-cultured with C2C12 murine myoblasts, in a 1:4 ratio.

Co-immunostaining with human-nuclei (red) and myosin heavy chain (MHC, green) antibodies, and staining of all nuclei with Hoechst 33342 (blue), revealed the formation of myotubes incorporating human nuclei only in Reversine pre-treated hASCs (Figure 17, pink arrow heads in the merge panels), expressing sarcomeric myosin in the cytoplasm. Overall, we observed the incorporation of human nuclei inside MHC positive myotubes with a frequency of roughly 30%, calculated by dividing the number of myotubes containing at least one human nuclei by the overall number of myotubes for each field. Control cells, did not show appreciable presence of human nuclei in the formed myotubes. No pink nuclei could be detected inside the myotubes, but just nuclei stained by Hoechst 33342, as revealed in the merge panels (Figure 17, merge of controls, blue arrow heads).
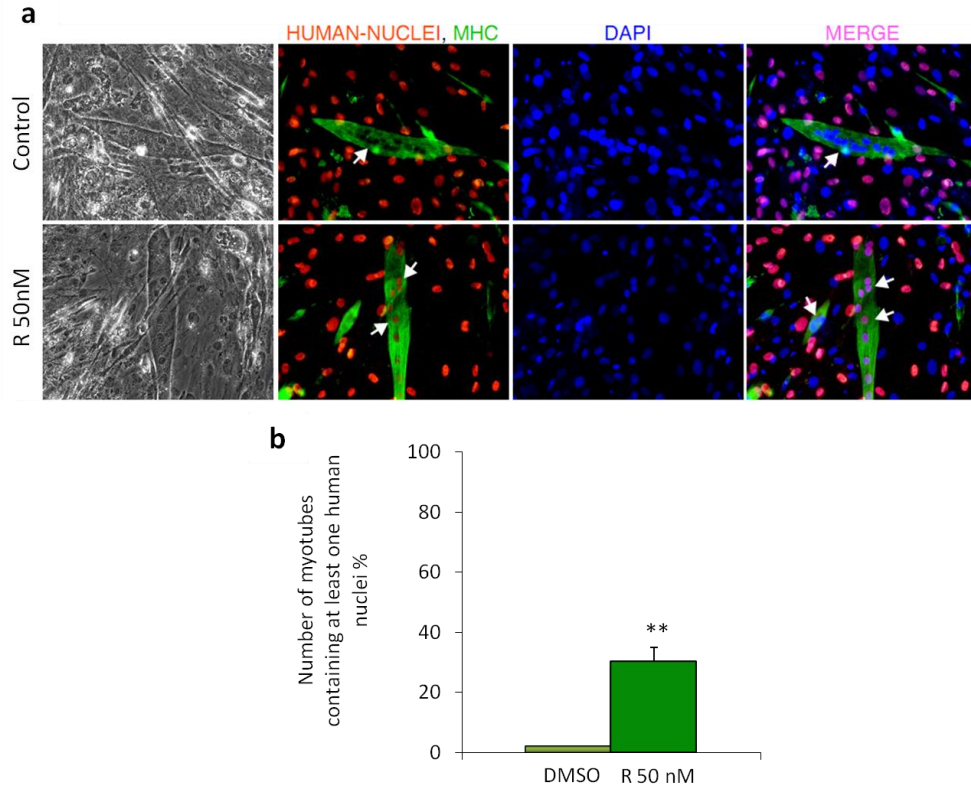
Figure 17. Co-immunostaining with human-nuclei (red) and myosin heavy chain (MHC, green) antibodies, and staining of all nuclei with Hoechst 33342 (blue) revealed the formation of myotubes incorporating human nuclei (pink arrow) in undifferentiated and muscle skeletal-differentiated, untreated and Reversine pre-treated hASCs (a). Quantification of the incorporation of human nuclei inside MHC expressing myotubes (mean ± SD) (n=4). **p<.01.

Finally, with the aim to understand the mechanism of action promoted by Reversine, key genes which have been shown to be crucial in adult cell reprogramming have been analyzed. Real-Time PCR analysis of mRNA extracted from hASCs revealed a 2.5-fold increase in Klf-4 in 5 µM Reversine pre-treated cells, while no significant changes could be detected at 50 nM or in c-Myc and Oct 4, and Nanog remained undetectable (Figure 18).
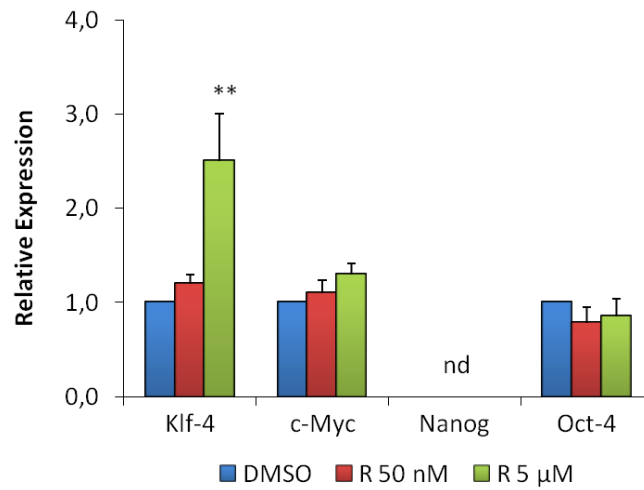
Figure 18. Real-Time PCR expression of key "*reprogramming factors*" (Klf-4, c-Myc, Nanog and Oct-4) used to genetically de-differentiate adult cells into pluripotent stem cells (iPSCs) in reversine treated and untreated hASCs (mean ± SD). **p<.01.

Analysis of hASCs Immunoselected CD34+ and L-NGFR+ Subpopulation Compared with the Whole hASCs Population

In this study, we compared the whole hASCs population, purified by plastic adherence (PA hASCs), with two immunoselected subpopulations (L-NGFR+ and CD34+ hASCs), evaluating their immunophenotype and their ability to differentiate.

hASCs populations were divided in three fractions: one obtained by plastic adherence (PA), and the others obtained by immunoselection for CD34 and L-NGFR markers. Starting from a variable number of cells, the percentage of immunoselected L-NGFR+ cells was 4.4±6.3% and the purity of the immunoselected population was 88.5±10.6% (Table 4 and Figure 19). The mean percentage of CD34+ cells was 13.7±19.5% and the purity after immunoseparation was 82.6±12.9% (Table 4 and Figure 19).

	n	Cellular Yield	Immunoselected hASCs
CD34	7	13.7±19.5%	2.4×10^6 - 5.9×10^6
L-NGFR	6	4.4±6.3%	4.8×10^6 - 2.5×10^6

Table 4. Average cellular yield of CD34+ and L-NGFR+ obtained after immunoselection of hASCs.

The freshly purified L-NGFR+ and CD34+ cells appeared small round cells that rapidly adhered to the plastic and expressed surface markers associated with a primitive phenotype. Despite the high variability among donors, immunomagnetic separation allowed us to identify 2 distinct subpopulations: a high percentage of L-NGFR+ cells co-expressed the stem markers CD34 (78.0±10.6%), while CD117 and CD105 were variably expressed (45.9±36.5 and 24.8±32.3%, respectively). The endothelial-committed progenitor markers KDR and P1H12 were mainly expressed on CD34+ cells (12.2±21.9 and 36.0±23.0%, respectively) (Figure 19).

Interestingly, CD34 was always highly expressed on L-NGFR+ cells, whereas a variable but smaller percentage of CD34+ cells expressed the L-NGFR antigen (28.0±34.7%). As shown in Table 5, both CD34 and L-NGFR expressions were progressively down-modulated during culture and definitively lost within 5-8 weeks. CD34 expression was reduced of about 36% at early passages and progressively decrease at late passages (-70%), whereas L-NGFR

expression was constant during early passages in culture to reducing of 80% at late passages (Table 5).
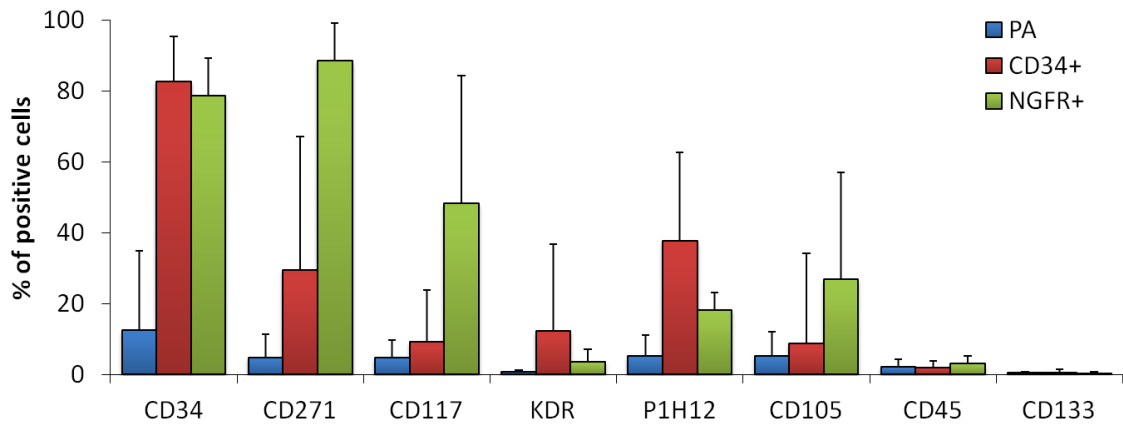
Figure 19. Immunophenotype of fresh human adipose-derived stem cells (hASCs) fractions, analyzed immediately after isolation (PA) or immunoselection (CD34+ and L-NGFR+ or CD271+) (mean ± SD).

	Early Passages	Late Passages
CD34	13.7±19.5	2.9±0.7
L-NGFR	4.4±6.3	0.7±0.1

Table 5. Modulation of CD34 and L-NGFR expression during culture in hASCs PA fraction. analysed by FACS. Data are expressed as % of CD34 and L-NGFR positive cells until passage 3 (early passages) and after passage 5 (late passages) (mean ± SD).

The L-NGFR- and CD34- populations were also analyzed. Both fractions showed a strong decrease in stem cell markers expression compared to the positive cells: in CD34- cells (CD34 expression: 0.4±0.5%) L-NGFR, KDR, and P1H12 positivity diminished to 0.9±0.8%, 0.6±0.8% and 1.7±1.9%, respectively; in the L-NGFR- cells (L-NGFR expression: 0.7±1.1%) CD34, CD117, and CD105 decreased to 6.8±1.0%, 7.2±4.5%, and 4.1±3.5%, respectively (data not shown).

In Figure 20 is reported a representative trend of PA, CD34+ and L-NGFR+ hASCs deriving from one donor. After about 5 weeks, cells start to rapidly proliferate without any signs of cellular aging for additional 20 weeks. The 3 cellular populations proliferated similarly; however, in the long period, PA cells reduced their dividing potential in comparison to the immunoseparated cells (Figure 20).
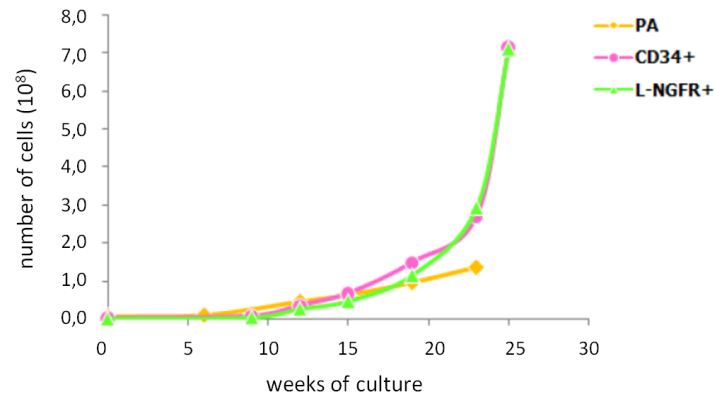
Figure 20. Proliferation rate of PA, CD34+ and L-NGFR+ hASCs isolated from the same donors. Proliferation rate was evaluated by cells count at each passage in culture.

At early weeks of culture, all the 3 populations showed the typical fibroblast-like aspect. Furthermore, the morphology of the 3 fractions became quite different after 15-20 weeks: PA hASCs grew with a larger and latten shape, with cells gathered in clusters and cytoplasm rich in granules, in contrast to the immunoselected cells that still appeared homogeneous, spindle-shaped, and with well-defined shape and nuclei (Figure 21).
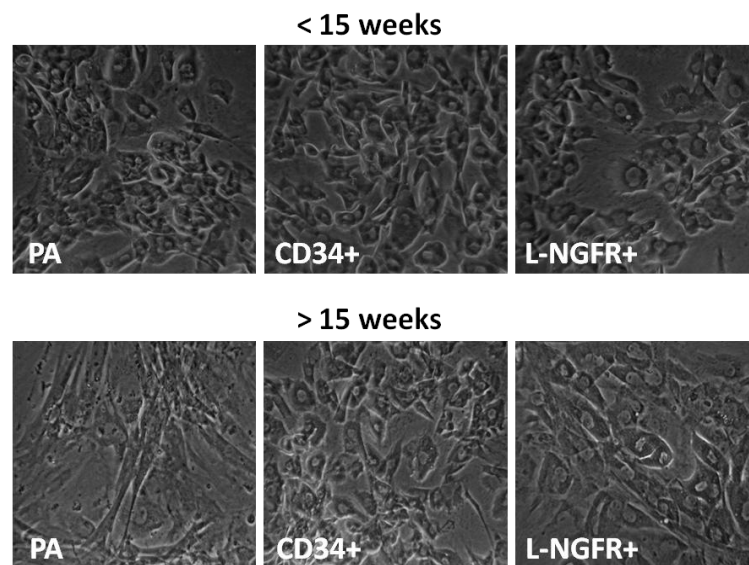
Figure 21. Morphologic appearance of PA, CD34+, and L-NGFR+ cells at 9th week (upper panel) and 18th week (lower panel) of culture (400X magnification).

A great variability was found among different donors in term of clonogenic potential. At early passages, we did not observe any significant differences among the 3 populations; at late passages, we observed a decrease in the colony-forming ability in all the 3 populations,

and in particular a reduction of 10-fold in PA hASCs and 50% in CD34+ and L-NGFR+ hASCs respect to the early passages (Figure 22).
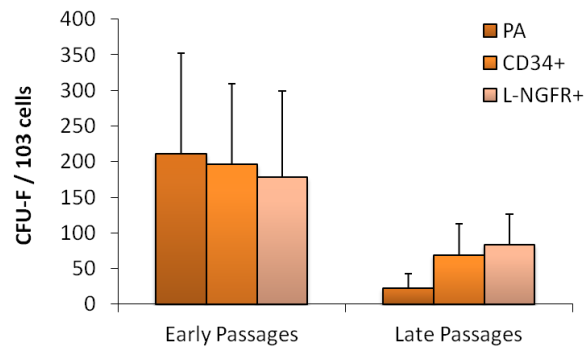
Figure 22. Clonogenic potential of PA, CD34+ and L-NGFR+ hASCs at early and late passages in culture (mean ± SD).

When maintained in adipogenic medium, hASCs from the 3 fractions showed, already after few days of differentiations, some morphological changes: cells became bigger and rounder in comparison to undifferentiated ones, with the presence of several lipid vacuoles in the cytoplasm, indicating their multipotent features.

After 21 days, PA, CD34+ and L-NGFR+ hASCs showed a significant increase of vacuoles production of 384.1, 676.0 and 711.4%, respectively, in comparison to undifferentiated ones (Figure 23a). Moreover, CD34+ and L-NGFR+ cells presented significant increase in differentiation ability compared to the unselected cells: at early passages the average increments were of 40.1 and 47.9% for CD34+ and L-NGFR+ hASCs, respectively (Figure 23b). We have also analysed the adipogenic differentiation ability of the 3 populations during culture: at late passages, despite the reduced adipogenic ability of the immunoselected cells, they still generated more lipid vacuoles compared to the unselected ones (+33.5 and +36.0% for CD34+ and L-NGFR+ cells, respectively).

Figure 23. Quantification of lipid deposition in undifferentiated (CTRL) and adipogenic-differentiated hASCs in PA, CD34+ and L-NGFR+ fractions (a). Quantification of lipid vacuoles in PA, CD34+, and L-NGFR+ cells isolated from a representative donor, after different periods of culture (b) (IPA, isopropanol).
ADIPO vs CTRL: ***$p<.001$; Immunoselected vs PA: §§§$p<.001$.

When the 3 fractions of cells were induced to differentiate towards osteoblast-like cells, after 21 days, all the hASCs nicely differentiated; indeed a 96.2, 427.1 and 389.6% of calcium deposition was determined respect to the cells maintained in CTRL medium. CD34+ and L-NGFR+ hASCs showed a significant increase in their differentiation ability compared to PA cells: at early passages, the average increment was 680.7% for CD34+ hASCs, and 345.0% for L-NGFR+ cells (Figure 24b). This difference was maintained in the long term, although the calcified matrix deposition strongly decreased for all of cells (Figure 24b).
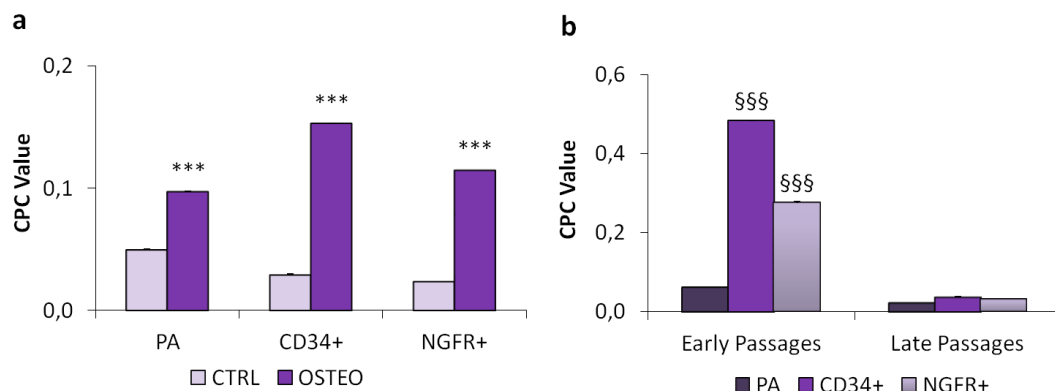
Figure 24. Quantification of extracellular calcified matrix deposition in undifferentiated (CTRL) and adipogenic-differentiated hASCs in PA, CD34+ and L-NGFR+ fractions (a). Quantification of calcium depots in PA, CD34+, and L-NGFR+ cells isolated from a representative donor, after different periods of culture (b).
OSTEO vs CTRL: ***$p<.001$; Immunoselected vs PA: §§§$p<.001$.

We have also studied the chondrogenic potential of the 3 hASCs populations evaluating GAGs production in cells differentiated in 3D culture condition for 21 days (Figure 25).
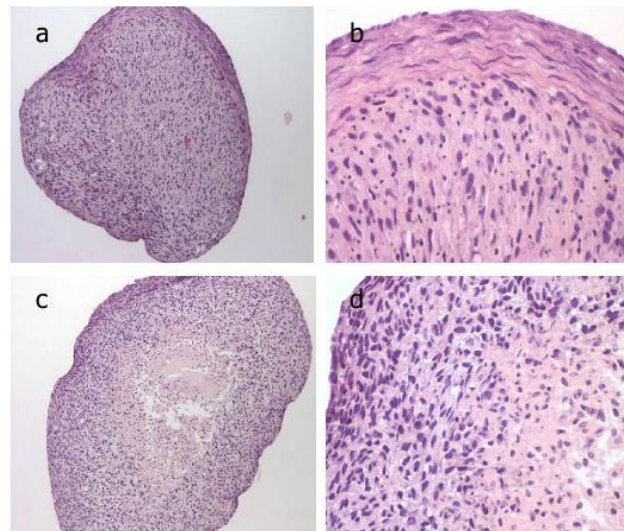
Figure 25. Chondrogenic differentiation in pellet culture conditions. Sections of micromasses maintained for 21 days in undifferentiated media (a, b - 4X and 10X magnification, respectively) and in chondrogenic medium (c, d - 4X and 10X magnification, respectively) stained with haematoxylin/eosin.

Surprisingly, we found that DNA content of each pellet in PA and CD34+ chondrogenic micromasses was about 2-fold higher compared to pellets cultured in control medium, whereas there was no significant difference between differentiated and undifferentiated L-NGFR+ micromasses (Table 6), suggesting that the L-NGFR positive cells do not proliferate if maintained in 3D culture for 21 days like the other cells did.

	μg DNA/ Pellet		
	PA	**CD34+**	**L-NGFR+**
CTRL	4.40±1.65	3.53±1.88	4.39±2.64
CHONDRO	7.30±2.56*	8.20±3.45*	4.38±1.30

Table 6. DNA content in each pellet formed by PA, CD34+, and L-NGFR+ cells maintained in either control or chondrogenic medium (n= 6) CHONDRO vs CTRL: *p<.01.

All the three hASCs factions were able to chondro-differentiate showing significant increases of 125.4, 28.9 and 86.0% of GAGs production, in PA, CD34+ and L-NGFR+ hASCs, respectively, in comparison to the same cells maintained in CTRL medium (Figure 26a).

The immunopurified populations showed a similar differentiation potential when compared to PA hASCs. In Figure 26b, we analysed GAGs production in the 3 hASCs populations isolated from a single donor and differentiated at different times during culture: at early passages not significant differences were observed between PA and CD34+ hASCs, whereas

a significant production of GAGs was observed (+40.1%). Moreover, at late passages, we observed a general and progressive decrease in GAGs production with no relevant differences among the populations.
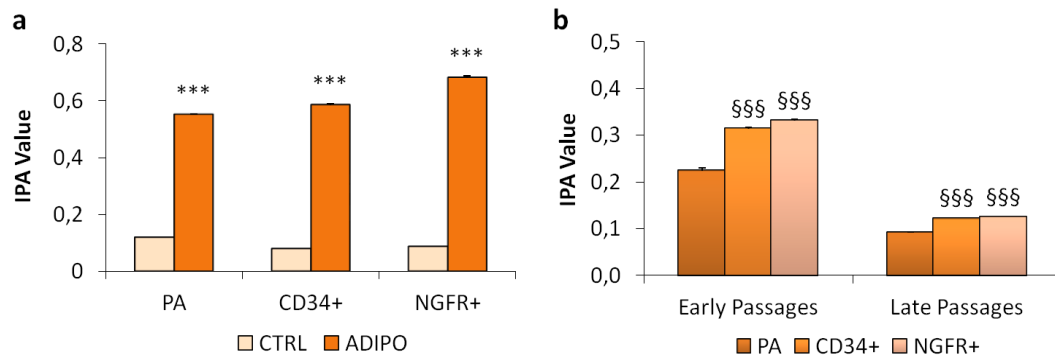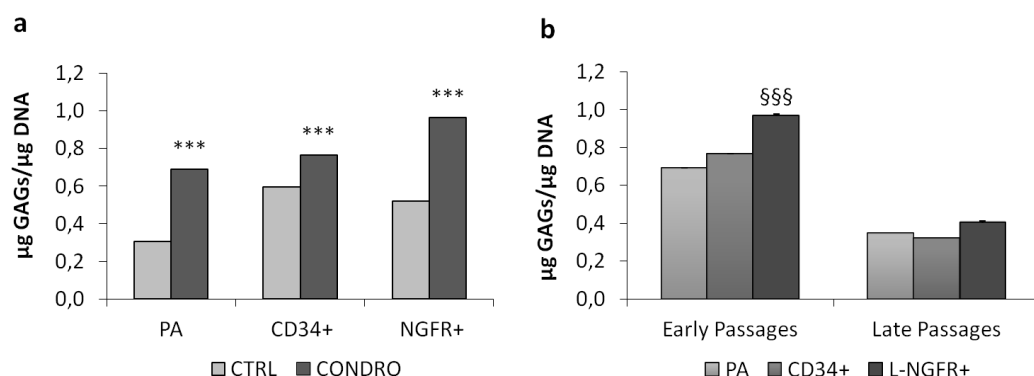

Figure 26. Quantification of GAGs production in undifferentiated (CTRL) and chondrogenic-differentiated hASCs in PA, CD34+ and L-NGFR+ fractions (a). Quantification of GAGs in PA, CD34+, and L-NGFR+ cells isolated from a representative donor, after different periods of culture (b). CHONDRO vs CTRL: ***p<.001; Immunoselected vs PA: §§§p<.001.

The multipotentiality of these cells clearly decreased keeping them in culture for many passages; so we suggest to use these cells until passage 15 and to cryopreserving them, take advantages of the fact that cryopreserved cells maintained their multipotentiality.

DISCUSSION

In the last few years, tissue engineering and regenerative medicine are becoming prominent fields in research and modern medicine due to the aging population and the shortage of donor tissues [Fraser et al., 2006b]. A convenient cell source for autologous cells will aid the approach of regenerative medicine and mesenchymal stem cells derived from adipose tissue present several advantages compared to bone marrow MSCs. Indeed, fat is routinely available in large amount from liposuction and a great number of MSCs can be isolated from a minimal amount of withdrawn tissue, and with a minimal discomfort for the patient. Moreover, the number of purified progenitor cells is quite abundant [De Ugarte et al., 2003]. In our previous data we have demonstrated the ability of human ASCs to constantly proliferate over an extended period of time, showing clonogenic activity and a stable phenotypic profile [de Girolamo/ Arrigoni et al., 2008]. Moreover, hASCs differentiated *in vitro* toward chondrocyte and adipocyte-like cells, showing an enhancement of GAGs deposition and lipidic vacuoles production, respectively. The broad clinical potential application of hASCs is also able be based on their ability to differentiate towards endothelial [Scherberich et al., 2007; Zannettino et al., 2008] and muscle cells [Mizuno et al., 2002], making them a promising tool for regeneration of highly vascularised tissues such as bone and in the cardiovascular field, respectively. In particular, we have focused our interest on the osteogenic potential: hASCs were induced to differentiate into osteoblast-like cells both by biochemical stimuli and by the physical interaction with scaffolds [de Girolamo/ Arrigoni et al., 2008; Lopa/ Arrigoni et al., 2011]. Interestingly, the adherence of hASCs to the tested scaffolds induced progenitor cells to spontaneously differentiate, showing the osteoinductive features of tested biomaterials. Few years ago several authors have also demonstrated that ASCs can be isolated from the adipose tissue of various animal models such as rat [Tholpady et al., 2003; Yoshimura et al., 2007], rabbit

[Torres et al., 2007], pig [Qu et al., 2007] and horse [Vidal et al., 2007]. Moreover, various ASCs-based preclinical models have been reported in bone tissue engineering. In an our work, we have isolated ASCs from small, medium and large animal models, such as rat (rASCs), rabbit (rbASCs) and pig (pASCs), comparing the features of these cells in the undifferentiated state and their ability to differentiate *in vitro*, with particular interest to their osteogenic differentiation potential [Arrigoni et al., 2009]. All these cell types possess suitable osteogenic potential as assessed by up-regulation of specific markers of such as alkaline phosphatase, osteocalcin and osteonectin, and as confirmed by the ability of these cells to produce a large amount of calcified extracellular matrix. In addition, the ability of these cells to adhere and grow on suitable scaffolds, such as hydroxyapatite, suggests that this biomaterial may be an efficient support for future *in vivo* applications. Rabbits and pigs are interesting animal models in the field of regenerative medicine for muscle-skeletal tissue. In particular, rabbits are useful for screening some experimental conditions because of their low cost of maintenance, whereas pigs represent a more predictive model due to their greater similarity to human beings with regard to diet, weight and working load.

Starting from our *in vitro* results, in collaboration with the Faculty of Veterinary Medicine of the University of Milan and the IRCCS Orthopaedic Galeazzi Institute of Milan, we have established an autologous rabbit model of critical-size bone defect by using rbASCs in association with disks of hydroxyapatite (HA), in order to assess the *in vivo* integration of the cells/scaffold construct with the surrounding bone tissue.

The results of our preclinical study suggest that culture-expanded undifferentiated autologous rbASCs seeded on HA scaffolds are able to promote a good bone healing already after 8 weeks from implantation in rabbit critical-size bone defects [de Girolamo/ Arrigoni et al., 2011; Arrigoni et al., submitted].

Many authors have demonstrated the efficacy of MSCs loaded onto osteoconductive scaffolds, both in small and in large animal models [Bruder et al., 1997; Kadiyala et al., 1997; Kon et al., 2000; Viateau et al., 2007]. It is known that bone healing is strongly dependent on the type of used graft substitute [Hing et al., 2007]; in particular, in bone tissue engineering, the adequate biomaterial should provide the biomechanical support, until tissue regeneration is completed, and during this process, it needs to progressively disappear to allow new tissue formation and cell colonization. Nowadays bioceramic scaffolds are considered particularly suitable for bone regeneration due to their

osteoconductivity and their osteointegration ability [Heise et al., 1990; Elsinger and Leal, 1996; Ge et al., 2004; Mastrogiacomo et al., 2006]. The first demonstration of their efficacy was by Goshima et al., who showed that rat expanded BMSCs seeded on ceramic scaffold were able to deposit bone when implanted in immunodeficient mouse subcutaneously [Goshima et al., 1991]. More recent studies confirmed the same ability of BMSCs in other animals, both implanting scaffolds subcutaneously and in experimental bone defects. Kon et al. have shown the efficacy of autologous BMSCs loaded on ceramic constructs of HA to repair a critical-size tibia gaps in sheep: 2 months after implantation, bone formation was found to occur both within the internal macropore space and around the HA cylinder resulting in a faster bone repair [Kon et al., 2000]. Another study reports the efficacy of BM stem cells in regenerating critical-size bone defects in a swine mandible model, showing that these cells were able to engraft and regenerate bone 6 months post-surgery with a good restoration of the orofacial skeletal tissue [Zheng et al., 2009]. Moreover, in a more recent work, both the osteogenic potential and the influence of platelet-rich plasma (PRP) on BMSCs and ASCs were evaluated in a large animal model: cells were seeded on mineralized collagen sponges and implanted into a critical size defect of the sheep tibia for 26 weeks. Radiographic and histological evaluations revealed a significantly more abundant amount of newly formed bone in the BMSCs-group compared to the ASCs-group suggesting that ASCs seem to have a reduced osteogenic potential compared to BMSCs; however the addition of PRP seems to partially filled this functional gap [Niemeyer et al., 2010]. In addition to these works, there are several studies documenting that adipose-derived stem cells are an alternative cells source for bone regeneration. Autologous osteo-differentiated ASCs were used with coral scaffolds to repair a cranial bone defect in a canine model [Cui et al., 2007]: bilateral full-thickness defects of parietal bone were created, and treated animals were sacrificed 6 month after surgery. Radiographic analysis and histological examination revealed that the defect was repaired by bone tissue just in the experimental group, while only minimal bone formation with fibro-connective tissue was observed with coral scaffolds only. More recently, Hao et al. produced a novel biomimetic construct based on a combination of rabbit ASCs encapsulated in collagen I gel with a PLGA-β-TCP scaffold. The composites implanted into a 15-mm length critical-sized segmental radial defect, showed a consistent degradation of the scaffold with an enhanced *in vivo* osteogenesis of these cells and bone defect healing after 24 weeks [Hao et al., 2010b].

Respect to the above mentioned studies, we performed a wider full-thickness defects compared to those usually considered critical in rabbit [Cui et al., 2007; Pearce et al., 2007; Lee et al., 2010]. We have chosen a very severe lesion in order to accurately evaluate the ability of autologous rbASCs to improve bone healing. Indeed, the combination of bone self-regeneration and the osteoconductive properties of HA might have been sufficient to achieve a fast regeneration in smaller defects, thus hiding a possible contribution of rbASCs. Moreover, due to the known faster bone remodeling process in rabbit, respect to human [Pearce et al., 2007], we have chosen a quite short follow-up, in order to better highlight differences between the experimental conditions.

The *in vitro* characterization of rbASC populations, used in our study, showed some inter-donor differences, both in term of proliferation, clonogenic ability, and osteogenic differentiation, as already reported in previous studies [Arrigoni et al., 2009]. Our *in vivo* results showed neither bone resorption, or abnormal bone callus formation, or infections and severe inflammatory reactions, thus suggesting the feasibility of using rbASCs in this kind of applications.

Differently from previous studies [Viateau et al., 2007; Hao et al., 2010a], gross and radiographic examinations did not reveal a dramatically different filling of the untreated specimens respect to the treated ones. This can be related to the kind of defect: we performed circular full-thickness defects instead of an osteo-periosteal segmental one, which is normally more difficult and slow to be repaired. We chose such type of defect in order to avoid the use of mechanical stabilization devices, which are known to be able to affect bone healing, providing different mechanical stimulation in relation to the kind of chosen device. Moreover, it is very difficult to perform an adequate and reproducible stabilization in the chosen small animal model.

The different defects' treatment did not affect the BMD of the areas surrounding the lesions (R1 and R3), which are comparable to the normal tibia values. However, for R2 region, corresponding to the defect site, although not significant, the group D BMD was higher than the group B one, suggesting that in the first period of the defect healing, the bone deposition activity is predominant respect to the remodeling activity [Mastrogiacomo et al., 2006]. However, the histological analysis revealed strong differences in term of quality of new-formed tissue: in untreated specimens just a periosteal reaction participated to the defect repair, and no osteoblasts were observed. When treated with the semi-liquid

rbASCs suspension, defects were filled by a woven matrix, indicating an immature bone tissue. These data suggest that rbASCs are able to respond to the microenvironment signals inducing the differentiation into osteogenic-like cells. After a short period from the implant of cells and in the absence of a three-dimensional scaffold on which arrange themselves, rbASCs did not show to be able to form a well-organized tissue; anyway, they significantly participate in the bone defect regeneration. In both cell-seeded and unseeded scaffolds, a good osteointegration was observed, even if a significant amount of hydroxyapatite was not resorbed yet. In these treated groups, an initially bone formation occurred mostly in the part of the scaffolds close to the bone ridge. Indeed, accordingly to previous studies [Kon et al., 2000], little new bone formation occurred also within cell-free scaffold pores, indicating the ability of this scaffold to be colonized by the resident cells and to induce their osteogenesis. However, in the group treated with the construct rbASCs-HA a uniform spatial distribution of newly formed tissue was observed, indicating the presence of bone tissue not only along the walls of the pores, but also in their inner part, and suggesting that the bone maturation process is more advanced in the cell-treated defects, where lamellar bone was largely represented.

Furthermore, defects treated with rbASCs showed good mechanical properties, suggesting an improved capability to bear mechanical loading. This is quite evident when low forces (1mN, corresponding to 200 nm of penetration depth) are applied. This result might be explained by a higher mineral content present in the lesions treated with rbASCs-HA and representing a more advanced step in the healing process. Instead, at higher maximum depth no differences have been observed, and the response is dominated by the deformation mechanisms occurring in tissue, namely the debonding between the collagen fibres and the slippage at the mineral-collagen interfaces [Fantner et al., 2005; Mercer et al., 2006]. These results are qualitatively consistent with Pelled et al. who found that a decrease in the elastic modulus and hardness values correlated with an increasing maximum load [Pelled at al., 2007].

Moreover, with the aim to minimally manipulate cells, we seeded non osteogenic-induced rbASCs on HA. As already reported, some authors demonstrated the efficacy of engineered bioconstruct using pre-osteogenic-induced MSCs: Hao et al. cultured rabbit ASCs on collagen I gel PLGA-TCP for 2 weeks in osteogenic medium, before using these hybrid composites to treat rabbit segmental bone defects [Hao et al., 2010a]; also Viateau et al. at

first suspended BMSCs in osteogenic medium, and then they seeded them on coral scaffolds [Viateau et al., 2007]. Although in both cases these authors obtained satisfactory results, our data, together with other previous study [Kon et al., 2000; Cowan et al., 2004; Mastrogiacomo et al., 2006], support the idea that a pre-osteogenic induction of MSCs is not strictly necessary to achieve a good bone regeneration, probably due to the combined effect of the surrounding bone microenvironment with the selected scaffold. Indeed, HA is able to promote osteogenic differentiation *in vitro*: collagen type I is expressed in rbASCs seeded on HA fragments, and cultured in non-inductive medium, confirming the osteoconductive effect of HA on rbASCs. We believe that this osteoconductive feature of HA accelerate the osteogenic differentiation of rbASCs and consequently the bone deposition process. This evidence may be very useful in a hypothetic one-step bone defect treatment, where mesenchymal stem cells could be purified from the donor tissue, directly seeded on scaffold, and immediately implanted in the defect, without the necessity of a pre-stimulation. However, the marked osteogenic differentiation variability among the different cell populations, as we have found *in vitro* and as it has been already reported in several papers concerning animal or human ASCs [Arrigoni et al., 2009; de Girolamo/ Arrigoni et al., 2009; Quirici/ Arrigoni et al., 2010] seems not to affect bone healing . Indeed, we have not observed any relevant differences among rabbit tibia, both in terms of bone formation, distribution and mechanical properties: the best "*in vitro* performing rabbit" did not show the best results *in vivo* compared to the others. We suggest that the microenvironment may promote the bone healing masking the inter-donor variability, and it allows all different cellular populations to adequately contribute to the bone regeneration process suggesting also that the exogenous cells could recruit and lead the endogenous ones in the reparative process. So, the treatment of bone defects with autologous rbASCs-hydroxyapatite bioconstructs might be a promising approach improving bone healing and reducing the rehabilitation period for the patients.

Few months ago, we have also concluded a new pre-clinical study in a large animal model using autologous and heterologous porcine ASCs in association with OPF [oligo(poly(ethylene glycol) fumarate] hydrogel (MayoClinic, Rochester, Minnesota, USA) to repair a critical osteochondral defect in the knee of minipigs.

Briefly, always in collaboration with the vet team of the University of Milan and the IRCCS Galeazzi Orthopaedic Institute of Milan, we have at first isolated ASCs from the

interscapular region of 7 male minipigs, we have expanded and characterized these cells *in vitro*, and about 4 weeks after isolation we have loaded $3x10^6$ of either autologous or heterologous ASCs (female pig) on cylinders of OPF hydrogel and implanted in a critical size osteochondral defects at the level of the right knee (four defects/ joint). The follow up has been of 6 month and right now the histological, immunohistochemical and bio-mechanical analyses are in progress. All the minipigs have been fine during the follow up, except one animals which sufferer the first 3 day after surgery of a local inflammation at the knee that in a week has disappeared. If the results of this study will be promising we will try to apply for a phase I trial. However, there are several aspects that need to be consider dealing with humans: may the "quality" of human ASCs be affected by the donor's physiological or pathological conditions? and in this case may the use of selected pharmacological treatment enhance the cellular plasticity? or may the use of allogenic hASCs overcome some hASCs deficiency? or may the use of immunoselected hASCs be more advantageous in the field of muscle-skeletal tissue regeneration?

It is well known that MSCs play an essential role in the maintaining tissue homeostasis and in participating in tissue repair during the lifespan of an individual.

The decline in their proliferative and differentiation potential can contribute to aging and to the onset of age-related diseases [Rao and Mattson, 2001; Van Zant and Liang, 2003] and, for this reason, the use of autologous MSCs in tissue engineering applications should take into account the possibility that the proliferative and differentiative potential decreases in relation of the donor's age [Pal et al., 2009; Carrion et al., 2010].

In recent years, several studies both in animals and in humans, have reported that age induce some alterations in term of MSCs cellular yield, doubling time, ability to produce colonies and differentiation potential [Baxter et al., 2004; Fehrer and Lepperdinger, 2005; Bonab et al., 2006].

For this reason we have analyzed and compared hASCs harvested from female donors aged under 35 and over 45 years. The significantly more abundant hASCs yield per ml of raw adipose tissue from the over 45 year-old donors may be related to the hormonal disequilibrium in this period of a woman's life, which may enhance the number of progenitor mesenchymal cells in adipose tissue, known to increase with age. On the other hand, the number of CFU-F was just slightly reduced from older donors. No significant differences were detected in terms of the *in vitro* adipogenic differentiation potential of

hASCs from younger or older donors; indeed, in both cases cells were able to differentiate into adipocyte-like cells. On the contrary, age affected the hASCs *in vitro* osteogenic differentiation potential: a reduced differentiation capacity of hASCs>45 y/o was observed, as assessed by ALP activity and calcium deposition. Hence our data suggest the potential use of autologous hASCs, although inter-individual differences related to sex, age and tissue inflammatory state [Barry, 2003; van Harmelen et al., 2003] need to be taken into account for regenerative medicine application, together with the opportune indications for this kind of treatment.

Now, in collaboration with a group of the University of Rome, we are evaluating the effect of obesity, on hASCs features from obese subcutaneous adipose tissue, in comparison to hASCs from healthy donors. It is known that adipose tissue is an endocrine organ able to secrete hormones, growth factors and cytokines involve in the regulation of the physiological homeostasis and also to contribute to the development of pathological states as obesity. This disease and the associated metabolic pathologies affect over 50% of the adult population, and are associated with a reduced pressure of oxygen that induced a chronic inflammatory response characterized by abnormal production of cytokines and activation of inflammatory signalling pathways that could affect the properties of adipose-derived stem cells. For this reason, we are studying if the inflammatory status of the human tissue *in vivo* reduces the pool of mesenchymal stem cells and their differentiation potential. Preliminary data indicate that hASCs isolated from adipose tissues of normal-weight (n-hASCs) and obese (ob-hASCs) donors showed different morphological and functional features [Tissue Engineering and Regenerative Medicine International Society (TERMIS), 2011; 35° Congresso Nazionale della Società Italiana di Farmacologia (SIF), 2011]. The proliferation rate of n-hASCs was higher compared to those cells obtained from obese patients with an average doubling time of 123.9±10.6 and 173.4±10.4 hours, respectively. We have also confirmed the different presence of progenitor cells: n-hASCs showed a clonogenic potential 77% higher than stem cells isolated from obese donors. Moreover, the osteogenic potential of hASCs seems also to be affected by obesity: indeed, n-hASCs and ob-hASCs in the presence of osteogenic stimuli showed a significant up-regulation of ALP activity of 326 and 48%, in comparison to the undifferentiated ones, respectively. It is important to mention that osteo-differentiated ob-hASCs presented about 10-fold lower ALP basal levels respect to n-hASCs. We have also cultured hASCs in hypoxic conditions:

both cell types were responsive to hypoxic environment resulting in the activation of pro-inflammatory genes such as hypoxia-inducible factor (HIF-1α), vascular endothelial growth factor (VEGF-α), suppressor of cytokine signalling (SOCS-1) and cyclooxygenase-2 (COX2). So, obesity seems to negatively affect the self-renewal and the differentiation ability of hASCs, likely due to the inflammatory state related to this condition. Indeed, both hASCs from healthy and obese donors are responsive to hypoxic environment resulting in the activation of pro-inflammatory genes, with major influence for n-hASCs in comparison to ob-hASCs, that could be due to an adaptation of ob-hASCs to an inflammatory microenvironment *in vivo*.

As the use of MSCs in regenerative medicine applications requires tissue engineering skills [Atala, 2007], and the selection of a suitable scaffold is fundamental in order to set up hybrid constructs [Mano and Reis, 2007], we have shown that hASCs may be used conveniently to screen several biomaterials, natural and synthetic, with potential clinical application [de Girolamo/ Arrigoni et al., 2009; Lopa/ Arrigoni et al., 2011]. We seeded undifferentiated hASCs on hydroxyapatite (HA) and on SiC-PECVD, a suitable ameliorative biocompatible coating layer [Santavirta et al., 1998], and then compared their ability to differentiate into osteoblast-like cells with cells cultured on polystyrene (PA). With regard to physiological condition of age, hASCs from younger donors, when cultured on both HA and SiC-PECVD, produced higher ALP activity and a greater amount of calcium deposition compared with cells derived from older donors. As expected, HA showed a strong and direct osteoinductive effect on hASCs; indeed, cells derived from both young and old donors, when cultured on HA, showed greater ALP activity compared with cells grown on PA, even if maintained in control medium.

From these results, it is possible conclude that, the outcome of the use of autologous hASCs in tissue engineering applications may depend on the physio/pathological conditions of the donors which should be considered before proposing the use of progenitor cells for a cellular therapy.

For this reason, with the aim to improve the use of MSCs, we pharmacologically treated hASCs to improve their plasticity.

As previously demonstrated [de Girolamo/ Arrigoni et al., 2009], there are some cases in which mesenchymal stem cells give unsatisfactory differentiation yields, especially when used for the regeneration of skeletal or cardiac muscle, where reports in the literature

could be classified as "*proof of concept*" studies, more than realistic strategies for cell therapy [Mizuno, 2009]. Therefore, we tested whether Reversine, a synthetic purine that has been shown to increase cell plasticity of adult differentiated cells, could enhance mesenchymal stem cell differentiation. In particular, in this study, we have focused our attention on adipose-derived stem cells differentiation toward osteogenic and myogenic cell lineages.

Initially, we have decided to treat hASCs with 5 µM Reversine, which Anastasia et al. had previously found as the optimal concentration for fibroblast de-differentiation [Anastasia et al., 2006]. However, this dose was toxic for hASCs and we treated them with 50 nM Reversine, which was already used in another study [Chen et al., 2007], and which gave the best results in terms of differentiation ability toward osteoblast and smooth muscle cells, without reduction in cell proliferation. Moreover, since the main goal of our study was to determine whether we could improve the differentiation yields of mesenchymal stem cells in those cases where they normally give really poor results, we tried to induce Reversine-pretreated hASCs to differentiate into myocytes. Reversine treated hASCs co-differentiated with murine myoblasts C2C12, produced the formation of myotubes expressing the muscle differentiation marker MHC and containing human nuclei that could only be generated from hASCs, clearly demonstrating the differentiation of hASCs into skeletal muscle. It is not known the mechanism of action of Reversine yet, and we have shown that genes such as c-Myc, Oct-4, Kfl-4 and Nanog are not modulated by the treatment in these cells. Along this line, several studies are in progress to elucidate and clarify the Reversine mechanism of action.

Another aspect that we have considered, was the possibility to isolate, specific progenitor cells, such as CD34 and L-NGFR positive cells from hASCs population (PA) by immunoselection. The enrichment of MSCs by selection with a monoclonal antibody raised against L-NGFR and bound to magnetic beads has been previously described in BMSCs [Quirici et al., 2002], where a subset of cells showed a high proliferative, clonogenic, and multipotential differentiation ability. More recently, Yamamoto et al. isolated and analyzed L-NGFR+ cells from mouse subcutaneous adipose tissue, showing that the rate of differentiation into adipocytes, osteoblasts, and neuronal cells was higher than for L-NGFR-hASCs [Yamamoto et al., 2007].

As already reported, Lee et al. isolated a population of muscle-derived CD34+ stem cells able to improve both muscle regeneration and bone healing [Lee et al., 2000], whereas Garcia-Pacheco et al. found that human decidual stromal cells positive for both CD34 and STRO-1 are related to BM stromal precursors [Garcia-Pacheco et al., 2001]. Moreover, expression of CD34 had been already reported in BMSCs, although it was rapidly lost after *in vitro* culture [Simmons and Torok-Storb, 1991; Deans and Moseley, 2000; Quirici et al., 2002]. In human adipose tissue, L-NGFR and CD34 MoAbs were able to identify 2 fractions expressing surface markers associated with a primitive phenotype. Accordingly, we observed that L-NGFR and CD34 expressions are progressively down-modulated during culture, in parallel with both the reduction of hASCs clonogenic and multi-differentiative ability and the acquisition of a fibroblast phenotype. The developmentally programmed loss of marker expression is reminiscent of what was observed in the case of the CD34 [Civin et al., 1987], L-NGFR [Quirici et al., 2002], and Stro-1 [Simmons and Torok-Storb, 1991] antigens on BMSCs, supporting the hypothesis that they are markers of primitive cells. Both immunoseparated cellular fractions showed higher proliferative and differentiative ability throughout the time of culture compared to PA hASCs. Nevertheless, the immunoselected subpopulations better responded both to the physical stimuli and to the hypoxia condition of the 3-dimensional culture, positively affecting the chondrogenic differentiation [Vinatier et al., 2009]. Indeed, just the 3D condition induced CD34+ and L-NGFR+ cells to produce similar or even higher levels of GAGs than PA hASCs cultured in chondrogenic medium: this could be due to the greater ability of the selected hASCs to respond to the 3D physical stimuli. Furthermore, DNA quantification showed a higher proliferative effect of the chondrocyte-inductive TGF-β on PA and CD34+ fractions in comparison to L-NGFR+ cells, maybe depending on the large number of primitive cells able to differentiate and survive in conditions of stress and able to rapidly differentiate.

All together, these data suggest that the selection by anti-L-NGFR MoAb allows us to obtain a more homogeneous and primitive population: the almost total co-expression of CD34, the expression of the stem markers CD117 and CD105, and the higher proliferative, clonogenic, and differentiative potential, in particular at early passages, seem to support this observation. The role of L-NGFR in MSCs is still unclear, although its expression has been described in BM and in other tissues [Jones et al., 2004] and it has been shown to be involved in several functions including morphogenesis [Sariola et al., 1991; Campagnolo et

al., 2001; Suzuki et al., 2008], growth factor presentation [Glass et al., 1991], and apoptosis in response to NGF stimulation [Trim et al., 2000]. We observed a higher heterogeneity in CD34+ population, with <30% of cells co-expressing L-NGFR and low levels of CD117 and CD105 expression. In the last years, some authors have isolated from human adipose tissue CD34+/CD31- cells including adipocytes progenitor cells and CD34+/CD31+ cells defined as capillary endothelial cells [Miranville et al., 2004]. They proposed that adipocytes and endothelial cells might share a common precursor, as also suggested by Planat-Benard et al. [Planat-Benard et al., 2004], which could play a determinant role in the excessive development of the adipose tissue by contributing to neo-vascularisation and to the apparent adipocyte hyperplasia. Moreover, Traktuev et al. recently described a hASCs subset (CD34+/CD140a+/CD140b+/CD31−/CD45−/CD117−/CD144−) with pericytic properties that participate in vascular stabilization by mutual structural and functional interactions with endothelial cells, maintaining the ability to differentiate into multiple lineages [Traktuev et al., 2008]. These evidences suggest that CD34+ hASCs could be preferentially used for bone tissue engineering, due to their ability to promote the neo-vascularization process, which is known to be a critical point in the healing of bone defects. These cells could be also combined with other terminally differentiated cells to allow a satisfactory vascularization of the "repaired" tissue.

 Nowadays, in the field of regenerative medicine, physicians prefer one-step surgical procedures in order to reduce patients' discomfort, risks of pathogens transmission, and social costs. In this context, the possibility to rapidly select subpopulations of cells more prone to differentiate into a specific lineage would be very advantageous, and could be useful tools in regenerative medicine applications.

In conclusion, ASCs can be considered good candidates in the field of tissue engineering and regenerative medicine, in particular in the field of skeletal-muscle tissues.

In our pre-clinical studies, we have demonstrated that rbASCs seeded on hydroxyapatite disks, are able to repair a critical-size bone defect producing, in the defect site, a new tissue with the characteristics of mature and healthy bone tissue [de Girolamo/ Arrigoni et al., 2011; Arrigoni et al., submitted].

However, before moving to the clinic is important consider if some physio/ pathological conditions of the donors can influence the features of hASCs. Indeed, we have demonstrated that age [de Girolamo/ Arrigoni et al., 2009] and obesity [Stanco/ Arrigoni et

al., manuscript in preparation], could be considered important to predict the outcome of a regenerative medicine treatment by hASCs, and possible strategies to overcome differentiation deficiency could be the pharmacological treatment with Reversine to enhance the differentiative potential of hASCs [Conforti/ Arrigoni et al., 2011], the use of immunoselected subpopulation of hASCs [Quirici/ Arrigoni et al., 2010], or the use of allogenic hASCs from young healthy donors that may produce a better results. In collaboration with Prof. Sacerdote at the Department of Medical Pharmacology of the University of Milan, we have obtained preliminary results on hASCs, co-cultured for 24 hours together with heterologous peripheral blood lymphocytes, where they do not induce any T-cells activation and any significant release of Th1 and Th2-specific cytokines confirming the low immunogenicity of these hASCs, as already shown by others [Calderon et al., 2011; McIntosh KR, 2011] and making us believing feasible to perform allotransplant.

<u>ACKNOWLEDGEMENTS</u>

Department of Human Morphology - Università degli Studi di Milano

Dr. Claudia Dellavia

LaBS - Laboratory of Biological Structure Mechanics Structural Engineering Department - Politecnico di Milano

M.Eng. Davide Carnelli

Fondazione Matarelli, Department of Medical Pharmacology - Università degli Studi di Milano

Dr. Nadia Quirici

Dr. Cinzia Scavullo

IRCCS Policlinico San Donato, Milano

Prof. Luigi Anastasia

Dr. Erika Conforti

Dr. Marco Piccoli

Experimental Medicine and Pathology Department - Università di Roma "La Sapienza"

Prof. Elisa Petrangeli

Dr. Luisa Salvatori

Dr. Giuseppe Coroniti

Department of Medical Pharmacology - Università degli Studi di Milano

Prof. Alberto Panerai

Prof. Paola Sacerdote

Dr. Silvia Franchi

Dr. Donatella Lattuada

Dr. Giuseppe Rossoni

REFERENCES

Aalami, O.O., R.P. Nacamuli, K.A. Lenton, C.M. Cowan, T.D. Fang, K.D. Fong, Y.Y. Shi, H.M. Song, D.E. Sahar, M.T. Longaker (2004) Applications of a mouse model of calvarial healing: differences in regenerative abilities of juveniles and adults: Plast Reconstr Surg. United States, pp 713-720.

Abdallah, B.M., M. Kassem (2008) Human mesenchymal stem cells: from basic biology to clinical applications. Gene Ther *15(2)*: 109-116.

Aerssens, J., S. Boonen, J. Joly, J. Dequeker (1997) Variations in trabecular bone composition with anatomical site and age: potential implications for bone quality assessment. J Endocrinol *155(3)*: 411-421.

Aerssens, J., S. Boonen, G. Lowet, J. Dequeker (1998) Interspecies differences in bone composition, density, and quality: potential implications for in vivo bone research. Endocrinology *139(2)*: 663-670.

Ahdjoudj, S., F. Lasmoles, X. Holy, E. Zerath, P.J. Marie (2002) Transforming growth factor beta2 inhibits adipocyte differentiation induced by skeletal unloading in rat bone marrow stroma. J Bone Miner Res *17(4)*: 668-677.

Al-Hajj, M., M.S. Wicha, A. Benito-Hernandez, S.J. Morrison, M.F. Clarke (2003) Prospective identification of tumorigenic breast cancer cells: Proc Natl Acad Sci U S A. United States, pp 3983-3988.

Ambrosio, A.M., J.S. Sahota, Y. Khan, C.T. Laurencin (2001) A novel amorphous calcium phosphate polymer ceramic for bone repair: I. Synthesis and characterization: J Biomed Mater Res. United States, 2001 John Wiley & Sons, Inc., pp 295-301.

Anastasia, L., G. Pelissero, B. Venerando, G. Tettamanti (2010) Cell reprogramming: expectations and challenges for chemistry in stem cell biology and regenerative medicine: Cell Death Differ. England, pp 1230-1237.

Anastasia, L., M. Sampaolesi, N. Papini, D. Oleari, G. Lamorte, C. Tringali, E. Monti, D. Galli, G. Tettamanti, G. Cossu, B. Venerando (2006) Reversine-treated fibroblasts acquire myogenic competence in vitro and in regenerating skeletal muscle: Cell Death Differ. England, pp 2042-2051.

Andrade-Zaldivar, H., L. Santos, A. De Leon Rodriguez (2008) Expansion of human hematopoietic stem cells for transplantation: trends and perspectives. Cytotechnology *56(3)*: 151-160.

Anokye-Danso, F., C.M. Trivedi, D. Juhr, M. Gupta, Z. Cui, Y. Tian, Y. Zhang, W. Yang, P.J. Gruber, J.A. Epstein, E.E. Morrisey (2011) Highly efficient miRNA-mediated reprogramming of mouse and human somatic cells to pluripotency: Cell Stem Cell. United States, 2011 Elsevier Inc, pp 376-388.

Arai, F., O. Ohneda, T. Miyamoto, X.Q. Zhang, T. Suda (2002) Mesenchymal stem cells in perichondrium express activated leukocyte cell adhesion molecule and participate in bone marrow formation. J Exp Med *195(12)*: 1549-1563.

Arrigoni, E., L. de Girolamo, A. Di Giancamillo, D. Stanco, C. Dellavia, D. Carnelli, M. Campagnol, C. Domeneghini, A.T. Brini (submitted) Adipose-derived stem cells in association with hydroxyapatite enhance bone regeneration in rabbits. J Orthop Res (under revision).

Arrigoni, E., S. Lopa, L. de Girolamo, D. Stanco, A.T. Brini (2009) Isolation, characterization and osteogenic differentiation of adipose-derived stem cells: from small to large animal models. Cell Tissue Res *338(3)*: 401-411.

Atala, A. (2007) Engineering tissues, organs and cells. J Tissue Eng Regen Med *1(2)*: 83-96.

Aubin, J.E. (1998) Advances in the osteoblast lineage. Biochem Cell Biol *76(6)*: 899-910.

Augello, A., C. De Bari (2010) The regulation of differentiation in mesenchymal stem cells. Hum Gene Ther *21(10)*: 1226-1238.

Bae, S.E., D.H. Choi, D.K. Han, K. Park (2010) Effect of temporally controlled release of dexamethasone on in vivo chondrogenic differentiation of mesenchymal stromal cells: J Control Release. Netherlands, 2009 Elsevier B.V, pp 23-30.

Banas, A., T. Teratani, Y. Yamamoto, M. Tokuhara, F. Takeshita, G. Quinn, H. Okochi, T. Ochiya (2007) Adipose tissue-derived mesenchymal stem cells as a source of human hepatocytes. Hepatology *46(1)*: 219-228.

Barbosa, I., S. Garcia, V. Barbier-Chassefiere, J.P. Caruelle, I. Martelly, D. Papy-Garcia (2003) Improved and simple micro assay for sulfated glycosaminoglycans quantification in biological extracts and its use in skin and muscle tissue studies: Glycobiology. England, pp 647-653.

Barrallo-Gimeno, A., M.A. Nieto (2005) The Snail genes as inducers of cell movement and survival: implications in development and cancer: Development. England, pp 3151-3161.

Barry, F.P. (2003) Biology and clinical applications of mesenchymal stem cells. Birth Defects Res C Embryo Today *69(3)*: 250-256.

Barry, F.P., J.M. Murphy (2004) Mesenchymal stem cells: clinical applications and biological characterization: Int J Biochem Cell Biol. England, pp 568-584.

Baskin, D.S., P. Ryan, V. Sonntag, R. Westmark, M.A. Widmayer (2003) A prospective, randomized, controlled cervical fusion study using recombinant human bone morphogenetic protein-2 with the CORNERSTONE-SR allograft ring and the ATLANTIS anterior cervical plate. Spine (Phila Pa 1976) *28(12)*: 1219-1224; discussion 1225.

Baxter, M.A., R.F. Wynn, S.N. Jowitt, J.E. Wraith, L.J. Fairbairn, I. Bellantuono (2004) Study of telomere length reveals rapid aging of human marrow stromal cells following in vitro expansion. Stem Cells *22(5)*: 675-682.

Beier, D., P. Hau, M. Proescholdt, A. Lohmeier, J. Wischhusen, P.J. Oefner, L. Aigner, A. Brawanski, U. Bogdahn, C.P. Beier (2007) CD133(+) and CD133(-) glioblastoma-derived cancer stem cells show differential growth characteristics and molecular profiles: Cancer Res. United States, pp 4010-4015.

Bodo, M., C. Lilli, C. Bellucci, P. Carinci, M. Calvitti, F. Pezzetti, G. Stabellini, S. Bellocchio, C. Balducci, F. Carinci, T. Baroni (2002) Basic fibroblast growth factor autocrine loop controls human osteosarcoma phenotyping and differentiation: Mol Med. United States, pp 393-404.

Bonab, M.M., K. Alimoghaddam, F. Talebian, S.H. Ghaffari, A. Ghavamzadeh, B. Nikbin (2006) Aging of mesenchymal stem cell in vitro. BMC Cell Biol *7*: 14.

Bosetti, M., L. Zanardi, L. Hench, M. Cannas (2003) Type I collagen production by osteoblast-like cells cultured in contact with different bioactive glasses. J Biomed Mater Res A *64(1)*: 189-195.

Brown, B.N., J.E. Valentin, A.M. Stewart-Akers, G.P. McCabe, S.F. Badylak (2009) Macrophage phenotype and remodeling outcomes in response to biologic scaffolds with and without a cellular component: Biomaterials. England, pp 1482-1491.

Bruder, S.P., N. Jaiswal, S.E. Haynesworth (1997) Growth kinetics, self-renewal, and the osteogenic potential of purified human mesenchymal stem cells during extensive subcultivation and following cryopreservation: J Cell Biochem. United States, pp 278-294.

Burns, C.E., L.I. Zon (2002) Portrait of a stem cell: Dev Cell. United States, pp 612-613.

Cabrita, G.J., B.S. Ferreira, C.L. da Silva, R. Goncalves, G. Almeida-Porada, J.M. Cabral (2003) Hematopoietic stem cells: from the bone to the bioreactor: Trends Biotechnol. England, pp 233-240.

Calabro, A., M. Benavides, M. Tammi, V.C. Hascall, R.J. Midura (2000) Microanalysis of enzyme digests of hyaluronan and chondroitin/dermatan sulfate by fluorophore-assisted carbohydrate electrophoresis (FACE): Glycobiology. England, pp 273-281.

Calderon, D.,V. Planat-Benard, V. Bellamy, V. Vanneaux, C. Khun, S. Peyrard, J. Larghero, M. Desnos, L. Casteilla, M. Pucéat, P. Menasché, L. Chatenoud (2011) Immune response to human embryonic stem cell-derived cardiac progenitors and adipose-derived stromal cells. J Cell Mol Med. 2011 Sep 5.

Campagnolo, L., M.A. Russo, A. Puglianiello, A. Favale, G. Siracusa (2001) Mesenchymal cell precursors of peritubular smooth muscle cells of the mouse testis can be identified by the presence of the p75 neurotrophin receptor. Biol Reprod *64(2)*: 464-472.

Caplan, A.I. (2007) Adult mesenchymal stem cells for tissue engineering versus regenerative medicine. J Cell Physiol *213(2)*: 341-347.

Capretto, L., S. Mazzitelli, G. Luca, C. Nastruzzi (2010) Preparation and characterization of polysaccharidic microbeads by a microfluidic technique: application to the encapsulation of Sertoli cells: Acta Biomater. England, pp 429-435.

Carrion, F., E. Nova, C. Ruiz, F. Diaz, C. Inostroza, D. Rojo, G. Monckeberg, F.E. Figueroa (2010) Autologous mesenchymal stem cell treatment increased T regulatory cells with no effect on disease activity in two systemic lupus erythematosus patients. Lupus *19(3)*: 317-322.

Castaneda, S., R. Largo, E. Calvo, F. Rodriguez-Salvanes, M.E. Marcos, M. Diaz-Curiel, G. Herrero-Beaumont (2006) Bone mineral measurements of subchondral and trabecular bone in healthy and osteoporotic rabbits. Skeletal Radiol *35(1)*: 34-41.

Castro-Malaspina, H., R.E. Gay, G. Resnick, N. Kapoor, P. Meyers, D. Chiarieri, S. McKenzie, H.E. Broxmeyer, M.A. Moore (1980) Characterization of human bone marrow fibroblast colony-forming cells (CFU-F) and their progeny. Blood *56(2)*: 289-301.

Celil, A.B., P.G. Campbell (2005) BMP-2 and insulin-like growth factor-I mediate Osterix (Osx) expression in human mesenchymal stem cells via the MAPK and protein kinase D signaling pathways: J Biol Chem. United States, pp 31353-31359.

Chamberlain, G., J. Fox, B. Ashton, J. Middleton (2007) Concise review: mesenchymal stem cells: their phenotype, differentiation capacity, immunological features, and potential for homing: Stem Cells. United States, pp 2739-2749.

Chang, C.H., T.F. Kuo, F.H. Lin, J.H. Wang, Y.M. Hsu, H.T. Huang, S.T. Loo, H.W. Fang, H.C. Liu, W.C. Wang (2011) Tissue engineering-based cartilage repair with mesenchymal stem cells in a porcine model. J Orthop Res *29(12)*: 1874-1880.

Chen, H.C., Y.C. Hu (2006) Bioreactors for tissue engineering. Biotechnol Lett *28(18)*: 1415-1423.

Chen, S., S. Takanashi, Q. Zhang, W. Xiong, S. Zhu, E.C. Peters, S. Ding, P.G. Schultz (2007) Reversine increases the plasticity of lineage-committed mammalian cells: Proc Natl Acad Sci U S A. United States, pp 10482-10487.

Chen, S., Q. Zhang, X. Wu, P.G. Schultz, S. Ding (2004) Dedifferentiation of lineage-committed cells by a small molecule. J Am Chem Soc *126(2)*: 410-411.

Choi, C.H., J.H. Jung, Y.W. Rhee, D.P. Kim, S.E. Shim, C.S. Lee (2007) Generation of monodisperse alginate microbeads and in situ encapsulation of cell in microfluidic device. Biomed Microdevices *9(6)*: 855-862.

Ciocca, L., F. De Crescenzio, M. Fantini, R. Scotti (2009) CAD/CAM and rapid prototyped scaffold construction for bone regenerative medicine and surgical transfer of virtual planning: a pilot study: Comput Med Imaging Graph. United States, pp 58-62.

Civiale, C., M. Licciardi, G. Cavallaro, G. Giammona, M.G. Mazzone (2009) Polyhydroxyethylaspartamide-based micelles for ocular drug delivery: Int J Pharm. Netherlands, pp 177-186.

Civin, C.I., M.L. Banquerigo, L.C. Strauss, M.R. Loken (1987) Antigenic analysis of hematopoiesis. VI. Flow cytometric characterization of My-10-positive progenitor cells in normal human bone marrow. Exp Hematol *15(1)*: 10-17.

Conforti, E., E. Arrigoni, M. Piccoli, S. Lopa, L. de Girolamo, A. Ibatici, A. Di Matteo, G. Tettamanti, A.T. Brini, L. Anastasia (2011) Reversine increases multipotent human mesenchymal cells differentiation potential. J Biol Regul Homeost Agents *25(2 Suppl)*: S25-33.

Cook, S.D., L.P. Patron, S.L. Salkeld, D.C. Rueger (2003) Repair of articular cartilage defects with osteogenic protein-1 (BMP-7) in dogs. J Bone Joint Surg Am *85-A Suppl 3*: 116-123.

Corcione, A., F. Benvenuto, E. Ferretti, D. Giunti, V. Cappiello, F. Cazzanti, M. Risso, F. Gualandi, G.L. Mancardi, V. Pistoia, A. Uccelli (2006) Human mesenchymal stem cells modulate B-cell functions: Blood. United States, pp 367-372.

Cowan, C.M., Y.Y. Shi, O.O. Aalami, Y.F. Chou, C. Mari, R. Thomas, N. Quarto, C.H. Contag, B. Wu, M.T. Longaker (2004) Adipose-derived adult stromal cells heal critical-size mouse calvarial defects. Nat Biotechnol *22(5)*: 560-567.

Cui, L., B. Liu, G. Liu, W. Zhang, L. Cen, J. Sun, S. Yin, W. Liu, Y. Cao (2007) Repair of cranial bone defects with adipose derived stem cells and coral scaffold in a canine model: Biomaterials. England, pp 5477-5486.

Damadzadeh, B., H. Jabari, M. Skrifvars, K. Airola, N. Moritz, P.K. Vallittu (2010) Effect of ceramic filler content on the mechanical and thermal behaviour of poly-L-lactic acid and poly-L-lactic-co-glycolic acid composites for medical applications. J Mater Sci Mater Med *21(9)*: 2523-2531.

Dausse, Y., L. Grossin, G. Miralles, S. Pelletier, D. Mainard, P. Hubert, D. Baptiste, P. Gillet, E. Dellacherie, P. Netter, E. Payan (2003) Cartilage repair using new polysaccharidic biomaterials: macroscopic, histological and biochemical approaches in a rat model of cartilage defect: Osteoarthritis Cartilage. England, 2003 OsteoArthritis Research Society International. Published by Elsevier Science Ltd., pp 16-28.

Davies, C.M., D.B. Jones, M.J. Stoddart, K. Koller, E. Smith, C.W. Archer, R.G. Richards (2006) Mechanically loaded ex vivo bone culture system 'Zetos': systems and culture preparation: Eur Cell Mater. Scotland, pp 57-75; discussion 75.

Day, T.F., X. Guo, L. Garrett-Beal, Y. Yang (2005) Wnt/beta-catenin signaling in mesenchymal progenitors controls osteoblast and chondrocyte differentiation during vertebrate skeletogenesis: Dev Cell. United States, pp 739-750.

de Girolamo, L., E. Arrigoni, D. Stanco, S. Lopa, A. Di Giancamillo, A. Addis, S. Borgonovo, C. Dellavia, C. Domeneghini, A.T. Brini (2011) Role of autologous rabbit adipose-derived stem cells in the early phases of the repairing process of critical bone defects. J Orthop Res *29(1)*: 100-108.

de Girolamo, L., S. Lopa, E. Arrigoni, M.F. Sartori, F.W. Baruffaldi Preis, A.T. Brini (2009) Human adipose-derived stem cells isolated from young and elderly women: their differentiation potential and scaffold interaction during in vitro osteoblastic differentiation. Cytotherapy *11(6)*: 793-803.

de Girolamo, L., M.F. Sartori, W. Albisetti, A.T. Brini (2007) Osteogenic differentiation of human adipose-derived stem cells: comparison of two different inductive media. J Tissue Eng Regen Med *1(2)*: 154-157.

de Girolamo, L., M.F. Sartori, E. Arrigoni, L. Rimondini, W. Albisetti, R.L. Weinstein, A.T. Brini (2008) Human adipose-derived stem cells as future tools in tissue regeneration: osteogenic differentiation and cell-scaffold interaction. Int J Artif Organs *31(6)*: 467-479.

De Ugarte, D.A., K. Morizono, A. Elbarbary, Z. Alfonso, P.A. Zuk, M. Zhu, J.L. Dragoo, P. Ashjian, B. Thomas, P. Benhaim, I. Chen, J. Fraser, M.H. Hedrick (2003) Comparison of multi-lineage cells from human adipose tissue and bone marrow: Cells Tissues Organs. Switzerland, 2003 S. Karger AG, Basel, pp 101-109.

Deans, R.J., A.B. Moseley (2000) Mesenchymal stem cells: biology and potential clinical uses. Exp Hematol *28(8)*: 875-884.

den Boer, F.C., P. Patka, F.C. Bakker, B.W. Wippermann, A. van Lingen, G.Q. Vink, K. Boshuizen, H.J. Haarman (1999) New segmental long bone defect model in sheep: quantitative analysis of healing with dual energy x-ray absorptiometry. J Orthop Res *17(5)*: 654-660.

Denizot, F., R. Lang (1986) Rapid colorimetric assay for cell growth and survival. Modifications to the tetrazolium dye procedure giving improved sensitivity and reliability. J Immunol Methods *89(2)*: 271-277.

Deschaseaux, F., L. Sensebe, D. Heymann (2009) Mechanisms of bone repair and regeneration: Trends Mol Med. England, pp 417-429.

Devine, M.J., C.M. Mierisch, E. Jang, P.C. Anderson, G. Balian (2002) Transplanted bone marrow cells localize to fracture callus in a mouse model. J Orthop Res *20(6)*: 1232-1239.

Devine, S.M., S. Peter, B.J. Martin, F. Barry, K.R. McIntosh (2001) Mesenchymal stem cells: stealth and suppression. Cancer J *7 Suppl 2*: S76-82.

Dimar, J.R., S.D. Glassman, K.J. Burkus, L.Y. Carreon (2006) Clinical outcomes and fusion success at 2 years of single-level instrumented posterolateral fusions with recombinant human bone morphogenetic protein-2/compression resistant matrix versus iliac crest bone graft: Spine (Phila Pa 1976). United States, pp 2534-2539; discussion 2540.

Donath, K., G. Breuner (1982) A method for the study of undecalcified bones and teeth with attached soft tissues. The Sage-Schliff (sawing and grinding) technique. J Oral Pathol *11(4)*: 318-326.

Ducy, P., M. Starbuck, M. Priemel, J. Shen, G. Pinero, V. Geoffroy, M. Amling, G. Karsenty (1999) A Cbfa1-dependent genetic pathway controls bone formation beyond embryonic development. Genes Dev *13(8)*: 1025-1036.

Duque, G., M. Macoritto, R. Kremer (2004) 1,25(OH)2D3 inhibits bone marrow adipogenesis in senescence accelerated mice (SAM-P/6) by decreasing the expression of peroxisome proliferator-activated receptor gamma 2 (PPARgamma2): Exp Gerontol. England, pp 333-338.

Egermann, M., J. Goldhahn, E. Schneider (2005) Animal models for fracture treatment in osteoporosis. Osteoporos Int *16 Suppl 2*: S129-138.

Ehrlich, P.J., L.E. Lanyon (2002) Mechanical strain and bone cell function: a review. Osteoporos Int *13(9)*: 688-700.

Elsinger, E.C., L. Leal (1996) Coralline hydroxyapatite bone graft substitutes. J Foot Ankle Surg *35(5)*: 396-399.

Engler, A.J., S. Sen, H.L. Sweeney, D.E. Discher (2006) Matrix elasticity directs stem cell lineage specification: Cell. United States, pp 677-689.

Erbs, S., A. Linke, V. Schachinger, B. Assmus, H. Thiele, K.W. Diederich, C. Hoffmann, S. Dimmeler, T. Tonn, R. Hambrecht, A.M. Zeiher, G. Schuler (2007) Restoration of microvascular function in the infarct-related artery by intracoronary transplantation of bone marrow progenitor cells in patients with acute myocardial infarction: the Doppler Substudy of the Reinfusion of Enriched Progenitor Cells and Infarct Remodeling in Acute Myocardial Infarction (REPAIR-AMI) trial: Circulation. United States, pp 366-374.

Erickson, G.R., J.M. Gimble, D.M. Franklin, H.E. Rice, H. Awad, F. Guilak (2002) Chondrogenic potential of adipose tissue-derived stromal cells in vitro and in vivo: Biochem Biophys Res Commun. United States, pp 763-769.

Esposito, E., R. Cortesi, G. Luca, C. Nastruzzi (2001) Pectin-based microspheres: a preformulatory study. Ann N Y Acad Sci *944*: 160-179.

Everts, V., J.M. Delaisse, W. Korper, D.C. Jansen, W. Tigchelaar-Gutter, P. Saftig, W. Beertsen (2002) The bone lining cell: its role in cleaning Howship's lacunae and initiating bone formation. J Bone Miner Res *17(1)*: 77-90.

Fantner, G.E., T. Hassenkam, J.H. Kindt, J.C. Weaver, H. Birkedal, L. Pechenik, J.A. Cutroni, G.A. Cidade, G.D. Stucky, D.E. Morse, P.K. Hansma (2005) Sacrificial bonds and hidden length dissipate energy as mineralized fibrils separate during bone fracture. Nat Mater *4(8)*: 612-616.

Fehrer, C., G. Lepperdinger (2005) Mesenchymal stem cell aging. Exp Gerontol *40(12)*: 926-930.

Foster, B.L., M.J. Somerman (2005) Regenerating the periodontium: is there a magic formula?: Orthod Craniofac Res. England, pp 285-291.

Franceschi, R.T., C. Ge, G. Xiao, H. Roca, D. Jiang (2007) Transcriptional regulation of osteoblasts: Ann N Y Acad Sci. United States, pp 196-207.

Fraser, J.K., R. Schreiber, B. Strem, M. Zhu, Z. Alfonso, I. Wulur, M.H. Hedrick (2006a) Plasticity of human adipose stem cells toward endothelial cells and cardiomyocytes: Nat Clin Pract Cardiovasc Med. England, pp S33-37.

Fraser, J.K., I. Wulur, Z. Alfonso, M.H. Hedrick (2006b) Fat tissue: an underappreciated source of stem cells for biotechnology. Trends Biotechnol *24(4)*: 150-154.

Friedenstein, A.J., K.V. Petrakova, A.I. Kurolesova, G.P. Frolova (1968) Heterotopic of bone marrow. Analysis of precursor cells for osteogenic and hematopoietic tissues. Transplantation *6(2)*: 230-247.

Frisbie, D.D., S. Morisset, C.P. Ho, W.G. Rodkey, J.R. Steadman, C.W. McIlwraith (2006) Effects of calcified cartilage on healing of chondral defects treated with microfracture in horses: Am J Sports Med. United States, pp 1824-1831.

Fujimura, J., R. Ogawa, H. Mizuno, Y. Fukunaga, H. Suzuki (2005) Neural differentiation of adipose-derived stem cells isolated from GFP transgenic mice: Biochem Biophys Res Commun. United States, pp 116-121.

Garcia-Pacheco, J.M., C. Oliver, M. Kimatrai, F.J. Blanco, E.G. Olivares (2001) Human decidual stromal cells express CD34 and STRO-1 and are related to bone marrow stromal precursors. Mol Hum Reprod *7(12)*: 1151-1157.

Ge, Z., S. Baguenard, L.Y. Lim, A. Wee, E. Khor (2004) Hydroxyapatite-chitin materials as potential tissue engineered bone substitutes. Biomaterials *25(6)*: 1049-1058.

Giannoudis, P.V., H. Dinopoulos, E. Tsiridis (2005) Bone substitutes: an update: Injury. Netherlands, pp S20-27.

Gilsanz, V., T.F. Roe, D.T. Gibbens, E.E. Schulz, M.E. Carlson, O. Gonzalez, M.I. Boechat (1988) Effect of sex steroids on peak bone density of growing rabbits. Am J Physiol *255(4 Pt 1)*: E416-421.

Gimble, J.M. (2003) Adipose tissue-derived therapeutics. Expert Opin Biol Ther *3(5)*: 705-713.

Glass, D.J., S.H. Nye, P. Hantzopoulos, M.J. Macchi, S.P. Squinto, M. Goldfarb, G.D. Yancopoulos (1991) TrkB mediates BDNF/NT-3-dependent survival and proliferation in fibroblasts lacking the low affinity NGF receptor. Cell *66(2)*: 405-413.

Gomes, M.E., V.I. Sikavitsas, E. Behravesh, R.L. Reis, A.G. Mikos (2003) Effect of flow perfusion on the osteogenic differentiation of bone marrow stromal cells cultured on starch-based three-dimensional scaffolds. J Biomed Mater Res A *67(1)*: 87-95.

Goshima, J., V.M. Goldberg, A.I. Caplan (1991) Osteogenic potential of culture-expanded rat marrow cells as assayed in vivo with porous calcium phosphate ceramic. Biomaterials *12(2)*: 253-258.

Gotterbarm, T., S.J. Breusch, U. Schneider, M. Jung (2008) The minipig model for experimental chondral and osteochondral defect repair in tissue engineering: retrospective analysis of 180 defects. Lab Anim *42(1)*: 71-82.

Gupta, P.B., C.L. Chaffer, R.A. Weinberg (2009) Cancer stem cells: mirage or reality?: Nat Med. United States, pp 1010-1012.

Hadjidakis, D.J., Androulakis, II (2006) Bone remodeling: Ann N Y Acad Sci. United States, pp 385-396.

Haleem, A.M., A.A. Singergy, D. Sabry, H.M. Atta, L.A. Rashed, C.R. Chu, M.T. El Shewy, A. Azzam, M.T. Abdel Aziz (2010) The Clinical Use of Human Culture-Expanded Autologous Bone Marrow Mesenchymal Stem Cells Transplanted on Platelet-Rich Fibrin Glue in the Treatment of Articular Cartilage Defects: A Pilot Study and Preliminary Results. Cartilage *1(4)*: 253-261.

Halvorsen, Y.D., D. Franklin, A.L. Bond, D.C. Hitt, C. Auchter, A.L. Boskey, E.P. Paschalis, W.O. Wilkison, J.M. Gimble (2001) Extracellular matrix mineralization and osteoblast gene expression by human adipose tissue-derived stromal cells. Tissue Eng *7(6)*: 729-741.

Hanks, C.T., J.C. Wataha, Z. Sun (1996) In vitro models of biocompatibility: a review. Dent Mater *12(3)*: 186-193.

Hao, W., J. Dong, M. Jiang, J. Wu, F. Cui, D. Zhou (2010a) Enhanced bone formation in large segmental radial defects by combining adipose-derived stem cells expressing bone morphogenetic protein 2 with nHA/RHLC/PLA scaffold. Int Orthop *34(8)*: 1341-1349.

Hao, W., L. Pang, M. Jiang, R. Lv, Z. Xiong, Y.Y. Hu (2010b) Skeletal repair in rabbits using a novel biomimetic composite based on adipose-derived stem cells encapsulated in collagen I gel with PLGA-beta-TCP scaffold. J Orthop Res *28(2)*: 252-257.

Harman, B.D., S.H. Weeden, D.K. Lichota, G.W. Brindley (2006) Osteochondral autograft transplantation in the porcine knee: Am J Sports Med. United States, pp 913-918.

Hay, E., J. Lemonnier, O. Fromigue, H. Guenou, P.J. Marie (2004) Bone morphogenetic protein receptor IB signaling mediates apoptosis independently of differentiation in osteoblastic cells: J Biol Chem. United States, pp 1650-1658.

Heino, T.J., K. Kurata, H. Higaki, H.K. Vaananen (2009) Evidence for the role of osteocytes in the initiation of targeted remodeling: Technol Health Care. Netherlands, pp 49-56.

Heise, U., J.F. Osborn, F. Duwe (1990) Hydroxyapatite ceramic as a bone substitute. Int Orthop *14(3)*: 329-338.

Hemavathy, K., S.I. Ashraf, Y.T. Ip (2000) Snail/slug family of repressors: slowly going into the fast lane of development and cancer: Gene. Netherlands, pp 1-12.

Hing, K.A., L.F. Wilson, T. Buckland (2007) Comparative performance of three ceramic bone graft substitutes. Spine J *7(4)*: 475-490.

Hoemann, C.D., J. Sun, A. Legare, M.D. McKee, M.D. Buschmann (2005) Tissue engineering of cartilage using an injectable and adhesive chitosan-based cell-delivery vehicle: Osteoarthritis Cartilage. England, pp 318-329.

Hollister, S.J. (2009) Scaffold engineering: a bridge to where?: Biofabrication. England, p 012001.

Hu, H., M.J. Hilton, X. Tu, K. Yu, D.M. Ornitz, F. Long (2005) Sequential roles of Hedgehog and Wnt signaling in osteoblast development: Development. England, pp 49-60.

Huangfu, D., R. Maehr, W. Guo, A. Eijkelenboom, M. Snitow, A.E. Chen, D.A. Melton (2008) Induction of pluripotent stem cells by defined factors is greatly improved by small-molecule compounds: Nat Biotechnol. United States, pp 795-797.

Hwang, Y.J., J.Y. Choi (2010) Addition of mesenchymal stem cells to the scaffold of platelet-rich plasma is beneficial for the reduction of the consolidation period in mandibular distraction osteogenesis: J Oral Maxillofac Surg. United States, 2010. Published by Elsevier Inc., pp 1112-1124.

Idikio, H.A. (2011) Human cancer classification: a systems biology- based model integrating morphology, cancer stem cells, proteomics, and genomics. J Cancer *2*: 107-115.

Inada, M., T. Yasui, S. Nomura, S. Miyake, K. Deguchi, M. Himeno, M. Sato, H. Yamagiwa, T. Kimura, N. Yasui, T. Ochi, N. Endo, Y. Kitamura, T. Kishimoto, T. Komori (1999) Maturational disturbance of chondrocytes in Cbfa1-deficient mice: Dev Dyn. United States, pp 279-290.

Izadpanah, R., C. Trygg, B. Patel, C. Kriedt, J. Dufour, J.M. Gimble, B.A. Bunnell (2006) Biologic properties of mesenchymal stem cells derived from bone marrow and adipose tissue. J Cell Biochem *99(5)*: 1285-1297.

Jiang, W.H., A.Q. Ma, Y.M. Zhang, K. Han, Y. Liu, Z.T. Zhang, T.Z. Wang, X. Huang, X.P. Zheng (2005) Migration of intravenously grafted mesenchymal stem cells to injured heart in rats. Sheng Li Xue Bao *57(5)*: 566-572.

Jones, E.A., A. English, K. Henshaw, S.E. Kinsey, A.F. Markham, P. Emery, D. McGonagle (2004) Enumeration and phenotypic characterization of synovial fluid multipotential mesenchymal progenitor cells in inflammatory and degenerative arthritis. Arthritis Rheum *50(3)*: 817-827.

Josiah, D.T., D. Zhu, F. Dreher, J. Olson, G. McFadden, H. Caldas (2010) Adipose-derived stem cells as therapeutic delivery vehicles of an oncolytic virus for glioblastoma: Mol Ther. United States, pp 377-385.

Kadiyala, S., R.G. Young, M.A. Thiede, S.P. Bruder (1997) Culture expanded canine mesenchymal stem cells possess osteochondrogenic potential in vivo and in vitro: Cell Transplant. United States, pp 125-134.

Karsenty, G., E.F. Wagner (2002) Reaching a genetic and molecular understanding of skeletal development: Dev Cell. United States, pp 389-406.

Kassem, M., M. Kristiansen, B.M. Abdallah (2004) Mesenchymal stem cells: cell biology and potential use in therapy: Basic Clin Pharmacol Toxicol. Denmark, pp 209-214.

Katagiri, T., N. Takahashi (2002) Regulatory mechanisms of osteoblast and osteoclast differentiation. Oral Dis *8(3)*: 147-159.

Kayser, O., A. Lemke, N. Hernandez-Trejo (2005) The impact of nanobiotechnology on the development of new drug delivery systems. Curr Pharm Biotechnol *6(1)*: 3-5.

Kim, H.J., J.H. Kim, S.C. Bae, J.Y. Choi, H.M. Ryoo (2003) The protein kinase C pathway plays a central role in the fibroblast growth factor-stimulated expression and transactivation activity of Runx2: J Biol Chem. United States, pp 319-326.

Kirkpatrick, C.J., V. Krump-Konvalinkova, R.E. Unger, F. Bittinger, M. Otto, K. Peters (2002) Tissue response and biomaterial integration: the efficacy of in vitro methods: Biomol Eng. Netherlands, pp 211-217.

Kirouac, D.C., P.W. Zandstra (2008) The systematic production of cells for cell therapies: Cell Stem Cell. United States, pp 369-381.

Ko, H.C., B.K. Milthorpe, C.D. McFarland (2007) Engineering thick tissues--the vascularisation problem: Eur Cell Mater. Scotland, pp 1-18; discussion 18-19.

Komori, T. (2006) Regulation of osteoblast differentiation by transcription factors. J Cell Biochem *99(5)*: 1233-1239.

Komori, T. (2008) Regulation of bone development and maintenance by Runx2: Front Biosci. United States, pp 898-903.

Kon, E., A. Muraglia, A. Corsi, P. Bianco, M. Marcacci, I. Martin, A. Boyde, I. Ruspantini, P. Chistolini, M. Rocca, R. Giardino, R. Cancedda, R. Quarto (2000) Autologous bone marrow stromal cells loaded onto porous hydroxyapatite ceramic accelerate bone repair in critical-size defects of sheep long bones. J Biomed Mater Res *49(3)*: 328-337.

Kousteni, S., M. Almeida, L. Han, T. Bellido, R.L. Jilka, S.C. Manolagas (2007) Induction of osteoblast differentiation by selective activation of kinase-mediated actions of the estrogen receptor: Mol Cell Biol. United States, pp 1516-1530.

Krampera, M., G. Pizzolo, G. Aprili, M. Franchini (2006) Mesenchymal stem cells for bone, cartilage, tendon and skeletal muscle repair: Bone. United States, pp 678-683.

Krishnan, V., T.L. Moore, Y.L. Ma, L.M. Helvering, C.A. Frolik, K.M. Valasek, P. Ducy, A.G. Geiser (2003) Parathyroid hormone bone anabolic action requires Cbfa1/Runx2-dependent signaling: Mol Endocrinol. United States, pp 423-435.

Lambertini, E., T. Franceschetti, E. Torreggiani, L. Penolazzi, A. Pastore, S. Pelucchi, R. Gambari, R. Piva (2010) SLUG: a new target of lymphoid enhancer factor-1 in human osteoblasts: BMC Mol Biol. England, p 13.

Lambertini, E., G. Lisignoli, E. Torreggiani, C. Manferdini, E. Gabusi, T. Franceschetti, L. Penolazzi, R. Gambari, A. Facchini, R. Piva (2009) Slug gene expression supports human osteoblast maturation. Cell Mol Life Sci *66(22)*: 3641-3653.

Lecka-Czernik, B., I. Gubrij, E.J. Moerman, O. Kajkenova, D.A. Lipschitz, S.C. Manolagas, R.L. Jilka (1999) Inhibition of Osf2/Cbfa1 expression and terminal osteoblast differentiation by PPARgamma2: J Cell Biochem. United States, 1999 Wiley-Liss, Inc., pp 357-371.

Lee, J.H., D.M. Kemp (2006) Human adipose-derived stem cells display myogenic potential and perturbed function in hypoxic conditions: Biochem Biophys Res Commun. United States, pp 882-888.

Lee, J.Y., Z. Qu-Petersen, B. Cao, S. Kimura, R. Jankowski, J. Cummins, A. Usas, C. Gates, P. Robbins, A. Wernig, J. Huard (2000) Clonal isolation of muscle-derived cells capable of enhancing muscle regeneration and bone healing. J Cell Biol *150(5)*: 1085-1100.

Lee, M.J., S.K. Sohn, K.T. Kim, C.H. Kim, H.B. Ahn, M.S. Rho, M.H. Jeong, S.K. Sun (2010) Effect of hydroxyapatite on bone integration in a rabbit tibial defect model. Clin Orthop Surg *2(2)*: 90-97.

Lee, M.S., R.R. Makkar (2004) Stem-cell transplantation in myocardial infarction: a status report: Ann Intern Med. United States, pp 729-737.

Lendeckel, S., A. Jodicke, P. Christophis, K. Heidinger, J. Wolff, J.K. Fraser, M.H. Hedrick, L. Berthold, H.P. Howaldt (2004) Autologous stem cells (adipose) and fibrin glue used to treat widespread traumatic calvarial defects: case report: J Craniomaxillofac Surg. Scotland, pp 370-373.

Lerner, U.H. (2006) Bone remodeling in post-menopausal osteoporosis: J Dent Res. United States, pp 584-595.

Liebschner, M.A. (2004) Biomechanical considerations of animal models used in tissue engineering of bone: Biomaterials. England, pp 1697-1714.

Liu, H., E.B. Slamovich, T.J. Webster (2006) Less harmful acidic degradation of poly(lacticcoglycolic acid) bone tissue engineering scaffolds through titania nanoparticle addition. Int J Nanomedicine *1(4)*: 541-545.

Liu, W., S. Toyosawa, T. Furuichi, N. Kanatani, C. Yoshida, Y. Liu, M. Himeno, S. Narai, A. Yamaguchi, T. Komori (2001) Overexpression of Cbfa1 in osteoblasts inhibits osteoblast maturation and causes osteopenia with multiple fractures: J Cell Biol. United States, pp 157-166.

Lo Celso, C., H.E. Fleming, J.W. Wu, C.X. Zhao, S. Miake-Lye, J. Fujisaki, D. Cote, D.W. Rowe, C.P. Lin, D.T. Scadden (2009) Live-animal tracking of individual haematopoietic stem/progenitor cells in their niche: Nature. England, pp 92-96.

Lopa, S., L. De Girolamo, E. Arrigoni, D. Stanco, L. Rimondini, F.W. Baruffaldi Preis, L. Lanfranchi, M. Ghigo, R. Chiesa, A.T. Brini (2011) Enhanced biological performance of human adipose-derived stem cells cultured on titanium-based biomaterials and silicon carbide sheets for orthopaedic applications. J Biol Regul Homeost Agents *25(2 Suppl)*: S35-42.

Lu, C., A. Shervington (2008) Chemoresistance in gliomas. Mol Cell Biochem *312(1-2)*: 71-80.

Lu, L., S.J. Peter, M.D. Lyman, H.L. Lai, S.M. Leite, J.A. Tamada, S. Uyama, J.P. Vacanti, R. Langer, A.G. Mikos (2000) In vitro and in vivo degradation of porous poly(DL-lactic-co-glycolic acid) foams: Biomaterials. England, pp 1837-1845.

Lyons, F.G., A.A. Al-Munajjed, S.M. Kieran, M.E. Toner, C.M. Murphy, G.P. Duffy, F.J. O'Brien (2010) The healing of bony defects by cell-free collagen-based scaffolds compared to stem cell-seeded tissue engineered constructs: Biomaterials. England, 2010 Elsevier Ltd, pp 9232-9243.

Mano, J.F., R.L. Reis (2007) Osteochondral defects: present situation and tissue engineering approaches. J Tissue Eng Regen Med *1(4)*: 261-273.

Marion, R.M., K. Strati, H. Li, M. Murga, R. Blanco, S. Ortega, O. Fernandez-Capetillo, M. Serrano, M.A. Blasco (2009) A p53-mediated DNA damage response limits reprogramming to ensure iPS cell genomic integrity: Nature. England, pp 1149-1153.

Martin, Y., P. Vermette (2005) Bioreactors for tissue mass culture: design, characterization, and recent advances: Biomaterials. England, pp 7481-7503.

Maruyama, Z., C.A. Yoshida, T. Furuichi, N. Amizuka, M. Ito, R. Fukuyama, T. Miyazaki, H. Kitaura, K. Nakamura, T. Fujita, N. Kanatani, T. Moriishi, K. Yamana, W. Liu, H. Kawaguchi, T. Komori (2007) Runx2 determines bone maturity and turnover rate in postnatal bone development and is involved in bone loss in estrogen deficiency. Dev Dyn *236(7)*: 1876-1890.

Mastrogiacomo, M., S. Scaglione, R. Martinetti, L. Dolcini, F. Beltrame, R. Cancedda, R. Quarto (2006) Role of scaffold internal structure on in vivo bone formation in macroporous calcium phosphate bioceramics. Biomaterials *27(17)*: 3230-3237.

McCarthy, T.L., W.Z. Chang, Y. Liu, M. Centrella (2003) Runx2 integrates estrogen activity in osteoblasts: J Biol Chem. United States, pp 43121-43129.

McIntosh, K.R. (2011) Evaluation of cellular and humoral immune responses to allogeneic adipose-derived stem/stromal cells. Methods Mol Biol. 2011;702:133-50.

Mercer, C., M.Y. He, R. Wang, A.G. Evans (2006) Mechanisms governing the inelastic deformation of cortical bone and application to trabecular bone. Acta Biomater *2(1)*: 59-68.

Miranville, A., C. Heeschen, C. Sengenes, C.A. Curat, R. Busse, A. Bouloumie (2004) Improvement of postnatal neovascularization by human adipose tissue-derived stem cells. Circulation *110(3)*: 349-355.

Mitsui, K., Y. Tokuzawa, H. Itoh, K. Segawa, M. Murakami, K. Takahashi, M. Maruyama, M. Maeda, S. Yamanaka (2003) The homeoprotein Nanog is required for maintenance of pluripotency in mouse epiblast and ES cells. Cell *113(5)*: 631-642.

Miyazaki, M., H. Tsumura, J.C. Wang, A. Alanay (2009) An update on bone substitutes for spinal fusion. Eur Spine J *18(6)*: 783-799.

Mizuno, H. (2009) Adipose-derived stem cells for tissue repair and regeneration: ten years of research and a literature review: J Nihon Med Sch. Japan, pp 56-66.

Mizuno, H., P.A. Zuk, M. Zhu, H.P. Lorenz, P. Benhaim, M.H. Hedrick (2002) Myogenic differentiation by human processed lipoaspirate cells. Plast Reconstr Surg *109(1)*: 199-209; discussion 210-191.

Mosekilde, L., J. Kragstrup, A. Richards (1987) Compressive strength, ash weight, and volume of vertebral trabecular bone in experimental fluorosis in pigs. Calcif Tissue Int *40(6)*: 318-322.

Murphy, C.M., M.G. Haugh, F.J. O'Brien (2010) The effect of mean pore size on cell attachment, proliferation and migration in collagen-glycosaminoglycan scaffolds for bone tissue engineering: Biomaterials. England, pp 461-466.

Murphy, C.M., F.J. O'Brien (2010) Understanding the effect of mean pore size on cell activity in collagen-glycosaminoglycan scaffolds: Cell Adh Migr. United States, pp 377-381.

Nakamura, T., Y. Hara, M. Tagawa, M. Tamura, T. Yuge, H. Fukuda, H. Nigi (1998) Recombinant human basic fibroblast growth factor accelerates fracture healing by enhancing callus remodeling in experimental dog tibial fracture. J Bone Miner Res *13(6)*: 942-949.

Nandan, M.O., V.W. Yang (2009) The role of Kruppel-like factors in the reprogramming of somatic cells to induced pluripotent stem cells. Histol Histopathol *24(10)*: 1343-1355.

Neumann, E., G. Schett (2007) [Bone metabolism: molecular mechanisms]. Z Rheumatol *66(4)*: 286-289.

Newman, E., A.S. Turner, J.D. Wark (1995) The potential of sheep for the study of osteopenia: current status and comparison with other animal models: Bone. United States, pp 277S-284S.

Niemeyer, P., K. Fechner, S. Milz, W. Richter, N.P. Suedkamp, A.T. Mehlhorn, S. Pearce, P. Kasten (2010) Comparison of mesenchymal stem cells from bone marrow and adipose tissue for bone

regeneration in a critical size defect of the sheep tibia and the influence of platelet-rich plasma: Biomaterials. England, 2010 Elsevier Ltd, pp 3572-3579.

Nieto, M.A. (2002) The snail superfamily of zinc-finger transcription factors: Nat Rev Mol Cell Biol. England, pp 155-166.

Noort, W.A., A.B. Kruisselbrink, P.S. in't Anker, M. Kruger, R.L. van Bezooijen, R.A. de Paus, M.H. Heemskerk, C.W. Lowik, J.H. Falkenburg, R. Willemze, W.E. Fibbe (2002) Mesenchymal stem cells promote engraftment of human umbilical cord blood-derived CD34(+) cells in NOD/SCID mice: Exp Hematol. Netherlands, pp 870-878.

Noth, U., A.M. Osyczka, R. Tuli, N.J. Hickok, K.G. Danielson, R.S. Tuan (2002) Multilineage mesenchymal differentiation potential of human trabecular bone-derived cells. J Orthop Res *20(5)*: 1060-1069.

O'Brien, C.A., A. Pollett, S. Gallinger, J.E. Dick (2007) A human colon cancer cell capable of initiating tumour growth in immunodeficient mice: Nature. England, pp 106-110.

O'Brien, F.J., B.A. Harley, I.V. Yannas, L.J. Gibson (2005) The effect of pore size on cell adhesion in collagen-GAG scaffolds: Biomaterials. England, pp 433-441.

O'Loughlin, P.F., S. Morr, L. Bogunovic, A.D. Kim, B. Park, J.M. Lane (2008) Selection and development of preclinical models in fracture-healing research: J Bone Joint Surg Am. United States, pp 79-84.

Oliver, W.C., G.M. Pharr (1992) An improved technique for determining hardness and elastic modulus using load and displacement sensing indentation experiments. Journal of Materials Research 7:1564-1583.

Okita, K., M. Nakagawa, H. Hyenjong, T. Ichisaka, S. Yamanaka (2008) Generation of mouse induced pluripotent stem cells without viral vectors: Science. United States, pp 949-953.

Pal, R., N.K. Venkataramana, A. Bansal, S. Balaraju, M. Jan, R. Chandra, A. Dixit, A. Rauthan, U. Murgod, S. Totey (2009) Ex vivo-expanded autologous bone marrow-derived mesenchymal stromal cells in human spinal cord injury/paraplegia: a pilot clinical study. Cytotherapy *11(7)*: 897-911.

Panchision, D., T. Hazel, R. McKay (1998) Plasticity and stem cells in the vertebrate nervous system: Curr Opin Cell Biol. United States, pp 727-733.

Pearce, A.I., R.G. Richards, S. Milz, E. Schneider, S.G. Pearce (2007) Animal models for implant biomaterial research in bone: a review. Eur Cell Mater *13*: 1-10.

Pessina, A., A. Bonomi, V. Cocce, G. Invernici, S. Navone, L. Cavicchini, F. Sisto, M. Ferrari, L. Vigano, A. Locatelli, E. Ciusani, G. Cappelletti, D. Cartelli, C. Arnaldo, E. Parati, G. Marfia, R. Pallini, M.L. Falchetti, G. Alessandri (2011) Mesenchymal stromal cells primed with Paclitaxel provide a new approach for cancer therapy. PLoS One *6(12)*: e28321.

Phelps, E.A., A.J. Garcia (2009) Update on therapeutic vascularization strategies. Regen Med *4(1)*: 65-80.

Piscaglia, A.C. (2008) Stem cells, a two-edged sword: risks and potentials of regenerative medicine. World J Gastroenterol *14(27)*: 4273-4279.

Pittenger, M.F., A.M. Mackay, S.C. Beck, R.K. Jaiswal, R. Douglas, J.D. Mosca, M.A. Moorman, D.W. Simonetti, S. Craig, D.R. Marshak (1999) Multilineage potential of adult human mesenchymal stem cells. Science *284(5411)*: 143-147.

Pizzoferrato, A., G. Ciapetti, S. Stea, E. Cenni, C.R. Arciola, D. Granchi, L. Savarino (1994) Cell culture methods for testing biocompatibility. Clin Mater *15(3)*: 173-190.

Planat-Benard, V., J.S. Silvestre, B. Cousin, M. Andre, M. Nibbelink, R. Tamarat, M. Clergue, C. Manneville, C. Saillan-Barreau, M. Duriez, A. Tedgui, B. Levy, L. Penicaud, L. Casteilla (2004) Plasticity of human adipose lineage cells toward endothelial cells: physiological and therapeutic perspectives. Circulation *109(5)*: 656-663.

Pountos, I., P.V. Giannoudis (2005) Biology of mesenchymal stem cells: Injury. Netherlands, pp S8-S12.

Pratap, J., M. Galindo, S.K. Zaidi, D. Vradii, B.M. Bhat, J.A. Robinson, J.Y. Choi, T. Komori, J.L. Stein, J.B. Lian, G.S. Stein, A.J. van Wijnen (2003) Cell growth regulatory role of Runx2 during proliferative expansion of preosteoblasts. Cancer Res *63(17)*: 5357-5362.

Proff, P., P. Romer (2009) The molecular mechanism behind bone remodeling: a review. Clin Oral Investig *13(4)*: 355-362.

Qiao, L., Z. Xu, T. Zhao, Z. Zhao, M. Shi, R.C. Zhao, L. Ye, X. Zhang (2008) Suppression of tumorigenesis by human mesenchymal stem cells in a hepatoma model: Cell Res. China, pp 500-507.

Qu, C.Q., G.H. Zhang, L.J. Zhang, G.S. Yang (2007) Osteogenic and adipogenic potential of porcine adipose mesenchymal stem cells. In Vitro Cell Dev Biol Anim *43(2)*: 95-100.

Quirici, N., C. Scavullo, L. de Girolamo, S. Lopa, E. Arrigoni, G.L. Deliliers, A.T. Brini (2010) Anti-L-NGFR and -CD34 monoclonal antibodies identify multipotent mesenchymal stem cells in human adipose tissue. Stem Cells Dev *19(6)*: 915-925.

Quirici, N., D. Soligo, P. Bossolasco, F. Servida, C. Lumini, G.L. Deliliers (2002) Isolation of bone marrow mesenchymal stem cells by anti-nerve growth factor receptor antibodies. Exp Hematol *30(7)*: 783-791.

Rao, M.S., M.P. Mattson (2001) Stem cells and aging: expanding the possibilities. Mech Ageing Dev *122(7)*: 713-734.

Rigotti, G., A. Marchi, M. Galie, G. Baroni, D. Benati, M. Krampera, A. Pasini, A. Sbarbati (2007) Clinical treatment of radiotherapy tissue damage by lipoaspirate transplant: a healing process mediated by adipose-derived adult stem cells. Plast Reconstr Surg *119(5)*: 1409-1422; discussion 1423-1404.

Rodriguez, L.V., Z. Alfonso, R. Zhang, J. Leung, B. Wu, L.J. Ignarro (2006) Clonogenic multipotent stem cells in human adipose tissue differentiate into functional smooth muscle cells: Proc Natl Acad Sci U S A. United States, pp 12167-12172.

Roger, M., A. Clavreul, M.C. Venier-Julienne, C. Passirani, L. Sindji, P. Schiller, C. Montero-Menei, P. Menei (2010) Mesenchymal stem cells as cellular vehicles for delivery of nanoparticles to brain tumors: Biomaterials. England, 2010 Elsevier Ltd, pp 8393-8401.

Rosen, E.D., B.M. Spiegelman (2000) Molecular regulation of adipogenesis: Annu Rev Cell Dev Biol. United States, pp 145-171.

Rowlands, A.S., S.A. Lim, D. Martin, J.J. Cooper-White (2007) Polyurethane/poly(lactic-co-glycolic) acid composite scaffolds fabricated by thermally induced phase separation: Biomaterials. England, pp 2109-2121.

Roy, R.K., K.R. Lee (2007) Biomedical applications of diamond-like carbon coatings: a review. J Biomed Mater Res B Appl Biomater *83(1)*: 72-84.

Safford, K.M., S.D. Safford, J.M. Gimble, A.K. Shetty, H.E. Rice (2004) Characterization of neuronal/glial differentiation of murine adipose-derived adult stromal cells: Exp Neurol. United States, pp 319-328.

Saini, N., P. Sikri, H. Gupta (2011) Evaluation of the relative efficacy of autologous platelet-rich plasma in combination with beta-tricalcium phosphate alloplast versus an alloplast alone in the treatment of human periodontal infrabony defects: a clinical and radiological study: Indian J Dent Res. India, pp 107-115.

Saito, T., J.Q. Kuang, B. Bittira, A. Al-Khaldi, R.C. Chiu (2002) Xenotransplant cardiac chimera: immune tolerance of adult stem cells. Ann Thorac Surg *74(1)*: 19-24; discussion 24.

Sakaguchi, Y., I. Sekiya, K. Yagishita, S. Ichinose, K. Shinomiya, T. Muneta (2004) Suspended cells from trabecular bone by collagenase digestion become virtually identical to mesenchymal stem cells obtained from marrow aspirates: Blood. United States, pp 2728-2735.

Sandrini, E., C. Morris, R. Chiesa, A. Cigada, M. Santin (2005) In vitro assessment of the osteointegrative potential of a novel multiphase anodic spark deposition coating for orthopaedic and dental implants. J Biomed Mater Res B Appl Biomater *73(2)*: 392-399.

Santavirta, S., M. Takagi, L. Nordsletten, A. Anttila, R. Lappalainen, Y.T. Konttinen (1998) Biocompatibility of silicon carbide in colony formation test in vitro. A promising new ceramic THR implant coating material. Arch Orthop Trauma Surg *118(1-2)*: 89-91.

Sariola, H., M. Saarma, K. Sainio, U. Arumae, J. Palgi, A. Vaahtokari, I. Thesleff, A. Karavanov (1991) Dependence of kidney morphogenesis on the expression of nerve growth factor receptor. Science *254(5031)*: 571-573.

Sarkar, M.R., P. Augat, S.J. Shefelbine, S. Schorlemmer, M. Huber-Lang, L. Claes, L. Kinzl, A. Ignatius (2006) Bone formation in a long bone defect model using a platelet-rich plasma-loaded collagen scaffold: Biomaterials. England, pp 1817-1823.

Scherberich, A., R. Galli, C. Jaquiery, J. Farhadi, I. Martin (2007) Three-dimensional perfusion culture of human adipose tissue-derived endothelial and osteoblastic progenitors generates osteogenic constructs with intrinsic vascularization capacity. Stem Cells *25(7)*: 1823-1829.

Schimandle, J.H., S.D. Boden (1994) Spine update. The use of animal models to study spinal fusion. Spine (Phila Pa 1976) *19(17)*: 1998-2006.

Schmidt, C., A.A. Ignatius, L.E. Claes (2001) Proliferation and differentiation parameters of human osteoblasts on titanium and steel surfaces: J Biomed Mater Res. United States, 2000 John Wiley & Sons, Inc., pp 209-215.

Schmidt, P., C. Kopecky, A. Hombach, P. Zigrino, C. Mauch, H. Abken (2011) Eradication of melanomas by targeted elimination of a minor subset of tumor cells: Proc Natl Acad Sci U S A. United States, pp 2474-2479.

Selvaraj, V., J.M. Plane, A.J. Williams, W. Deng (2010) Switching cell fate: the remarkable rise of induced pluripotent stem cells and lineage reprogramming technologies: Trends Biotechnol. England, 2010 Elsevier Ltd, pp 214-223.

Seo, M.J., S.Y. Suh, Y.C. Bae, J.S. Jung (2005) Differentiation of human adipose stromal cells into hepatic lineage in vitro and in vivo: Biochem Biophys Res Commun. United States, pp 258-264.

Sharma, S., D.J. Patil, V.P. Soni, L.B. Sarkate, G.S. Khandekar, J.R. Bellare (2009) Bone healing performance of electrophoretically deposited apatite-wollastonite/chitosan coating on titanium implants in rabbit tibiae. J Tissue Eng Regen Med *3(7)*: 501-511.

Shi, Y., C. Desponts, J.T. Do, H.S. Hahm, H.R. Scholer, S. Ding (2008) Induction of pluripotent stem cells from mouse embryonic fibroblasts by Oct4 and Klf4 with small-molecule compounds: Cell Stem Cell. United States, pp 568-574.

Shinohara, T., K.E. Orwig, M.R. Avarbock, R.L. Brinster (2001) Remodeling of the postnatal mouse testis is accompanied by dramatic changes in stem cell number and niche accessibility: Proc Natl Acad Sci U S A. United States, pp 6186-6191.

Shinohara, T., K.E. Orwig, M.R. Avarbock, R.L. Brinster (2002) Germ line stem cell competition in postnatal mouse testes. Biol Reprod *66(5)*: 1491-1497.

Simmons, P.J., B. Torok-Storb (1991) CD34 expression by stromal precursors in normal human adult bone marrow. Blood *78(11)*: 2848-2853.

Singh, S.K., I.D. Clarke, M. Terasaki, V.E. Bonn, C. Hawkins, J. Squire, P.B. Dirks (2003) Identification of a cancer stem cell in human brain tumors. Cancer Res *63(18)*: 5821-5828.

Singh, S.K., C. Hawkins, I.D. Clarke, J.A. Squire, J. Bayani, T. Hide, R.M. Henkelman, M.D. Cusimano, P.B. Dirks (2004) Identification of human brain tumour initiating cells: Nature. England, pp 396-401.

Son, M.J., K. Woolard, D.H. Nam, J. Lee, H.A. Fine (2009) SSEA-1 is an enrichment marker for tumor-initiating cells in human glioblastoma: Cell Stem Cell. United States, pp 440-452.

Sotiropoulou, P.A., S.A. Perez, A.D. Gritzapis, C.N. Baxevanis, M. Papamichail (2006) Interactions between human mesenchymal stem cells and natural killer cells: Stem Cells. United States, pp 74-85.

Sun, C., G. Huang, F.B. Christensen, M. Dalstra, S. Overgaard, C. Bunger (1999) Mechanical and histological analysis of bone-pedicle screw interface in vivo: titanium versus stainless steel. Chin Med J (Engl) *112(5)*: 456-460.

Suzuki, K., M. Tanaka, N. Watanabe, S. Saito, H. Nonaka, A. Miyajima (2008) p75 Neurotrophin receptor is a marker for precursors of stellate cells and portal fibroblasts in mouse fetal liver. Gastroenterology *135(1)*: 270-281 e273.

Takahashi, K., S. Yamanaka (2006) Induction of pluripotent stem cells from mouse embryonic and adult fibroblast cultures by defined factors: Cell. United States, pp 663-676.

Tarnowski, M., A.L. Sieron (2006) Adult stem cells and their ability to differentiate: Med Sci Monit. Poland, pp RA154-163.

Tholpady, S.S., A.J. Katz, R.C. Ogle (2003) Mesenchymal stem cells from rat visceral fat exhibit multipotential differentiation in vitro. Anat Rec A Discov Mol Cell Evol Biol *272(1)*: 398-402.

Thorwarth, M., S. Schultze-Mosgau, P. Kessler, J. Wiltfang, K.A. Schlegel (2005) Bone regeneration in osseous defects using a resorbable nanoparticular hydroxyapatite. J Oral Maxillofac Surg *63(11)*: 1626-1633.

Timper, K., D. Seboek, M. Eberhardt, P. Linscheid, M. Christ-Crain, U. Keller, B. Muller, H. Zulewski (2006) Human adipose tissue-derived mesenchymal stem cells differentiate into insulin, somatostatin, and glucagon expressing cells: Biochem Biophys Res Commun. United States, pp 1135-1140.

Torres, F.C., C.J. Rodrigues, I.N. Stocchero, M.C. Ferreira (2007) Stem cells from the fat tissue of rabbits: an easy-to-find experimental source. Aesthetic Plast Surg *31(5)*: 574-578.

Toyosawa, S., S. Shintani, T. Fujiwara, T. Ooshima, A. Sato, N. Ijuhin, T. Komori (2001) Dentin matrix protein 1 is predominantly expressed in chicken and rat osteocytes but not in osteoblasts. J Bone Miner Res *16(11)*: 2017-2026.

Traktuev, D.O., S. Merfeld-Clauss, J. Li, M. Kolonin, W. Arap, R. Pasqualini, B.H. Johnstone, K.L. March (2008) A population of multipotent CD34-positive adipose stromal cells share pericyte and

mesenchymal surface markers, reside in a periendothelial location, and stabilize endothelial networks. Circ Res *102(1)*: 77-85.

Trim, N., S. Morgan, M. Evans, R. Issa, D. Fine, S. Afford, B. Wilkins, J. Iredale (2000) Hepatic stellate cells express the low affinity nerve growth factor receptor p75 and undergo apoptosis in response to nerve growth factor stimulation. Am J Pathol *156(4)*: 1235-1243.

Tullberg-Reinert, H., G. Jundt (1999) In situ measurement of collagen synthesis by human bone cells with a sirius red-based colorimetric microassay: effects of transforming growth factor beta2 and ascorbic acid 2-phosphate. Histochem Cell Biol *112(4)*: 271-276.

van Harmelen, V., T. Skurk, K. Rohrig, Y.M. Lee, M. Halbleib, I. Aprath-Husmann, H. Hauner (2003) Effect of BMI and age on adipose tissue cellularity and differentiation capacity in women. Int J Obes Relat Metab Disord *27(8)*: 889-895.

Van Zant, G., Y. Liang (2003) The role of stem cells in aging. Exp Hematol *31(8)*: 659-672.

Viateau, V., G. Guillemin, V. Bousson, K. Oudina, D. Hannouche, L. Sedel, D. Logeart-Avramoglou, H. Petite (2007) Long-bone critical-size defects treated with tissue-engineered grafts: a study on sheep. J Orthop Res *25(6)*: 741-749.

Vidal, M.A., G.E. Kilroy, M.J. Lopez, J.R. Johnson, R.M. Moore, J.M. Gimble (2007) Characterization of equine adipose tissue-derived stromal cells: adipogenic and osteogenic capacity and comparison with bone marrow-derived mesenchymal stromal cells. Vet Surg *36(7)*: 613-622.

Vinatier, C., D. Mrugala, C. Jorgensen, J. Guicheux, D. Noel (2009) Cartilage engineering: a crucial combination of cells, biomaterials and biofactors. Trends Biotechnol *27(5)*: 307-314.

Wakitani, S., T. Goto, S.J. Pineda, R.G. Young, J.M. Mansour, A.I. Caplan, V.M. Goldberg (1994) Mesenchymal cell-based repair of large, full-thickness defects of articular cartilage. J Bone Joint Surg Am *76(4)*: 579-592.

Wang, B.L., C.L. Dai, J.X. Quan, Z.F. Zhu, F. Zheng, H.X. Zhang, S.Y. Guo, G. Guo, J.Y. Zhang, M.C. Qiu (2006) Parathyroid hormone regulates osterix and Runx2 mRNA expression predominantly through protein kinase A signaling in osteoblast-like cells: J Endocrinol Invest. Italy, pp 101-108.

Wang, M. (2003) Developing bioactive composite materials for tissue replacement: Biomaterials. England, pp 2133-2151.

Wang, S., Y. Liu, D. Fang, S. Shi (2007) The miniature pig: a useful large animal model for dental and orofacial research: Oral Dis. Denmark, pp 530-537.

Wang, X., J.D. Mabrey, C.M. Agrawal (1998) An interspecies comparison of bone fracture properties. Biomed Mater Eng *8(1)*: 1-9.

Weiss, M.L., D.L. Troyer (2006) Stem cells in the umbilical cord: Stem Cell Rev. United States, pp 155-162.

Wickham, M.Q., G.R. Erickson, J.M. Gimble, T.P. Vail, F. Guilak (2003) Multipotent stromal cells derived from the infrapatellar fat pad of the knee. Clin Orthop Relat Res*(412)*: 196-212.

Xiao, G., D. Jiang, C. Ge, Z. Zhao, Y. Lai, H. Boules, M. Phimphilai, X. Yang, G. Karsenty, R.T. Franceschi (2005) Cooperative interactions between activating transcription factor 4 and Runx2/Cbfa1 stimulate osteoblast-specific osteocalcin gene expression: J Biol Chem. United States, pp 30689-30696.

Xie, T., A.C. Spradling (2000) A niche maintaining germ line stem cells in the Drosophila ovary: Science. United States, pp 328-330.

Yamamoto, N., H. Akamatsu, S. Hasegawa, T. Yamada, S. Nakata, M. Ohkuma, E. Miyachi, T. Marunouchi, K. Matsunaga (2007) Isolation of multipotent stem cells from mouse adipose tissue. J Dermatol Sci *48(1)*: 43-52.

Yoshimura, H., T. Muneta, A. Nimura, A. Yokoyama, H. Koga, I. Sekiya (2007) Comparison of rat mesenchymal stem cells derived from bone marrow, synovium, periosteum, adipose tissue, and muscle. Cell Tissue Res *327(3)*: 449-462.

Yu, G., Z.E. Floyd, X. Wu, Y.D. Halvorsen, J.M. Gimble (2011) Isolation of human adipose-derived stem cells from lipoaspirates. Methods Mol Biol *702*: 17-27.

Yu, J.M., E.S. Jun, Y.C. Bae, J.S. Jung (2008) Mesenchymal stem cells derived from human adipose tissues favor tumor cell growth in vivo. Stem Cells Dev *17(3)*: 463-473.

Zannettino, A.C., S. Paton, A. Arthur, F. Khor, S. Itescu, J.M. Gimble, S. Gronthos (2008) Multipotential human adipose-derived stromal stem cells exhibit a perivascular phenotype in vitro and in vivo. J Cell Physiol *214(2)*: 413-421.

Zappia, E., S. Casazza, E. Pedemonte, F. Benvenuto, I. Bonanni, E. Gerdoni, D. Giunti, A. Ceravolo, F. Cazzanti, F. Frassoni, G. Mancardi, A. Uccelli (2005) Mesenchymal stem cells ameliorate experimental autoimmune encephalomyelitis inducing T-cell anergy: Blood. United States, pp 1755-1761.

Zelle, S., T. Zantop, S. Schanz, W. Petersen (2007) Arthroscopic techniques for the fixation of a three-dimensional scaffold for autologous chondrocyte transplantation: structural properties in an in vitro model: Arthroscopy. United States, pp 1073-1078.

Zhai, Q.L., L.G. Qiu, Q. Li, H.X. Meng, J.L. Han, R.H. Herzig, Z.C. Han (2004) Short-term ex vivo expansion sustains the homing-related properties of umbilical cord blood hematopoietic stem and progenitor cells. Haematologica *89(3)*: 265-273.

Zheng, Y., Y. Liu, C.M. Zhang, H.Y. Zhang, W.H. Li, S. Shi, A.D. Le, S.L. Wang (2009) Stem cells from deciduous tooth repair mandibular defect in swine. J Dent Res *88(3)*: 249-254.

Ziros, P.G., T. Georgakopoulos, I. Habeos, E.K. Basdra, A.G. Papavassiliou (2004) Growth hormone attenuates the transcriptional activity of Runx2 by facilitating its physical association with Stat3beta. J Bone Miner Res *19(11)*: 1892-1904.

Zuk, P.A., M. Zhu, P. Ashjian, D.A. De Ugarte, J.I. Huang, H. Mizuno, Z.C. Alfonso, J.K. Fraser, P. Benhaim, M.H. Hedrick (2002) Human adipose tissue is a source of multipotent stem cells. Mol Biol Cell *13(12)*: 4279-4295.

Zuk, P.A., M. Zhu, H. Mizuno, J. Huang, J.W. Futrell, A.J. Katz, P. Benhaim, H.P. Lorenz, M.H. Hedrick (2001) Multilineage cells from human adipose tissue: implications for cell-based therapies. Tissue Eng *7(2)*: 211-228.